S100A1 and Nectin 4 Biomarkers in Ovarian Cancer

A DISSERTATION
SUBMITTED TO THE FACULTY OF THE GRADUATE SCHOOL
OF THE UNIVERSITY OF MINNESOTA
BY

Melissa Sue DeRycke

IN PARTIAL FULFILLMENT OF THE REQUIREMENTS
FOR THE DEGREE OF
DOCTOR OFPHILOSOPHY

Amy P.N. Skubitz (adviser)

May 2010

Acknowledgements

I would first like to thank my advisor, Dr. Amy Skubitz; throughout my time in her lab, Amy has always strongly supported all of my efforts; she has always been available to help troubleshoot problems and encouraged my development as a graduate student. Amy's enthusiasm for research is always evident and an inspiration.

I would also like to thank my thesis committee members, Drs. Sundaram Ramakrishnan, James McCarthy, Bruce Walcheck, and Doug Yee. Their guidance and advice during my graduate education has been invaluable in helping me focus my research and develop as a researcher.

Third, Dr. Kristin Boylan and Dr. Peter Argenta deserve thanks for always being willing to read and offer constructive criticism on manuscripts I have written. I appreciate the time and effort and believe their comments have greatly improved the manuscripts and helped me improve my writing. Kristin has also been invaluable in troubleshooting protocols and advice on my research projects.

I would also like to thank the MICaB program, NIH, CanCurables, Minnesota Ovarian Cancer Alliance, and the Graduate school for funding supporting the research.

Last, I would like to thank my family and friends. Throughout my education, they have unwaveringly encouraged my efforts. Without the support from these groups, the work completed would not have been possible.

Dedication

This thesis and the work described herein are dedicated to my grandparents, Cyriel and Madeleine DeRycke. Their examples of hard work and tenacity to improve their lives by moving to America inspired me to follow my dreams.

Abstract

This doctoral thesis focuses on the use of protein biomarkers for ovarian cancer detection, diagnosis, and determination of prognosis. Ovarian cancer is frequently detected after metastasis has occurred; at this point, it is difficult to remove all the residual disease, resulting in poor survival. We hypothesize that discovering and validating novel biomarkers will allow for more sensitive, specific tests which may allow earlier detection and increase survival for women diagnosed with ovarian cancer.

Work presented in this dissertation focuses on two biomarkers of ovarian cancer, S100A1 and nectin 4. S100A1 is a calcium binding protein involved in several cellular processes, including metabolism, regulation of cell cytoskeleton components, and the contractility of muscle tissue. S100A1 is differentially expressed in epithelial ovarian cancer subtypes and its expression in endometrioid ovarian cancers is an indicator of poor prognosis. Defining a subset of endometrioid ovarian cancers with a poor prognosis has useful implications for patient management and treatment. S100A1 positive patients may benefit from more aggressive chemotherapy and more frequent checkups following initial debulking surgery.

Nectin 4 is also overexpressed in ovarian cancer and there is differential expression among the subtypes. A soluble form of nectin 4 is detectable in patient sera. Compared to CA125, nectin 4 is more specific but less sensitive. When combined with CA125 for the detection of ovarian cancer, both the specificity and positive predictive value (PPV) were increased.

Nectin 4 expression increases proliferation in ovarian cancer cells but does not alter survival to either cisplatin or taxol. Both nectin 4 expressing and control cells are able to form spheroids equally well.

Together, these results demonstrate that biomarkers can improve diagnosis and detection of ovarian cancer. Future studies may clarify how S100A1 and nectin 4 influence ovarian cancer progression. Both proteins are potential targets for therapy. Targeting S100A1 in endometrioid ovarian cancer may increase survival. Nectin 4 expression in normal tissues is restricted to the placenta. This makes it an ideal target to utilize in therapy as there should be little killing of noncancerous tissues.

Table of Contents

List of Tables

List of Figures

List of Figures

Abbreviations

ADAM17: A Disintegrin and Metalloproteinase-17

ADIP: α-actinin-binding protein

AJ: adherens junction

AUC: area under the curve

BRCA: breast cancer susceptibility gene

BSA: bovine serum albumin

Ct: threshold cycle

ECM: extracellular matrix

ELISA: enzyme-linked immunosorbent assay

ER: estrogen receptor

EV: empty vector

FCS: fetal calf serum

FFPE: formalin-fixed, paraffin-embedded

FIGO: International Federation of Gynecology and Obstetrics

HDAC: histone deacetylases

IHC: immunohistochemical

LMO7: LIM domain only protein

LMP: low malignant potential

MTT: 3-(4,5-dimethylthiazol-2-yl)-2,5-diphenyltetrazodiom bromide

N4: nectin 4

NOSE: normal ovarian surface epithelial (cells)

NPV: negative predictive value

NSCLC: non small cell lung cancer

OSE: ovarian surface epithelial (cells)

PBS: phosphate buffered saline

PPV: positive predictive value

PR: progesterone receptor

RAGE: receptor for advanced glycation end products

RCC: renal cell carcinoma

ROC: receiver-operating characteristics

TMA: tissue microarray

WST-1: 2-(4-Iodophenyl)-3-(4-nitrophenyl)-5-(2,4-disulfophenyl)-2H-tetrazolium, monosodium salt

Chapter 1

Introduction

OVARIAN CANCER

Overview

Ovarian cancer is the most lethal gynecological cancer, with an estimated 204,499 new cases and 124,860 deaths world-wide in 2002 (1). In the United States, an estimated 21,550 new cases and 14,600 deaths occurred in 2009 (2).

Ovarian cancer accounts for 3% of all the female cancers diagnosed, but 5% of the female cancer deaths (2). In Minnesota alone, it is estimated that 240 women died from ovarian cancer in 2009 (2). Although the death rate has decreased slightly over the years (9.51 deaths per 100,000 women in 1991 to 8.62 deaths per 100,000 women in 2005), the five year survival rate for ovarian cancer patients is still dismal (2). When detected while still localized, the five year survival is 93%; however this drops to 71% for patients with regional metastasis, and to 31% for patients with distant metastasis (2). Unfortunately, fewer than 20% of cases are detected when the tumor is still localized; over 65% are detected after distant metastasis has occurred (2). Because of the late diagnosis in many cases, the overall five year survival is only 46%, compared to an 89% five year survival for breast cancer (2).

Origins

The precursor cell of ovarian cancer remains in dispute. Previously, it was thought that most ovarian cancers arose from either the ovarian surface epithelial (OSE) cells covering the surface of the ovary or from inclusion cysts (invaginated areas of OSE trapped in the ovarian stroma) inside the ovary (3-5). This hypothesis is based on several observations, including cellular atypia of the OSE cells adjacent to invasive carcinomas and increased inclusion cysts and cellular atypia of the OSE in women with a family history of ovarian cancer undergoing prophylactic removal of ovaries (3, 4). Several features of the OSE make it an attractive site for tumorogenesis. Although called

epithelium, the OSE is better described as a layer of uncommitted mesothelium cells; these cells are able to differentiate into several different lineages, including both epithelial and mesenchymal (3, 5). The cells are able to respond to environmental cues and can secrete growth factors and cytokines (3). This allows the cells to respond to events common during ovulation, such as when a follicle ruptures from the surface of the ovary (3, 5). Thus, the plasticity of the OSE allows for the repair of the break in the cell lining covering the ovary. Additionally, OSE cells secrete proteases that can degrade the extracellular matrix (ECM) (3). Degradation of ECM proteins by OSE highlights an important concept, that OSE cells are inherently invasive, thus they do not need to acquire this phenotype during tumor progression (3).

Although the OSE is a logical site for tumorigenesis, sufficient evidence to support the hypothesis is lacking (3, 4). Analysis of OSE is difficult; the OSE is only a single cell layer thick. During surgical removal, the OSE is frequently lost due to routine handling (4). Often the only OSE available to study is from crevices or invaginations of the ovarian surface (4). Reports differ on the amount of atypia seen in OSE adjacent to tumors, as well as how often there are increased numbers of inclusion cysts. When atypical OSE have been found, rarely have the cells had altered expression or mutations of commonly mutated genes including p53, Her2/neu, p21, and p27 (3, 4).

An emerging hypothesis for the origin of ovarian cancer is that the epithelial cells lining the fallopian tube give rise to what is commonly diagnosed as primary ovarian cancer (5, 6). Supporting this hypothesis are several observations. First, analysis of ovarian and tubal carcinomas has shown that they frequently harbor similar genetic alterations (5, 6). Analysis of the distal fimbrial tips of the fallopian tubes of women with ovarian cancer has demonstrated the presence of abnormal cells with identical genetic alterations present in the ovarian tumor (6). Additionally, in over 70% of women

undergoing prophylactic surgeries because of positive breast cancer susceptibility gene (BRCA) status, early tubal cancers are detected (6). Even if a woman has no family history or other risk factors for ovarian cancer, tubal cancers are detected in approximately half of primary ovarian and peritoneal serous cancers (6).

A third lesion often described as a precursor to ovarian cancer is endometriosis, which occurs when cells similar to those lining the uterus grow outside of the uterine cavity. Many clear cell (88%) and endometrioid (20%) ovarian cancers diagnoses have simultaneously diagnosed endometriosis (4, 5).

Grading of Ovarian Tumors

The grade of a tumor is often a prognostic indicator in ovarian cancer. In 2000, Silverberg described a system of grading ovarian cancers based on a three-tiered system, which has now become known as Silverberg grading (7). Tumors are assessed for their architecture, nuclear atypia, and the number of mitotic cells visible; each of these is assigned a score of 1 to 3. These three scores are then combined and assigned a grade of 1 (cumulative score of 3 – 5), 2 (cumulative score of 6 – 7), or 3 (cumulative score of 8 – 9). A score of 1 indicates a well-differentiated tumor, a score of 2 represents a tumor with moderate differentiation, while a score of 3 represents a tumor with poor differentiation (7).

Tumor architecture can be glandular (score of 1), papillary (score of 2), or solid (score of 3) (7). Determining the score for nuclear atypia involves assessing several characteristics. A tumor with a nuclear atypia score of 1 has a low nuclear to cytoplasmic ratio, no chromatin clumping or nucleoli visible. In a tumor with a score of 2, there may be some chromatin clumping, small but recognizable nucleoli, and no bizarre cells present. Increased nuclear to cytoplasmic ration, prominent chromatin clumping, large nucleoli, and bizarre cells are features of a score of 3 for nuclear atypia (7).

The final assessment in determining the Silverberg grade is determining the number of mitotic cells visible. This can be highly variable, as different areas of a tumor may display increased or decreased proliferation. To standardize this, the area that should be observed is the most mitotically active area, which is often the leading edge of the tumor. A score of 1 indicates a tumor with 0 – 9 mitotic figures in 10 high powered fields (400x). Ten to 24 mitotic figures in 10 high powered fields results in a score of 2, and >25 mitotic figures in 10 high powered fields results in a score of 3 (7).

Staging of Ovarian Tumors

Staging of ovarian tumors describes where the tumor is located, or how far it has metastasized. The International Federation of Gynecology and Obstetrics has described a staging system that is currently in practice (8).

Stage I and II tumors are considered to be early stage. Tumors that are limited to one or both ovaries are considered stage I tumors. Stage Ia tumors are only present in one ovary, have no ascites containing malignant cells, no tumor present on the surface of the ovary or capsule rupture. Stage Ib tumors differ from stage I tumors in that the tumor is present in both ovaries. Stage Ic tumors have either tumor on the surface of one or both ovaries, ascites with malignant cells, or capsule rupture. However, the tumor has not metastasized to other organs (8). Stage II tumors extend into the pelvic region. Stage IIa tumors are present in the uterus and/or fallopian tubes; IIb tumors extend to other pelvic tissues; IIc tumors have all the features of stage IIa or IIb and additionally have ascites with malignant cells, tumor on the surface of the ovaries, or capsule rupture (8).

Stage III and IV tumors are considered late stage. Stage III tumors have confirmed peritoneal implants, superficial metastasis to the liver, or metastasis to either the retroperitoneal or inguinal lymph nodes. Stage IIIa tumors are limited to the true

pelvis but have microscopic implants on abdominal surfaces and there is no metastasis to the lymph nodes. Stage IIIb tumors have abdominal implants not exceeding 2 cm in diameter and the lymph nodes are negative for metastasis. Stage IIIc ovarian cancer occurs when either the lymph nodes are positive for malignancy or there are peritoneal metastases >2 cm (8). Stage IV tumors have distant metastases to the lungs and liver. Metastases to liver must have invaded and involved the parenchyma to be deemed stage IV (8).

Subtypes of Ovarian Cancer

Three different types of cells within the ovary may give rise to ovarian cancer: epithelial cells, germ cells, and sex cord stromal cells (5). Since approximately 60% of all ovarian carcinomas are epithelial in nature, and these account for the most lethal types of ovarian cancer (5, 9), my research will focus on the epithelial cell derived types of ovarian cancer.

Epithelial ovarian cancers can be divided into eight subtypes based on histological characteristics: serous, endometrioid, clear cell, mucinous, transitional cell, squamous cell, mixed epithelial, and undifferentiated (9). Of the four most frequently diagnosed ovarian carcinomas, serous tumors account for 68%, clear cell tumors for 13%, endometrioid for 9%, and mucinous for 3% (9).

Serous tumors are characterized by slit-like spaces, small, complex papillary structures, and diffuse WT1 staining by immunohistochemistry (IHC) (Fig. 1-2A) (9). Diagnosis can be further divided into two types, low and high grade serous tumors. These types are different diseases, with different pathogenesis and underlying molecular changes (10-14). Low grade tumors, sometimes referred to as borderline or low malignant potential tumors, are often large, bilateral, and nearly half (47%) are diagnosed at stage 1 (12). There is little necrosis, a lack of multinucleated cells, and a

low mitotic index (≤12 mitoses per 10 high power fields) (11, 12, 14). Mutations in BRAF or KRAS are common, and both estrogen receptor (ER) and progesterone receptor (PR) are often strongly expressed while p53 mutations are rare (10, 13, 15). Low-grade serous tumors arise through a series of steps, from benign cystadenoma, borderline cystadenoma, borderline cystadenoma with micropapillary features, to an invasive low-grade serous tumor (15). Low-grade serous tumors are usually slow growing, which can increase survival times (9). However, low-grade serous tumors respond poorly to platinum-based chemotherapy, and thus will often recur and be fatal (9).

Compared to low-grade serous tumors, high-grade serous tumors are much more aggressive; while they initially respond to platinum-based chemotherapy and may allow for a disease-free interval, often resistance develops and recurrence is fatal (9, 15). Increased mitotic index (>12 mitoses per 10 high power fields), necrosis, the presence of psammoma bodies, and multinucleated cells distinguish high-grade serous tumors from low-grade tumors (11, 12, 14, 15). BRCA1/2 mutations are present in the majority (84%) of high grade serous tumors and mutations in p53 (50-80%), Her2/neu (5-66%), and Akt (12-36%) are common (13-15).

Endometrioid ovarian cancer tumors are composed of both solid and cystic areas, with rounded glandular spaces, longer papillary structures, and commonly have squamous elements (Fig. 1-2B) (9). Endometrioid tumors are often negative or only focally positive for WT1 and p53, while occasionally positive for vimentin by IHC (9). Mutations in β-catenin (16-54%) and p53 (42-63%) are common (4, 13, 14). Endometriosis is often diagnosed concurrently and often considered a precursor lesion for endometrioid ovarian carcinomas (4, 12-14, 16). Nearly half (43%) of endometrioid tumors are diagnosed at stage 1, leading to a better survival compared to serous tumors (12, 14).

Clear cell ovarian tumor characteristics include cells with clear cytoplasm and the presence of hobnail cells (Fig. 1-2C) (9). Additionally, there are often several types of growth patterns apparent and they may display solid, glandular, and papillary foci in one tumor. Both WT1 and p53 are often negative in clear cell carcinomas (9).

Mucinous ovarian tumors are often quite heterogeneous (14). They may present with areas of benign, borderline, and malignant areas in a single tumor (Fig. 1-2D) (14). KRAS mutations are an early event in mucinous ovarian tumor progression, with 33% of mucinous cystadenomas positive increasing to 86% of mucinous carcinomas (4, 13, 14). Two types of mucinous ovarian tumors exist, intestinal and endocervical/Müllerian (11). IHC may be the best way to distinguish the two types; both are often diffusely positive for CK7, but intestinal mucinous ovarian tumors often express the enteric markers CK20, CDX2, CEA, villin, and CA19.9 (9). Additionally, intestinal type mucinous tumors have cysts and papillae lined with atypical epithelium cells with goblet cells interspersed (9, 11). Endocervical mucinous ovarian carcinoma, usually expresses the Müllerian markers CA125, ER, and PR (9). Endocervical type mucinous tumors features include papillae lined by atypical epithelium with abundant mucin and diffuse invasion of the stroma by neutrophils (9, 11).

Treatment

Therapy for advanced ovarian cancer normally consists of a primary debulking surgery, including a complete hysterectomy, bilateral salpingo-oophrectomy (removal of both ovaries and fallopian tubes), and removal of the omentum (17). In women with earlier stage disease, removal of only the ovary with apparent tumor may be done to preserve fertility in young woman (18). During surgery, it is important for the surgeon to visibly stage the tumor and optimally debulk the tumor mass (19). Staging the tumor is critical; it is a prognostic indicator that can help determine the likelihood of relapse (19).

Optimal debulking of the tumor is also of primary importance; recurrence occurs earlier in patients with tumors that are not optimally debulked (20, 21).

After surgery, patients receive chemotherapy consisting of both platinum and taxane based agents (22-24). If a patient has had no increase in size of the residual tumor within six months, the tumor is said to be platinum-sensitive. If the tumor has progressed or recurred in six months, it is considered to be platinum-refractive (23).

After the initial debulking surgery, patients go to checkups every 3 months for one year, then every 4 to six months for several years after. Often, recurrence is monitored by CA125 levels. Levels that increase usually coincide with tumors that are growing in mass; steady levels usually correlate to no disease progression (25, 26).

Diagnosis

Ovarian cancer is referred to as the 'silent killer', as there are no specific symptoms associated with the disease. Symptoms, such as abdominal pain and/or bloating, early satiation, constipation, and trouble urinating may be temporary and are too general to specifically point to ovarian cancer (27-30). Thus, in the early stages of progression, the lack of identifiable symptoms severely decreases the chances of detection and subsequently decreasing overall survival.

Currently there are no diagnostic markers that are both specific and sensitive enough to monitor the general population for ovarian cancer. To reach a positive predictive value of 10%, (1 true cancer detected for every 10 tested), a test must be 75% specific and 99.6% sensitive (28). CA125 (cancer antigen 125, MUC16), a glycoprotein, has been widely studied for detection of ovarian carcinoma, but it is neither sensitive nor specific enough to screen the general population. Approximately 20% of early stage ovarian carcinomas do not express CA125, thus the most sensitive it can be is 80% (28, 31). Additionally, CA125 can be elevated in many other conditions, such as

endometriosis, menstruation, ovarian cysts, and pregnancy, reducing the specificity of the test (5, 28). Currently, CA125 levels are used to detect recurrence of ovarian cancer after primary debulking surgery (28).

Many imaging technologies have been studied to determine their effectiveness at detecting early stage ovarian cancer. MRIs, CAT scans, as well as transvaginal ultrasounds have all been used (5, 28). At present, none are able to detect early stage tumor; however, transvaginal ultrasounds may be useful in discriminating between benign cysts and ovarian cancer in some cases (28).

The lack of a sensitive and specific test that can be used to screen the general population results in the majority of ovarian cancer cases being diagnosed at late stages (2). At this point in disease progression, it is virtually impossible to remove all of the tumor mass from a patient. Often the chemotherapy that follows surgery is not able to effectively kill all the residual tumor cells either, possibly because of an ovarian cancer stem cell component that is highly resistant to chemotherapy. These factors make late stage ovarian cancer a lethal diagnosis. Early stage tumors have a favorable 5 year survival rate (2). Increasing the number of early stage ovarian cancer diagnoses has the potential to greatly reduce the mortality associated with the disease.

In recent years, much focus has been placed on biomarkers for early stage ovarian cancer detection. Many groups have looked in patient specimens (sera, plasma, and urine) to find overexpressed proteins that would specifically be from the tumor and could be used in a screening test (5, 28, 32). Often, these are compared to and used in conjunction with CA125 levels to get improved sensitivity and specificity. However, when combining more than one test, while the sensitivity usually goes up, the specificity is decreased, as there will be different false positives for each marker.

Mass spectrometry of sera samples to identify peaks of interest has been performed by numerous groups (32-37). This approach does have some limitations, however. Mass spectrometry will only identify the most abundant proteins in a sample; thus, if the ideal tumor marker is produced by a small proportion of cells, it will not be a major constituent of the blood. The overwhelming amount of normal proteins can make it extremely difficult to find a tumor marker if the abundant proteins are not first removed. Many groups have worked around this problem by depleting the most common proteins through various methods (32, 35). This may have unintended consequences, however; many small, potential tumor marker proteins may bind to the abundant proteins (such as albumin) and be depleted as well.

S100 PROTEINS

General Overview

The S100 protein family consists of twenty members of low molecular weight proteins (9 – 13 kDa) that function in calcium signaling (38-40). Expression of S100 proteins is both cell and tissue specific; the proteins share a similar structural form consisting of an N-terminal region, four alpha-helixes, and a C-terminal region. S100 proteins contain two EF-hand calcium binding sites (38, 40). The N-terminal binding site is unconventional and binds calcium with a weaker affinity than the canonical C-terminal region site (38). The majority of sequence differences occur in the hinge region between helices II and III and the C-terminal region, and likely account for specificity of target protein binding (38-40). Most S100 proteins function as dimers held together by covalent bonds; both homo- and heterodimers exist, depending on the particular S100 protein (38-40). Upon binding calcium, the S100 dimer undergoes a conformational change, opening a previously inaccessible region, allowing binding to target proteins (38-40).

In addition to intracellular calcium signaling, some S100 proteins are secreted and can act in a cytokine manner by activating the receptor for advanced glycation end products (RAGE) (41). RAGE belongs to the immunoglobulin superfamily of proteins and contains one V and two C immunoglobulin-like loops, a transmembrane region, and a cytoplasmic tail (40, 41). Binding to ligands is mediated by the V region; ligands bind based on their 3-dimensional structure more than their primary amino acid sequence (41). Many ligands have been identified, including amyloid A, various S100 proteins, bacteria, and prions (41). Binding of ligands can induce many different signals, including NF-κB, ERK1/2, MAP kinases, and JNK (40, 41). The exact signaling cascade that occurs depends both on the specific ligand that binds RAGE as well as the concentration of the ligand (40, 41).

S100A1

S100A1 expression in human tissues is highest in skeletal muscle, neurons, the heart, and kidneys (38, 42). S100A1 can form homodimers as well as heterodimers with S100B, S100A4, or S100P (40). Several binding targets have been reported for S100A1, including the transcription factor MyoD, fructose 1,6-bisphosphate aldolase, phosphoglucomutase, glycogen phosphoralase, and membrane bound guanylate cyclase, CapZα, microtubules, and intermediate filaments, resulting in modulation of muscle contraction, metabolism, and cell structure (43-51).

Increased expression of several S100 family members, including S100A1, has been reported in several tumors (40, 52). Several groups have identified increased S100A1 in renal cell cancer. The exact function of S100A1 is unclear, but it may be possible to discriminate between subtypes of the disease based on S100A1 expression, improving diagnosis and helping determine the appropriate therapy (53-56).

S100A1/S100A4 heterodimers have also been described in breast cancer (52, 57). Expression of S100A1 increased proliferation of tumor cells; however, S100A1 acted as an antagonist of S100A4, reducing S100A4 increased motility and invasive potential (57). S100A1 alone could not reduce motility or invasiveness below normal levels, only the increase provoked by S100A4 expression (57).

S100A1 is able to bind to and activate RAGE, although to date S100A1 has not been reported to be secreted from cells (40, 58). It has been proposed that cells in the center of tumors may become necrotic due to lack of nutrients and hypoxia, resulting in release of their cellular contents (59, 60). Release of S100A1 may impart a survival advantage to nearby tumor cells, by signaling through RAGE and preventing apoptosis through NF-κB signaling (40).

NECTIN PROTEINS

General Overview

Nectins are calcium-independent, immunoglobulin-like proteins important in the formation and stabilization of adherens junctions (AJs) (61-65). There are four members of the nectin family and they all share a very similar structure. They are composed of three Ig-like loops (V, C, C), a single transmembrane region, and a short cytoplasmic tail. Nectins 1 – 3 share a PDZ binding domain in their cytoplasmic tail, allowing them to bind to afadin (Fig. 1-1A) (61, 63, 64, 66-69). Although nectin 4 does not contain the same motif, it is still able to bind to afadin like the other nectin family members (64).

Splice variants of all nectin proteins exist. Nectin 1 has three variants, α, β, and γ; nectin 2 has two variants, α and δ; nectin 3 has three variants, α, β, and γ; nectin 4 has two variants which have not been assigned names (62-64, 67, 68, 70). All but nectin 1γ share the same general structure of three Ig-like loops, a transmembrane region, and

a cytoplasmic tail; nectin 1γ does not have a transmembrane region and is thus a secreted protein (62).

Nectins 1, 2, and 3 are ubiquitously expressed in several tissues and cell types, including epithelial cells, fibroblasts, and neurons (61-63, 67-70). Nectins 2 and 3 are also expressed in other cell types, such as B cells, monocytes, and spermatids (62, 67-69). Nectin 4 expression is limited to the placenta in human, although it is more widely expressed in mouse tissues (62, 71).

Nectins function by forming both cis- and trans-dimers (61). The second Ig loop is required for the formation of cis-dimers, while the first Ig loop is required for the formation of trans-dimers (62, 63, 71-73). Cis-dimers are always composed of the same nectin molecule (homodimers), while trans dimers can be either homo- or hetero-dimers; however, not all nectins are able to form trans-dimers with all of the other nectins (62, 63) . Thus, nectin 4 can transdimerize with itself or with nectin 1, but not with nectins 2 or 3 (Fig. 1-1B) (64). The interaction between hetero trans-dimers is stronger than that of homo trans-dimers (63).

In addition to their importance in cell junction formation, nectins 1, 2, and 3 also serve as entry receptors for alpha herpes viruses; no such function has been found for nectin 4 (61, 69). Disruption of expression by gene knockout or knockdown of nectins 1, 2, and 3 have shown specific defects, but none are lethal, suggesting that the functions of the nectins are at least partially redundant (74). Knockdown of nectin 4 expression has not yet been tested in a mouse model (74).

The formation of AJ complexes is a complex, multistep process in which nectins are key players (Fig. 1-2). When nectins trans-dimerize, the tyrosine kinase Src is activated, and this results in the activation of the small G protein RAP1 through Crk and C3G (61, 75). Src also phosphorylates FRG and Vav2, two guanine nucleotide

exchange factor proteins (61, 75). Activated RAP1 is then able to phosphorylate FRG, which activates CDC42 (61, 75, 76). Activation of CDC42 results in the formation of filopodia, which extend between the adjacent cells to increase the number of contact sites (61, 75). In addition, active CDC42 also enhances the activation of VAV2, which goes on to activate Rac. Rac activation results in the formation of lamelliopodia, which act like a zipper, closing gaps formed by the filopodia (Fig. 1-2) (61, 75, 76).

During this process, nectins become anchored to the actin cytoskeleton and recruit cadherins to forming AJ (Fig. 1-3). The cytoplasmic tail of nectins binds to afadin, a scaffolding protein that binds to F-actin and is important for organizing the many protein complexes required for AJ formation (Fig. 1-3A) (75). Trans-dimerization of nectins recruits ponsin to bind to afadin (75). When Rac and CDC42 are activated, cadherins are recruited to the forming AJ (75). Although the cadherins do not trans-interact, they are bound to both p120ctn and β-catenin through their cytoplasmic domain (Fig. 1-3B). α-catenin binds to both β-catenin and F-actin, linking the cadherins to the actin cytoskeleton (75). Multiple connector complex molecules that link nectins to cadherins are then recruited: ponsin binds to vinculin, α-actinin-binding-protein (ADIP) and LIM domain only protein-7 (LMO7) bind to both afadin and α-actinin (75, 77). These complexes link nectins and cadherins together and to the actin cytoskeleton. Cadherins are stabilized at this point and able to form trans-dimers (Fig. 1-3C) (75, 78). Activation of Rac prevents the endocytosis of cadherins, promoting the stability of the newly formed AJ (Fig. 1-3D) (75).

Nectin 4

Nectin 4 is the newest member of the nectin family of proteins. It encodes a 510 amino acid protein with a predicted molecular weight of 55.5 kDa; N glycosylation results in the molecular weight increasing to 66 kDa (71). One splice variant has been found

with a 24 amino acid sequence deleted (71). Unlike the other nectins, nectin 4 does not act as a receptor for α herpes viruses (71).

Nectin 4 can be cleaved from the cell surface by **A D**isintegrin **A**nd **M**etalloproteinase-**17** (ADAM17) to produce a 43 kDa protein (79). ADAM17 is an enzyme with many targets, including L-selectin, epidermal growth factor, and notch (79). After being released from the surface of a cell, the shed extracellular portion of nectin 4 is stable for at least 72 hours and likely longer (79).

Recently, overexpression of nectin 4 has been detected in both breast and lung cancer patients (80, 81). Fabre-Lafay et. al demonstrated that certain subsets of breast cancer had increased expression of nectin 4 compared to normal breast tissue (80). Additionally, the shed ectodomain of nectin 4 was detected in the sera of patients with breast cancer (80). Levels of nectin 4 correlated with the number of metastases and likelihood of survival; the authors concluded that monitoring serum nectin 4 levels in patients after treatment for breast cancer may increase detection of recurrence earlier than standard methods currently in use (80). The authors also investigated expression of nectin 4 in a limited number of ovarian cancer cell lines and sera from ovarian cancer patients. Fifty percent of the ovarian cancer cell lines tested expressed nectin 4; however, they were only able to detect shed nectin 4 in the sera of one patient out of 25 (80). Based on these results, the authors concluded that nectin 4 is not a useful biomarker for ovarian cancer.

In non small cell lung cancer (NSCLC) tissue samples, nectin 4 mRNA levels were five times higher in more than 85% of samples compared to normal lung tissues (81). The authors validated the results both by IHC and enzyme-linked immunosorbent assay (ELISA) analysis of patient serum. Decreased survival was associated with tumors expressing strong nectin 4 staining levels (81). A positive cutoff level of 1.0 ng/ml

was calculated for serum samples, and they found that nectin 4 was significantly increased in patients diagnosed with NSCLC compared to normal control patients as well as patients diagnosed with chronic obstructive pulmonary disease (81). Additionally, serum levels of nectin 4 decreased after surgery in NSCLC patients (81). Nectin 4 was 53.4% sensitive in detecting NSCLC, a significant increase compared to the two conventional NSCLC biomarkers, carcinoembryonic antigen (42.7% sensitive) and cytokeratin 19-fragment (39.0% sensitive) (81).

Additionally, the authors determined that nectin 4 expression in lung cancer cell lines *in vitro* resulted in increased viability and cell growth as well as promoted the formation of colonies in soft agar (81). Expression of nectin 4 resulted in Rac1 activation and the formation of lamelliopodia, indicating that the nectin 4 signaling cascade is similar to other nectins (81). When nectin 4 expressing or null NSCLC cells were injected subcutaneously into mice, nectin 4 promoted a significant increase in rapid tumor growth compared to control cells, indicating that nectin 4 is capable of exerting effects both *in vitro* and *in vivo* (81). Together, these results suggest that nectin 4 expression in lung cancer cells may increase both proliferation as well as metastatic activity, promoting tumor progression.

HYPOTHESIS

Diagnosis of ovarian cancer at late stages results in poor survival rates. When detected in early stages, the five year survival increases significantly. Currently there are no available tests that are sensitive and specific enough to test the general population, resulting in delayed diagnosis. Adding to the poor survival rate of advanced stage ovarian cancer is a lack of targeted therapy options. Development of new biomarkers that can diagnose ovarian cancer at earlier stages and may act as novel therapeutic

targets is critical to reduce the high mortality associated with ovarian cancer. Thus, we hypothesize that discovering and validating novel biomarkers will allow for earlier detection and increase survival for women diagnosed with ovarian cancer.

To test this, we focused on two genes previously identified in our lab as overexpressed in ovarian cancer tissues compared to normal ovarian tissue. We validated overexpression of protein levels for both genes and determined associations with subtype, stage, grade, and survival. In addition, we describe that cleaved nectin 4 ectodomain can be detected in the sera of women with ovarian cancer and may be useful in detection and diagnosis of ovarian cancer.

Figure 1-1. Nectin protein structure and interactions. A) General nectin protein structure consisting of 1 Ig-like V loop, 2 Ig-like C loops, a transmembrane region (TM) and a PDZ binding domain. B) Trans interactions of nectins can be formed by either homodimers or heterodimers.

Figure 1-1

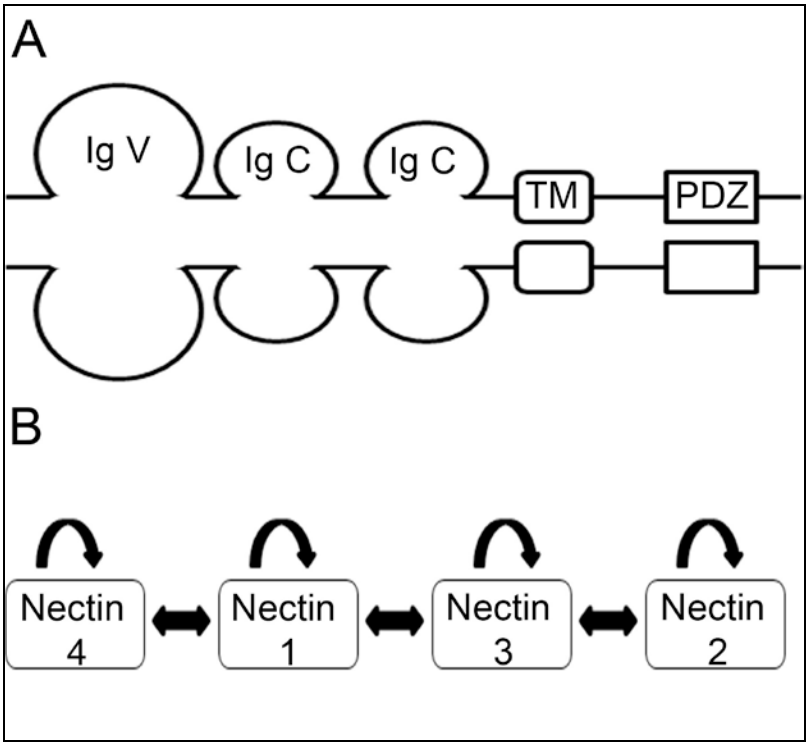

Figure 1-2. Function of nectins in adherens junction formation. Trans-dimerization of nectins results in activation of the tyrosine kinase Src. Src phosphorylates both VAV2 and FRG. RAP1 aids in activation of FRG; FRG then activates CDC42, resulting in the formation of filopodia, which increase the number of contact sites between adjacent cells. VAV2 activates Rac, resulting in the formation of lamelliopodia. The lamelliopodia act as a zipper and close gaps formed by the filopodia.

Figure 1-2

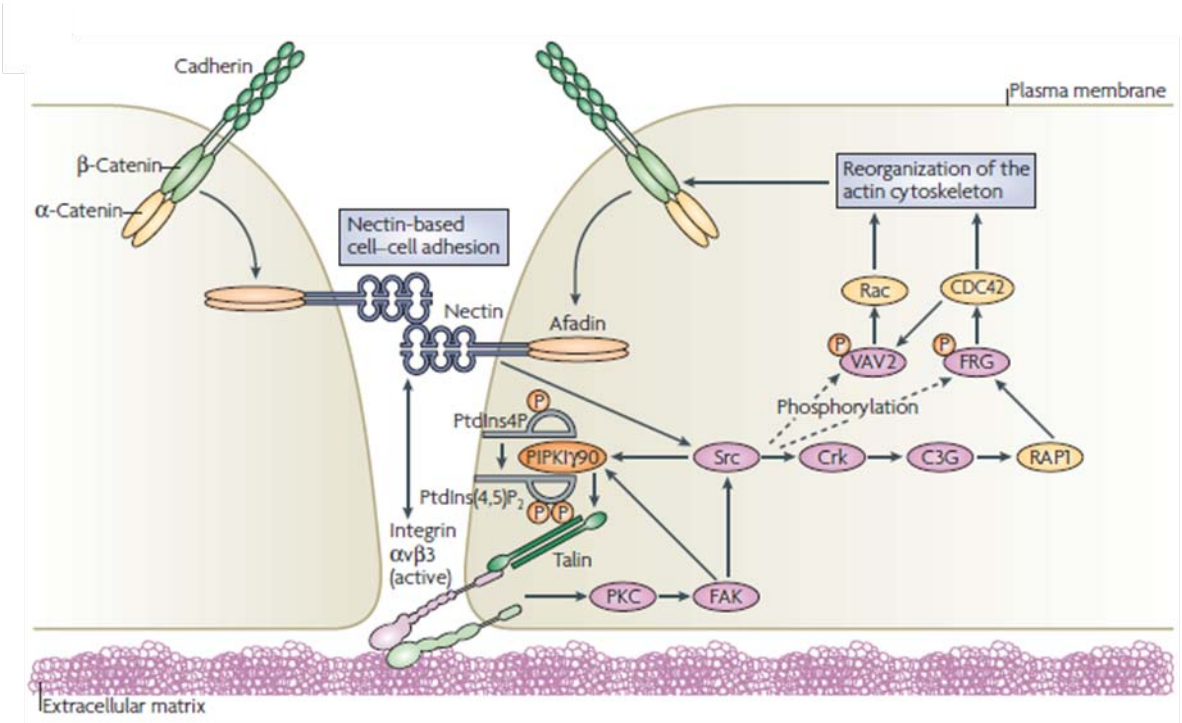
Cadherin
β-Catenin
α-Catenin
Nectin-based cell–cell adhesion
Nectin
Afadin
Plasma membrane
Reorganization of the actin cytoskeleton
Rac
CDC42
P
VAV2
P
FRG
Phosphorylation
P
PtdIns4P
PIPKIγ90
Src
Crk
C3G
RAP1
PtdIns(4,5)P2
P P
Integrin αvβ3 (active)
Talin
PKC
FAK
Extracellular matrix

Figure 1-3. Nectin recruitment of cadherins to the forming adherens junctions. A) Nectins bind to afadin through a PDZ binding domain in their cytoplasmic domain. Afadin acts as a scaffold for recruited proteins. B) Trans-interaction of nectins recruits ponsin to afadin. Activation of Rac and CDC42 recruits cadherins to the forming AJ. Cadherins are bound to p120ctn, α-catenin, and β-catenin but do not interact in trans yet. C) Vinculin, ADIP, and LMO7 are recruited and link cadherins to nectins and the cytoskeleton. Cadherins are stabilized and able to trans-dimerize. D) Rac activation prevents the endocytosis of cadherins, stabilizing the AJ.

Figure 1-3

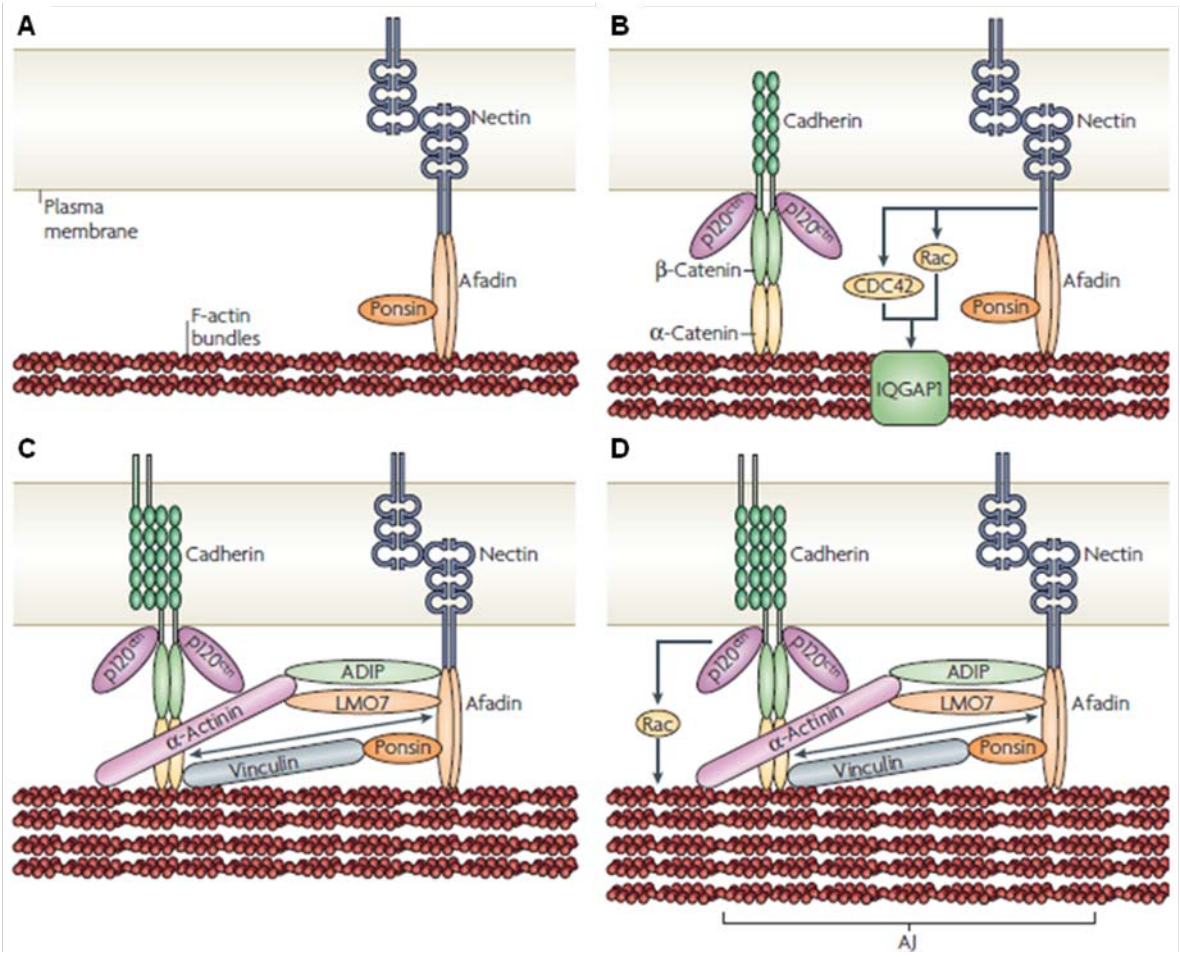
A
Nectin
Plasma membrane
Afadin
Ponsin
F-actin bundles
B
Cadherin
Nectin
p120ctn
p120ctn
β-Catenin
Rac
CDC42
Afadin
Ponsin
α-Catenin
IQGAP1
C
Cadherin
Nectin
p120ctn
p120ctn
ADIP
LMO7
Afadin
α-Actinin
Ponsin
Vinculin
D
Cadherin
Nectin
p120ctn
p120ctn
Rac
ADIP
LMO7
Afadin
α-Actinin
Ponsin
Vinculin
AJ

Chapter 2

S100A1 Expression in Ovarian and Endometrial Endometrioid Carcinomas is a Prognostic Indicator of Relapse-Free Survival

Melissa S. DeRycke[1], John D. Andersen[1], Katherine M. Harrington[1], Stefan E. Pambuccian[1], Steve E. Kalloger[2], Kristin L.M. Boylan[1], Peter A. Argenta[3], and Amy P.N. Skubitz[1*]

[1]Department of Laboratory Medicine and Pathology, University of Minnesota

[2]Cheryl Brown Ovarian Cancer Outcomes Unit, British Columbia Cancer Agency, Vancouver, Canada

[3]Division of Gynecologic Oncology, Department of Obstetrics and Gynecology, University of Minnesota

This research was originally published in *The American Journal of Clinical Pathology. Am J Clinc Pathol.* 2009. **132**:846-856.

ABSTRACT

We sought to investigate the expression levels of S100A1 in ovarian cancer cell lines and tissues in order to correlate S100A1 with subtype, stage, grade, and relapse-free survival.

S100A1 mRNA and protein were upregulated in ovarian cancer cell lines and tumors compared to normal ovarian cell lines and tissues by gene microarray analysis, RT-PCR, qRT-PCR, and western immunoblotting. Sixty-four percent of serous, 21% of clear cell, 11% of endometrioid, and 3% of mucinous ovarian cancers were S100A1 positive by immunohistochemical staining of tissue microarrays (n=500). S100A1 expression increased with increasing Silverberg grade but not stage in serous tumors. Endometrial tissue microarrays (n=126) were 9.5% S100A1 positive; no correlation with stage or grade and S100A1 was found. In the endometrioid subtype of both ovarian and endometrial cancer, relapse-free survival was decreased for S100A1 positive patients. These data suggest that S100A1 is a marker for poor prognosis of endometrioid subtypes of cancer.

INTRODUCTION

Ovarian cancer is the fifth leading cause of cancer-related death in women in the U.S., with over 22,000 new cases anticipated annually (82). The five-year survival rate, which exceeds 80% in early stage disease, drops to under 30% for disease diagnosed in later stages (82). Symptoms of early stage ovarian cancer are subtle and neither serum CA-125 nor ultrasound is predictive enough to be cost-effective in screening the general population. As a result, diagnosis typically occurs in later stages of disease, highlighting the need for novel tumor markers (83-85).

Our group previously reported a gene microarray analysis of ovarian cancer and over 400 normal and diseased tissues (85). In that study, we identified 66 genes that were upregulated two-fold or more in ovarian cancer relative to normal ovarian tissue; these genes, including S100A1, may potentially serve as tumor markers (85). Immunohistochemical (IHC) staining confirmed S100A1 protein expression as 100% sensitive and 60% specific to a small sampling of ovarian cancer tissues (85).

In this study, we report a comprehensive analysis of the expression of S100A1 mRNA and protein in a wide spectrum of ovarian cancer tissues and cell lines in an effort to validate our previous observation that S100A1 expression is elevated in ovarian cancer. We have also examined the implications of elevated S100A1 with regard to clinical specificity, disease progression, and outcomes.

MATERIALS AND METHODS

Reagents

Cell culture media and supplements were purchased from Invitrogen Corporation (Carlsbad, CA). Chemicals were purchased from Sigma Chemical (St. Louis, MO).

Cell Lines

Ovarian cancer cell lines SKOV3, ES-2, NIH:OVCAR3, HEY, C13, OV2008, OVCA429, OVCA433, A2780-s, and A2780-cp (provided by Dr. Barbara Vanderhyden), NIH:OVCAR5 (provided by Dr. Judah Folkman), MA148 (provided by Dr. Sundaram Ramakrishnan), and CAOV3 (provided by Dr. Robert Bast Jr.) were maintained as previously described (86-89). Immortalized normal ovarian surface epithelial (IOSE) cell lines 1816-575, 1816-686, HIO117, IMCC3, HIO3173-11, and HIO135 (provided by Dr. Patricia Kruk), IOSE-VAN and IOSE-MAR (provided by Dr. Nelly Auersperg) were also maintained as described (90, 91).

Tissue Samples

Snap-frozen tissues and formalin-fixed, paraffin-embedded tissue blocks were obtained from the University of Minnesota Cancer Center's Tissue Procurement Facility after IRB approval and patient consent. Snap-frozen tissue was obtained from 49 serous papillary ovarian cancers, 24 serous papillary ovarian cancer metastases to the omentum, 24 serous papillary ovarian cancer metastases to areas other than the omentum, 24 benign ovarian tumors, 59 normal ovaries, 441 normal tissues, 255 diseased tissues, and 148 other cancerous tissues, as listed in Fig. 2-1A (92). Tumor and normal samples were identified, dissected to ensure the presence of viable tumor or tissue, and snap-frozen in liquid nitrogen within 30 min of excision. Diagnoses were determined by the surgical pathologist and confirmed by two independent pathologists.

Gene Expression Analysis

RNA was prepared and gene expression determined at Gene Logic Inc. using the Affymetrix HU_133 array (92). Gene expression analysis was performed with the Gene Logic Genesis Enterprise System® Software, using the Gene Logic normalization algorithm (85, 92). The mean expression of S100A1 for each tissue type was calculated using the normalized expression values for Affymetrix probe 205334_at.

Reverse Transcriptase PCR

Total RNA was extracted from 7 serous ovarian cancer and 7 normal ovarian tissue homogenates using the RNeasy Midi Kit (Qiagen, Valencia, CA). One-step RT-PCR using the Access RT-PCR kit (Promega, Madison, WI) was performed using S100A1 primers (294-forward, 5'GAGCTAGACGAGAATGGAGAC; 497-reverse, 5'GGGTTATGGAGAGGGATAAGT) and β-actin primers (680- forward, 5'GGCCACGGCTGCTTC; 887-reverse, 5'GTTGGCGTACAGGTCTTTGC). Cycling conditions were: 45°C, 45 min; 94°C, 1 min; 35 cycles of: 94°C, 1 min; 54°C, 1 min; and 72°C, 30 sec; followed by an extension at 72°C for 3 min. Samples were separated on an agarose gel and visualized with ethidium bromide.

Quantitative Real Time PCR

Real time quantification of S100A1 was performed using the SYBR-green assay (Bio-Rad Laboratories, Hercules, CA) and the iQ5 Real-Time PCR thermocycler (Bio-Rad). Two microliters of cDNA was amplified in a 25 µl reaction containing 13 µl iQ SYBR green supermix (Bio-Rad), 1 µl each of S100A1 forward and reverse primers (353-forward, 5'TGCTCTCACAGTGGCCTGTA; 481-reverse, 5'TAAGTGGGGTGAGGTGGAAG), and 8 µl nuclease-free water. Following an initial denaturation step of 95°C for 3 min, 40 cycles of PCR were performed with the following

conditions: 95°C, 10 sec (denaturation) and 57°C, 30 sec (annealing/extension). Product size was verified by gel electrophoresis. Threshold cycle (Ct) values were calculated according to the iQ5 Real-time detection software. Standard curves for S100A1 and β-actin were generated by plotting Ct versus the log of the initial starting amount of RNA in nanograms (93). Each sample was normalized to the amount of β-actin mRNA present in the sample and the relative amount of each sample was determined as a fold-change increase over the lowest expressing cell line (IOSE-MAR).

Western Immunoblotting

Protein extraction. Protein was extracted from snap-frozen tissues in T-PER Tissue Protein Extraction Reagent (Thermo-Fisher Scientific, Waltham, MA) containing a protease inhibitor cocktail (Roche Applied Science, Basel, Switzerland). Protein concentration was determined using the BCA Protein Assay (Thermo-Fisher Scientific).

Immunoblotting. Fifty micrograms of protein was separated on a 10-20% gradient Tricine gel (Invitrogen) then transferred onto a polyvinylidene difluoride membrane. The membrane was blocked overnight then incubated with primary antibody at 1 μg/ml: rabbit-anti-human S100α polyclonal antibody (Abcam, Cambridge, MA), mouse-anti-human β-actin monoclonal antibody (clone AC-74, Sigma-Aldrich), rabbit IgG (Thermo-Fisher Scientific), or mouse IgG (Equitech-Bio, Inc, Kerrville, TX). After washing, the membrane was incubated with an HRP-conjugated secondary antibody diluted 1:5000. Proteins were visualized using SuperSignal West Femto Maximum Sensitivity substrates (Thermo-Fisher Scientific) and exposed to autoradiography film (Midwest Scientific, Valley Park, MO).

Tissue Sections

Individual tissue sections. Formalin-fixed, paraffin-embedded normal ovary (n=7), borderline ovarian tumor (n=5), and serous epithelial ovarian cancer (n=37) tissues were cut, adhered onto slides, then dried at 30°C overnight and for 30 min at 60°C immediately prior to staining to remove any residual water. Sections of normal ovary were only included in analysis if surface epithelium cells were present.

Immunohistochemical Staining of Tissues

Tissue sections were deparaffinized and rehydrated through a series of xylene and ethanol washes. Antigen retrieval was performed in a citrate buffer (Biocare, Concord, CA) and endogenous peroxidase activity was blocked with hydrogen peroxide. Slides were incubated with mouse-anti-human S100A1 monoclonal antibody (clone DAK-S100A1/1; DAKOCytomation, Glostrup, Denmark) or normal mouse IgG1 (clone 3-5D1-C9; AbCam) overnight at 1:2000. Slides were washed, then incubated with biotinylated horse-anti-mouse secondary antibody (Vector Laboratories, Burlingame, CA), followed with an avidin:biotin complex (Vector Laboratories). Staining was visualized with 3,3'-diaminobenzidine (Biocare). Slides were examined by a pathologist and assigned a score of 0 (no staining); 1 (<10% of neoplastic cells staining); 2 (10-50% of neoplastic cells staining); or 3 (>50% of neoplastic cells staining). For analysis, scores of 1, 2, and 3 were grouped and considered positive. Cardiac muscle was used as a positive control for antibody staining.

Tissue Microarrays

Tissue microarray slides of 500 cases of ovarian cancer and 126 cases of endometrial cancer (containing 0.6 mm duplicate core samples for each patient) were provided by the Cheryl Brown Ovarian Cancer Outcomes Unit (Vancouver,

Canada). Patients included in the TMA were chosen based on the fact that they were optimally debulked at initial surgery and had no macroscopic residual disease, thereby increasing the proportion of early stage cases on the TMA relative to the general population. None of the patients received neoadjuvant therapy, but all received platinum based chemotherapy following surgery. Because the 500 cases included on the ovarian TMA were originally diagnosed up to 18 years ago and the classification of ovarian cancer histologies has shifted over the years, care was taken to ensure that the current diagnostic criteria for subclassification of ovarian carcinoma based on cell type were uniformly applied (9, 94). Hematoxylin and eosin stained slides for all cases were reviewed by a gynecologic pathologist to confirm diagnosis, stage, tumor cell type, and grade prior to TMA inclusion; samples displaying multiple cell types (mixed tumors) were excluded from the study. Complete details about the cohort used for these TMAs are provided in Table 2-1 and in Gilks et al (95). Patients were followed for a median of 4.6 (0.1-18) years after the initial surgery. Relapse was defined by visible disease progression by a variety of diagnostic modalities including radiology and physical exam. Endometrial TMAs were composed of duplicate cores of 126 endometrial samples; complete details about the cohort have been previously reported in Weichert et al. (96).

Tissue microarray slides were treated and stained identically to the individual tissue sections described above.

Tissue Grading

Three-tiered grading of ovarian cancer tissues was done using the Silverberg grading system on the ovarian TMAs (7). Serous carcinomas were additionally divided

into low and high grade lesions, as reported in Malpica, et. al (97). Endometrial tissues were graded using the FIGO grading system (7).

Statistical Analysis

Significance of differential expression for S100A1 across the histopathological subtypes was quantified with the Pearson Chi-Square statistic. Univariable relapse-free survival for the entire cohort and each histopathologic subtype was examined with Kaplan-Meier survival curves. Results significant in univariable analysis were subjected to multivariable relapse-free survival using the Cox Proportional Hazards test. The level of significance for all comparisons was $p<0.05$. All statistical calculations were computed with JMP v. 6.0.3 (SAS Institute Inc., Carey, NC).

RESULTS

Gene Expression

To determine the tissue specificity of S100A1 mRNA expression, we extended our previous gene microarray analysis to include 934 samples (85, 92). S100A1 mRNA expression was increased in ovarian tumors and ovarian cancer metastases compared to normal ovaries and over 95% of the 844 other normal, diseased, and cancerous tissues examined (Fig. 2-1A). Interestingly, S100A1 was not upregulated in normal or cancerous cervix, myometrium, endometrium, uterus, intestine, colon, liver, or lung. Expression of S100A1 mRNA was high in normal skeletal muscle, as well as normal and diseased thyroid as previously described (Fig. 2-1A) (98).

Reverse Transcriptase PCR

S100A1 mRNA was highly expressed in five of seven serous ovarian cancer tissues relative to all seven normal ovarian tissues examined (Fig. 2-1B). However, surface epithelial cells, a postulated origin for ovarian cancer, comprise only a minute fraction of the entire normal ovary (99, 100). Thus, even if the normal ovarian surface epithelial cells had high levels of S100A1 mRNA, it may be masked by low or no expression of S100A1 in the ovarian stroma. It would therefore be difficult to detect S100A1 mRNA in normal ovarian surface epithelia by RT-PCR when using an entire piece of normal ovary. For this reason, qRT-PCR was performed on IOSE and ovarian cancer cell lines to better compare levels of expression in normal and cancerous epithelial cells, without concern for other contaminating cell types.

Real Time PCR

Twelve ovarian cancer cell lines and six IOSE cell lines were evaluated using qRT-PCR to quantify their expression levels of S100A1 mRNA (Fig. 2-1C). Overall, the

serous cell lines (A2780s, A2780cp, MA148, HEY, OVCAR3, OVCAR5, CAOV3) expressed the highest levels of S100A1 mRNA among the ovarian cancer subtypes, with a mean 5,779-fold increase (range 5 – 37,884) in S100A1 mRNA over the lowest expressing cell line (IOSE-MAR). S100A1 mRNA levels in clear cell carcinoma cell lines (OVCAR429, SKOV3, and ES-2) showed a mean 153-fold increase (range 7 – 418); while a mean 18-fold increase (range 12 – 25) was observed in endometrioid subtype cell lines (C13, OV2008). IOSE cell lines (HIO135, 1816-686, IOSE-VAN, HIO117, IMCC3) had only a mean 9-fold increase (range 1 – 32) in S100A1 mRNA compared to the lowest expressing cell line (Fig. 2-1C).

Western Immunoblotting

To confirm that mRNA levels correlated with S100A1 protein expression, protein extracts from seven serous papillary ovarian cancer tissues and five normal ovaries were analyzed by Western immunoblotting (Fig. 2-1D). Six of the seven cancer tissues had detectable S100A1 protein, while none of five normal ovarian tissues expressed S100A1 protein (Fig. 2-1D).

Immunohistochemical Staining

Immunohistochemistry for S100A1 was optimized in 49 individual FFPE tissue samples consisting of seven normal ovaries, five borderline, four stage I, one stage II, and 32 stage III serous subtype ovarian carcinomas. Staining was observed in both the nucleus and cytoplasm (Fig. 2-2A), as our group and others have reported previously (53, 85, 101). Three of the four stage I, the one stage II, and 29 of the 32 stage III ovarian cancer samples stained positively for S100A1, resulting in a sensitivity of 89%. One of the five cases of borderline tumor was positive. Six of the seven normal ovary tissues were negative for S100A1 expression (Fig. 2-2B), resulting in a specificity of 85.7%.

Several patient samples were analyzed by multiple techniques, and similar results were found, corroborating the results. For example, ovarian cancer tissue C5 had low levels of S100A1 mRNA expression by RT-PCR (Fig. 2-1B), and the tissue was negative for S100A1 protein by both Western immunoblot (Fig. 2-1D) and IHC (not shown). Ovarian cancer tissue C7 expressed high levels of S100A1 mRNA by RT-PCR (Fig. 2-1B) and S100A1 protein by Western immunoblot (Fig. 2-1D) and IHC (not shown). Similarly, normal ovarian tissues, N8 and N9, did not express protein by either Western immunoblot (Fig. 2-1D) or IHC.

To determine whether our IHC findings in serous ovarian tumors could be expanded and extrapolated to other histologic subtypes, tissue microarrays comprised of 500 ovarian cancer cases were stained for S100A1. Representative examples of the staining/scoring observed in the TMAs are shown in Fig. 2-2C. Differential expression was observed between the four major subtypes of ovarian cancer (serous, clear cell, endometrioid, and mucinous; $p<0.0001$) (Table 2-1). Sixty-four percent of the serous subtype stained positively for S100A1, while only 21% of clear cell, 11% of endometrioid, and 3% of mucinous subtypes stained positively (Fig. 2-3A).

S100A1 Expression by Cancer Grade and Stage

Expression of S100A1 increased significantly with increasing Silverberg grade in ovarian serous tumors, escalating from 25% to 50%, and finally to 72% for grades 1, 2 and 3 respectively (Fig. 2-3B, $p<0.0029$). No clear correlation was observed between grade and S100A1 expression in the other ovarian histologic subtypes. Likewise, S100A1 expression did not vary with stage in any histological subtype; for example, in serous tumors, S100A1 expression ranged from 60-70%, regardless of stage (Fig. 2-3C).

S100A1 Expression and Time to Disease Recurrence and Death

The medical records of those patients whose tissues were incorporated into the TMAs were examined to determine how long the patients remained disease-free before relapse or death occurred. In the ovarian cancer cohort, relapse free survival inversely correlated with S100A1 protein expression. Median relapse-free survival in patients with tumors not expressing S100A1 was 17.1 years, compared to 7.3 years for patients with tumors expressing S100A1 (data not shown). This finding is largely due to the subtype-specific differential expression of S100A1. In histologic subtype-specific relapse-free survival analysis, the S100A1 associated decrease in relapse-free survival time was only found to exist in the endometrioid subtype (Fig. 2-4A, p=0.004). Fifty percent of patients with S100A1 positive endometrioid ovarian cancer (7 of 14) had recurrent ovarian cancer 11 years after the primary diagnosis. In contrast, 87% of patients with S100A1 negative endometrioid ovarian cancer (97 of 111) remained disease-free up to 16 years (Fig. 2-4A). No correlation between S100A1 expression and relapse-free survival was observed for clear cell, mucinous, or serous subtypes of ovarian cancer (Fig. 2-4A). In multivariable analysis of the endometrioid subtype of ovarian cancer by stage, grade, and S100A1 expression, only stage and S100A1 expression remained significant (Table 2-2). This finding indicates that S100A1 expression is of independent prognostic significance.

S100A1 Expression in Endometrial Cancer

The small number of positive samples in the endometrioid subset of ovarian cancer (14 of 125) raised the possibility that the results were coincidental. To investigate the trend more thoroughly, we performed IHC on a TMA containing 126 cases of endometrial cancer of the endometrioid subtype. Endometrioid ovarian and endometrioid endometrial cancers are suspected to have similar origins (4, 7). Thus, we

hypothesized that the correlation between S100A1 expression and relapse-free survival may be similar in both types of cancer. Similar to endometrioid ovarian cancers, only a small percentage (i.e., 9.5%, 12 of 126 cases) of endometrioid endometrial cancers expressed S100A1 (Table 2-1). No correlation was found between S100A1 expression and stage or grade in endometrial endometrioid cancer (data not shown). Importantly, as in ovarian endometrioid carcinomas, the relapse-free survival time was significantly decreased in endometrial endometrioid cancers that were S100A1 positive (p=.0367) (Fig. 2-4B). Thus, we have shown that two gynecologic cancers with suspected similar origins have similar S100A1-dependent outcomes, making it highly unlikely that the results are due to chance partitioning.

DISCUSSION

In this comprehensive study, expression of S100A1 was found to be increased at both mRNA and protein levels in ovarian cancer tissues and cell lines as detected by several techniques, while expression in normal ovarian tissues and cell lines was low.

We also examined S100A1 expression on TMAs and correlated the results with tumor stage, grade, and survival. In the small subset of endometrioid subtype of ovarian cancers that expressed S100A1, relapse-free survival was significantly shorter. Half of the patients with S100A1 positive endometrioid tumors had recurrent ovarian cancer within 11 years of diagnosis, while fewer than 20% of patients with S100A1 negative endometrioid tumors had recurrent ovarian cancer at the end of the study (18 years). These findings were recapitulated in S100A1 positive endometrial endometrioid cancers as well, strengthening the results. Overall, the survival rates for endometrioid ovarian cancer are superior to that of other ovarian cancer subtypes (16). Our findings in this study suggest that S100A1 expression could represent a way to predict which patients will relapse earlier.

Previous reports have found a correlation between the presence of intraepithelial CD8-positive T cells and improved survival in ovarian cancer (102, 103). Using the same ovarian TMAs that we used in this study, Clarke et al stained for T cells using antibodies against CD3 (a pan T cell marker), CD4, and CD8 (T cell subset specific markers) (28). They found that while the presence of CD3-positive intraepithelial T cells improved disease-specific survival in the serous subtype, only the presence of CD8-positive intraepithelial T cells correlated with improved disease-specific survival in the entire cohort, including serous, endometrioid, and clear cell subtypes (104). When the T cell marker results were analyzed in conjunction with our S100A1 endometrioid ovarian

cancer data, an inverse correlation between CD3-positive T cells and S100A1 expression was found to be significant (p=0.004). Thus, S100A1-positive tumors tended to lack CD3-positive T cells, which may partially explain the shorter relapse-free survival of these patients. When expression of S100A1 and the presence of CD8-positive T cells were analyzed, however, there was no significant correlation (p=0.527).

Recent studies using the same TMAs have found type 1 histone deacetylases (HDAC) to be a marker for poor prognosis in endometrioid ovarian cancer (96). Specifically, expression of HDAC1 in multivariable survival analysis inversely correlated with relapse-free survival (96). A similar trend toward worse prognosis with HDAC1 expression in endometrioid endometrial cancers was also found (96). When analyzed with our IHC data for S100A1 staining, no significant correlation between the S100A1 and HDAC1 expression was found. Thus, the two markers identify different subsets of endometrioid ovarian cancer patients with decreased relapse-free survival. In prospective clinical trials, one could envision that tissues from patients with the endometrioid subset of ovarian cancer would be tested by IHC staining for both HDAC1 and S100A1. Those patients whose tissues stained positively for either marker would be monitored more closely for recurrence or could be candidates for additional therapy, due to the likelihood of a decreased relapse-free survival time.

High-grade serous tumors had increased S100A1 staining (66%) compared to low-grade serous tumors (25%). Although not fully understood, it is proposed that low- and high-grade serous tumors have different routes to pathogenesis. Malpica et al found that while 60% of low-grade serous tumors were associated with a serous neoplasm of low malignant potential, only 2% of high-grade serous tumors had a similar association (97). Although they have similar histological features, low- and high-grade

tumors likely arise from different molecular mechanisms, which could explain the difference in staining that we found in the TMAs.

The S100 family of proteins consists of over twenty calcium-binding proteins. Binding of calcium induces a conformational change, allowing interaction with target proteins (44). Increased expression of S100 family members, including S100A1, has been reported in several tumors. Several groups have identified increased S100A1 expression in renal cell carcinoma (RCC), and although the functional significance is not well understood, expression may be useful in differential diagnosis among RCC subtypes (53-56). In other tissues, S100A1 is involved in muscle contraction (45, 105, 106), metabolism (46, 47), and cell structure (50).

The role of S100A1 in ovarian cancer is unknown, but potentiation of anti-apoptotic pathways represents one possible mechanism. Exogenous S100A1 can activate the receptor for advanced glycation end products, resulting in activation of the NF-KB signaling pathway, increasing the anti-apoptotic protein Bcl-2 and survival (58). S100A1 can also activate the Erk1/2 signaling cascade, resulting in increased resistance to apoptosis.

To date, there have been no reports of S100A1 being secreted in cancer. However, bulky tumors harbor areas of central necrosis with relative hypoxemia (59, 60). Necrotic cells could release S100A1, providing it to nearby cells, preventing apoptosis, and imparting a survival advantage. Likewise, ovarian cancer cells are able to survive the relative hypoxia of ascitic fluid which may provide a similar stress stimulus (107).

Whether S100A1 will be an exploitable therapeutic target is unclear. Our seemingly discordant observations that S100A1 expressing serous ovarian cancer tumors were of higher grade but similar prognosis, while among endometrioid histologies

S100A1 expression did not correlate with grade or stage, but appeared to impart a significantly worsened prognosis, may be the coincidental result of subgroup analysis or overmatching. However, the results from the endometrial TMAs recapitulate the results from the endometrioid ovarian carcinomas, making this highly unlikely. Alternatively, the observed survival difference may represent a true decrease in the normally superior survival of endometrioid carcinomas in the group over-expressing S100A1 (to the level expected for serous or clear cell tumors), while the subset not expressing S100A1 retains a relatively favorable prognosis (16).

This is the first report demonstrating that S100A1 is specifically and frequently overexpressed in ovarian cancer. Though expression did not uniformly correlate with known prognostic indicators such as stage, it was associated with worsened cytological features in serous tumors and worse clinical outcomes in endometrioid ovarian cancer patients. Given our findings of worsened overall prognosis in a subset of patients, the role of S100A1 in ovarian cancer biology and tumor surveillance merits further study.

Figure 2-1. S100A1 expression levels in normal, diseased, and cancer tissues. A) Gene microarray analysis for S100A1 mRNA was performed on 934 tissues. (N)= number of samples per tissue type. Error bars represent the standard error of the mean. B) mRNA expression of S100A1 in ovarian cancer (C1-C7) and normal (N1-N7) ovary tissues was examined by RT-PCR. *, Reaction not run. C) qRT-PCR expression of S100A1 mRNA in ovarian cancer and IOSE cell lines as a function of fold-increase relative to IOSE-MAR. D) Western immunoblot of protein extracts from ovarian cancer (C5-C11) and normal (N8-N12) ovary tissues to detect S100A1 protein.

Figure 2-1A

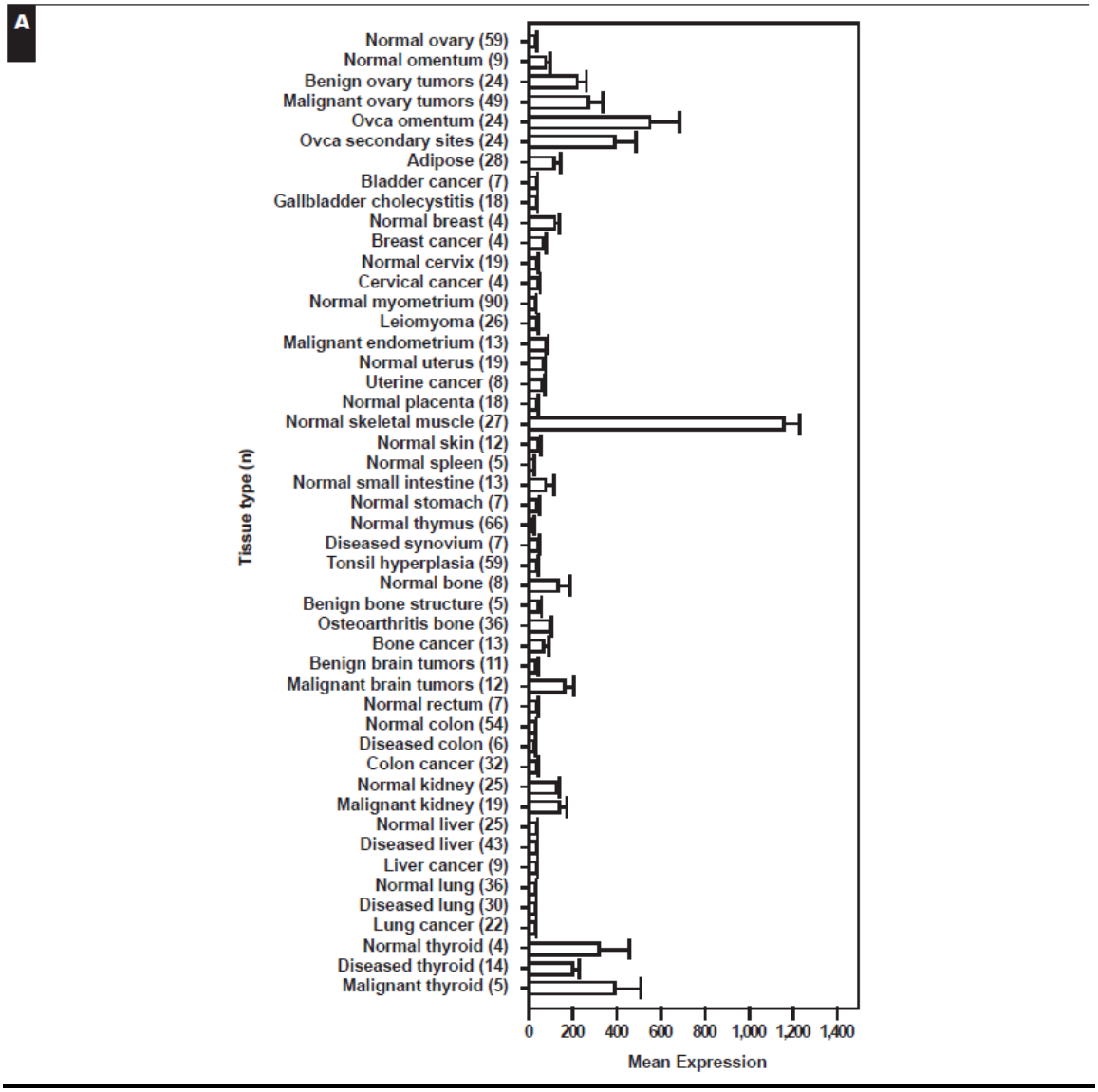
A
Normal ovary (59)
Normal omentum (9)
Benign ovary tumors (24)
Malignant ovary tumors (49)
Ovca omentum (24)
Ovca secondary sites (24)
Adipose (28)
Bladder cancer (7)
Gallbladder cholecystitis (18)
Normal breast (4)
Breast cancer (4)
Normal cervix (19)
Cervical cancer (4)
Normal myometrium (90)
Leiomyoma (26)
Malignant endometrium (13)
Normal uterus (19)
Uterine cancer (8)
Normal placenta (18)
Normal skeletal muscle (27)
Normal skin (12)
Normal spleen (5)
Normal small intestine (13)
Normal stomach (7)
Normal thymus (66)
Diseased synovium (7)
Tonsil hyperplasia (59)
Normal bone (8)
Benign bone structure (5)
Osteoarthritis bone (36)
Bone cancer (13)
Benign brain tumors (11)
Malignant brain tumors (12)
Normal rectum (7)
Normal colon (54)
Diseased colon (6)
Colon cancer (32)
Normal kidney (25)
Malignant kidney (19)
Normal liver (25)
Diseased liver (43)
Liver cancer (9)
Normal lung (36)
Diseased lung (30)
Lung cancer (22)
Normal thyroid (4)
Diseased thyroid (14)
Malignant thyroid (5)
Tissue type (n)
0
200
400
600
800
1,000
1,200
1,400
Mean Expression

Figure 2-1B-D

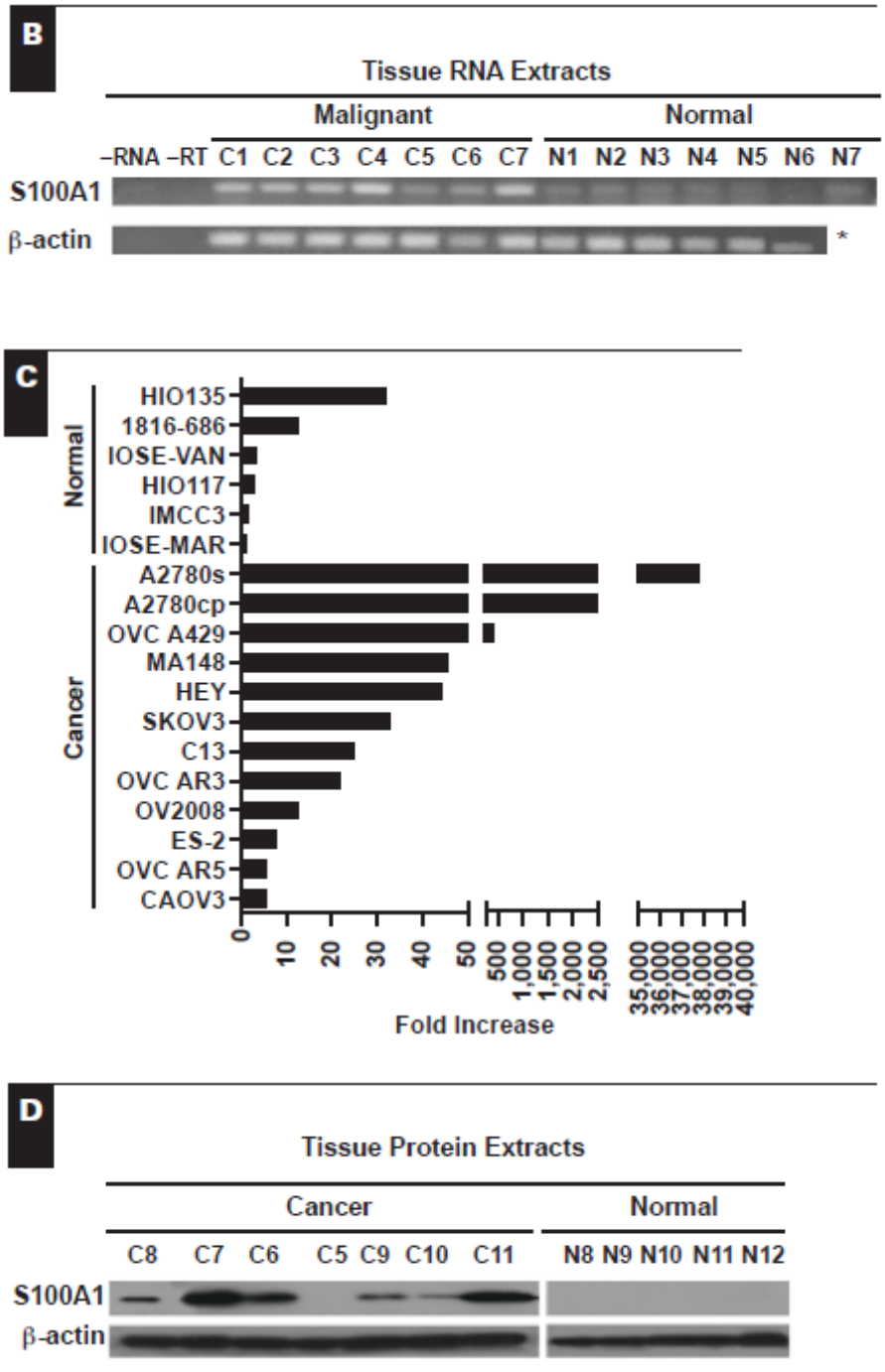
B
Tissue RNA Extracts
Malignant
Normal
–RNA –RT C1 C2 C3 C4 C5 C6 C7 N1 N2 N3 N4 N5 N6 N7
S100A1
β-actin
*
C
Normal
Cancer
HIO135
1816-686
IOSE-VAN
HIO117
IMCC3
IOSE-MAR
A2780s
A2780cp
OVC A429
MA148
HEY
SKOV3
C13
OVC AR3
OV2008
ES-2
OVC AR5
CAOV3
0
10
20
30
40
50
500
1,000
1,500
2,000
2,500
35,000
36,000
37,000
38,000
39,000
40,000
Fold Increase
D
Tissue Protein Extracts
Cancer
Normal
C8 C7 C6 C5 C9 C10 C11 N8 N9 N10 N11 N12
S100A1
β-actin

Table 2-1. Subtype, stage, Silverberg grade, and S100A1 score for tissue microarrays.

Ovarian Cancer	Median Age	Median PreOp Serum CA125*	Stage	N	S100A1 Positive (%)	Silverberg Grade	N	S100A1 Positive (%)	S100A1 Positive Overall (%)
Serous High Grade (n=200)	60.0 (37.6-86.0)	150 (0-23,000)	I	49	34 (69%)	1	0	0 (0%)	132 (66%)
			II	86	54 (63%)	2	56	28 (50%)	
			III	65	44 (68%)	3	144	104 (72%)	
Serous Low Grade (n=12)	59.2 (33.5-81.6)	65 (6-325)	I	1	1 (100%)	1	12	3 (25%)	3 (25%)
			II	7	2 (26%)	2	0	0 (0%)	
			III	4	0 (0%)	3	0	0 (0%)	
Endometrioid (n=125)	54.1 (29.4-88.1)	130 (8-13,000)	I	69	8 (12%)	1	82	8 (10%)	14 (11%)
			II	50	5 (10%)	2	35	5 (14%)	
			III	6	1 (17%)	3	8	1 (13%)	
Clear Cell (n=132)	55.0 (28.1-89.0)	64 (4-7,750)	I	68	19 (28%)	1	0†	N/A	28 (21%)
			II	56	7 (13%)	2	0†	N/A	
			III	8	2 (25%)	3	132	28 (21%)	
Mucinous (n=31)	56.4 (25.4-76.7)	45 (7-650)	I	18	0 (0%)	1	11	0 (0%)	1 (3%)
			II	12	0 (0%)	2	18	1 (6%)	
			III	1	1 (100%)	3	2	0 (0%)	
Total (n=500)	56.6 (25.4-89.0)	98 (0-23,000)	I	205	62 (30%)	1	105	11 (10%)	178 (36%)
			II	211	68 (32%)	2	109	34 (31%)	
			III	84	48 (57%)	3	286	133 (47%)	
Endometrial Cancer	**Age Range**	**Median PreOp Serum CA125**	**Stage**	**N**	**S100A1 Positive (%)**	**FIGO Grade**	**N**	**S100A1 Positive (%)**	**S100A1 Positive Overall (%)**
Endometrioid (n=126)	63.0 ± 13	N/D	I/II	119	12 (10%)	FIGO 1	81	7 (8.6%)	12 (9.5%)
			III	7	0 (0%)	FIGO 2	17	1 (6%)	
						FIGO 3	29	4 (29%)	

†PreOp, Pre operative

*All clear cell carcinomas are considered high grade.

Table 2-2. Subtype, stage, FIGO grade, and S100A1 Score for Tissue Microarrays in Endometrial Cancer*

	Mean ± SD Age (y)	S100A1 +	S100A1 + Overall
Endometrioid (n=127)	63.0 ± 13		12 (9.4)
Stage†			
I/II (n=119)	63.9 ± 12.4	12 (10)	
III (n=7)	59.1 ± 13.9	0 (0)	
FIGO grade			
1 (n=81)	63.6 ± 12.0	7 (9)	
2 (n=17)	63.0 ± 15.2	1 (6)	
3 (n=29)	63.9 ± 12.1	4 (14)	

FIGO, International Federation of Gynecology and Obstetrics

* Data are given as number (percentage) unless otherwise indicated. The preoperative serum CA125 level was not done.

† One sample was not staged.

Figure 2-2. Immunohistochemical staining of ovarian cancer and normal ovary tissue for S100A1. S100A1 stains both the nucleus (A, black arrows) and the cytoplasm, shown in a representative ovarian cancer tissue (A), but not normal ovary (B). C) Representative examples of TMA sections stained for S100A1 with a score of negative (top panel), or positive (bottom three panels, range of staining shown). Slides were examined by a pathologist and assigned a score of 0 (no staining); 1 (<10% of neoplastic cells staining); 2 (10-50% of neoplastic cells staining); or 3 (>50% of neoplastic cells staining). Original magnification 200x.

Figure 2-2

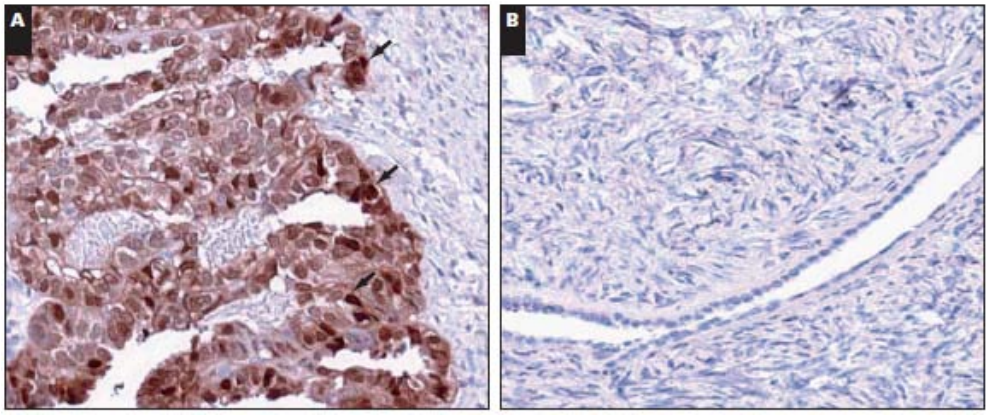

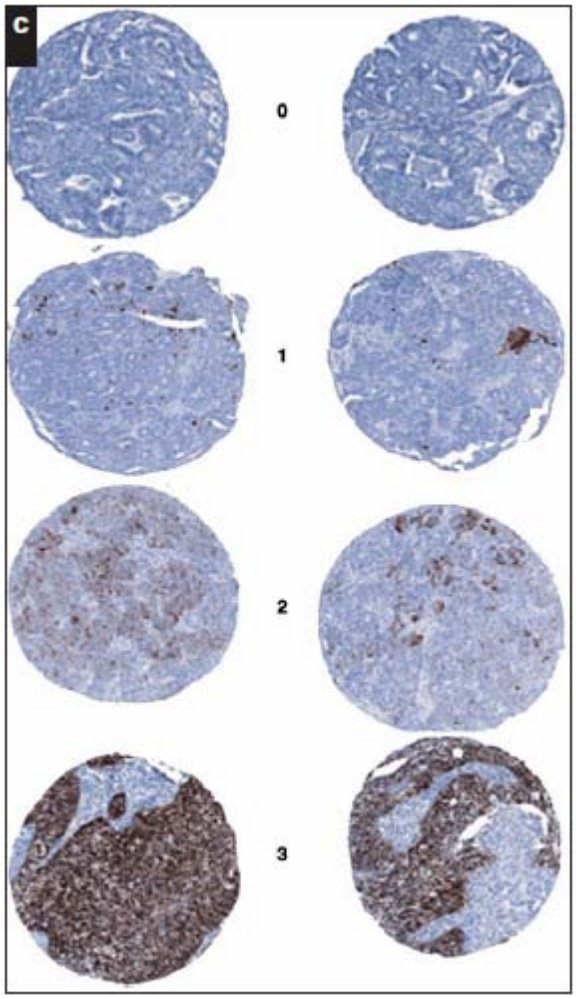

Figure 2-3. S100A1 staining of ovarian cancer TMAs by subtype, Silverberg grade, and stage. Percent of tissues staining positively by (A) subtype; (B) Silverberg grade of serous subtype of ovarian cancer; and (C) stage of serous subtype of ovarian cancer.

Figure 2-3

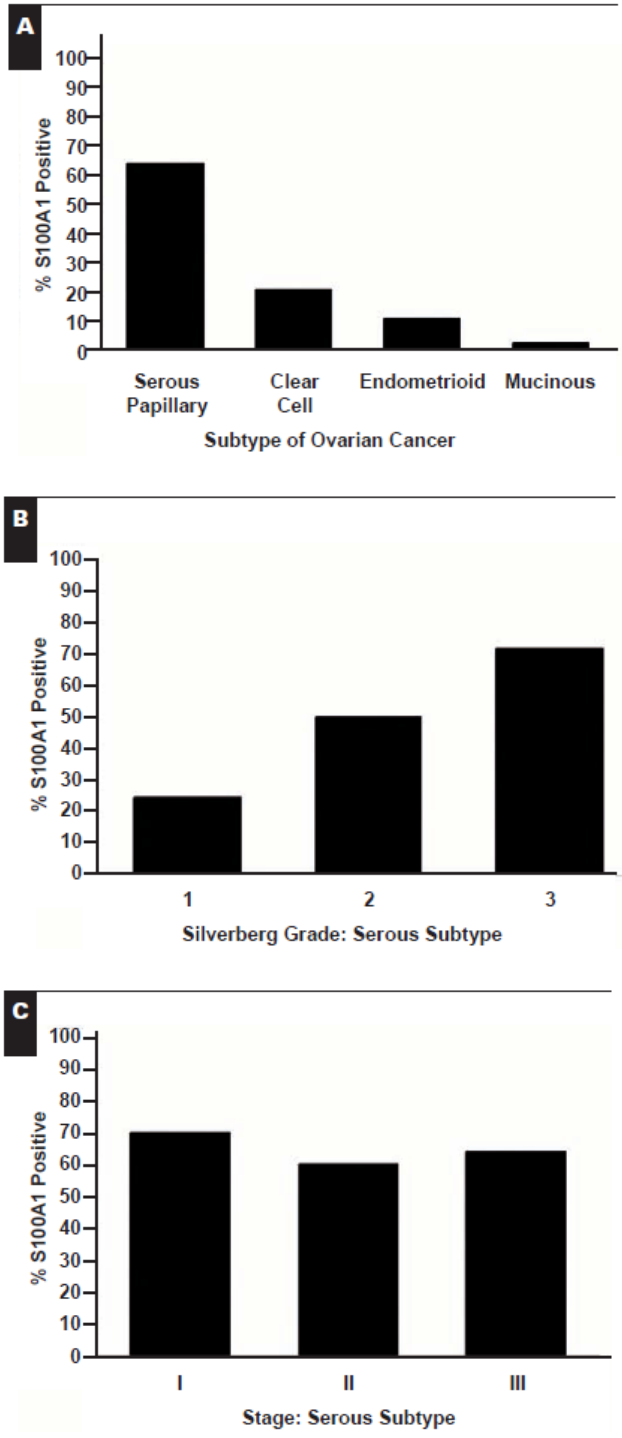
A
% S100A1 Positive
100
90
80
70
60
50
40
30
20
10
0
Serous Papillary
Clear Cell
Endometrioid
Mucinous
Subtype of Ovarian Cancer
B
% S100A1 Positive
1
2
3
Silverberg Grade: Serous Subtype
C
% S100A1 Positive
I
II
III
Stage: Serous Subtype

Figure 2-4. Kaplan-Meier relapse-free survival comparison of S100A1 positive and negative ovarian and endometrial cancer tissues. A) Relapse-free survival time was plotted as a function of S100A1 staining of ovarian cancer tissues by diagnosis, as labeled. B) Relapse-free survival time plotted as a function of S100A1 staining of endometrial endometrioid cancer. S100A1 positive, solid line; S100A1 negative, dashed line.

Figure 2-4

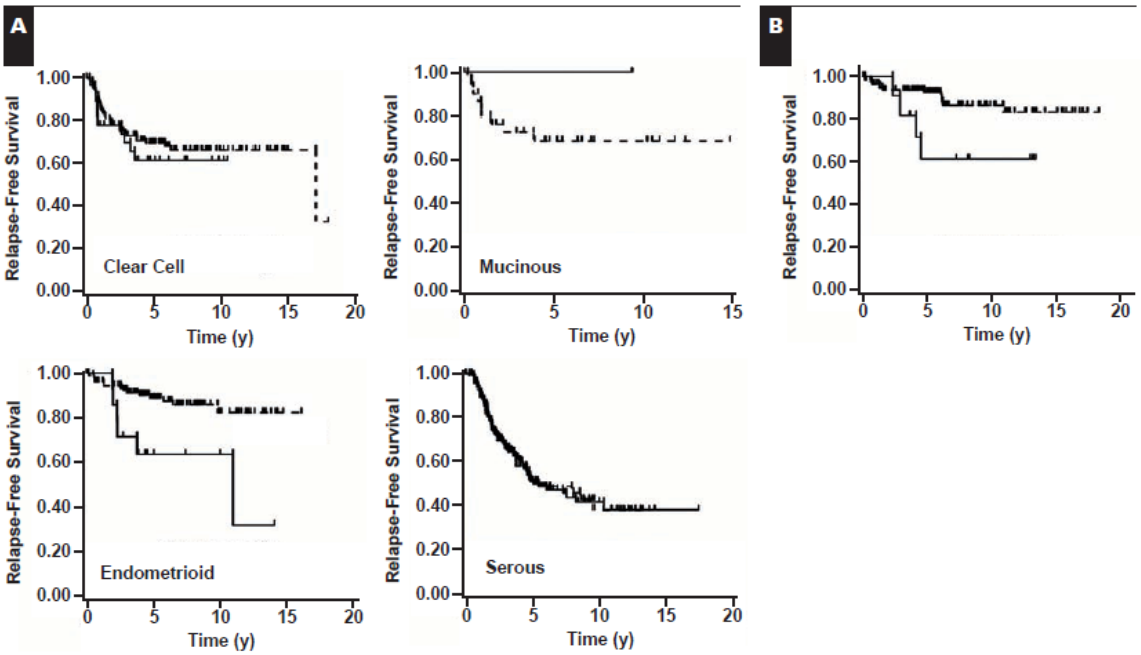
A
B
Relapse-Free Survival
1.00
0.80
0.60
0.40
0.20
0.00
0
5
10
15
20
Time (y)
Clear Cell
Mucinous
Endometrioid
Serous

Table 2-3: Multivariable relapse-free survival analysis of the 125 patients with endometrioid subtype of ovarian cancer as indicated by the Cox Proportional-Hazards Model.

Variable	Risk Ratio	Confidence Limits		p-value
		Lower	Upper	
Stage				0.0017
I	0.2886	0.1378	0.5682	
II	0.8262	0.4491	1.5265	
III	1.0000	1.0000	1.0000	
Silverberg Grade				0.3560
1	0.6811	0.2682	1.3975	
2	0.6183	0.2682	1.3975	
3	1.0000	1.0000	1.0000	
Age at Diagnosis	0.9999	0.9998	1.0000	0.8840
S100A1 Expression				0.0131
+	4.0586	1.3782	10.7851	
-	1.0000	1.0000	1.0000	

Chapter 3:

Nectin 4 overexpression in ovarian cancer tissues and sera:

Potential role as a serum biomarker

Melissa S. DeRycke[1], Stefan E. Pambuccian[1], C. Blake Gilks[2], Steve E. Kalloger[2], Abderrezak Ghidouche[3], Marc Lopez[3], Robin L. Bliss[4], Melissa A. Geller[5], Peter A. Argenta[5], Katherine M. Harrington[1], and Amy P.N. Skubitz[1]

[1]Department of Laboratory Medicine and Pathology, University of Minnesota; Minneapolis, MN,
[2]Cheryl Brown Ovarian Cancer Outcomes Unit, British Columbia Cancer Agency, Vancouver, Canada,
[3] Inserm UMR 891, Centre de Recherche en Cancérologie de Marseille (CRCM), Institut Paoli-Calmettes, Marseille, France,
[4]Biostatistics and Informatics Core, University of Minnesota; Minneapolis, MN,
[5]Department of Obstetrics, Gynecology, and Women's Health, University of Minnesota; Minneapolis, MN

This research has been accepted for publication in *The American Journal of Clinical Pathology.*

ABSTRACT

Early detection of ovarian cancer is difficult due to the lack of specific and sensitive tests available. Previously, we found expression of nectin 4 to be increased in ovarian cancer compared to normal ovaries. RT-PCR and qRT-PCR validated the over expression of nectin 4 mRNA in ovarian cancer compared to normal ovarian cell lines and tissues. Protein levels of nectin 4 were elevated in ovarian cancer cell lines and tissue compared to normal ovarian cell lines as demonstrated by Western immunoblotting, flow cytometry, and immunohistochemical staining of tissue microarray slides. Cleaved nectin 4 was detectable in a number of patient sera by ELISA. In patients with benign gynecological diseases with high serum CA125, nectin 4 was not detected in the majority of cases, suggesting that nectin 4 may serve as a potential biomarker that helps discriminate benign gynecological diseases from ovarian cancer in a panel with CA125.

Introduction

Ovarian cancer is the seventh leading cause of cancer-related death in women worldwide; 204,000 new cases were diagnosed and 125,000 women died in 2002 (1). In the United States, more than 20,000 women were diagnosed with ovarian cancer, resulting in over 14,000 deaths (2). Survival is greatly increased when ovarian cancer is diagnosed in early stages; however, approximately 70% of cases are diagnosed at stage III or IV, when the five-year survival rate decreases dramatically (82). Subtle symptoms and the lack of a specific, sensitive diagnostic test contribute to the delay in diagnosis, highlighting the need for both improved screening methods as well as novel targeting strategies for treatment (83-85). Currently, elevated serum CA125 is used to detect recurrent ovarian cancer; however, its use in screening the general population is precluded due to a lack of specificity and modest sensitivity in the detection of early stage disease.

Our group has previously identified nectin 4 (LNIR, PVRL4) upregulation in ovarian cancer tissues as part of an effort to identify novel ovarian cancer biomarkers (85). Nectins are a family of immunoglobulin-like cell adhesion molecules important in the formation and maintenance of adherens junctions and tight junctions. All nectins share a similar structure: three immunoglobulin-like extracellular loops, a single transmembrane region, and a short cytoplasmic domain that can bind to afadin (72, 108-110). Nectins function by first forming homo cis-dimers on the cell surface and then trans-dimers on adjacent cells in both a homophilic and heterophilic manner. The specificity of binding is different for each nectin (63, 72, 73). For example, nectin 4 can form trans-homodimers as well as trans-heterodimers with nectin 1, but not with nectins 2 or 3 (71).

Four nectin proteins have been described; nectin 1 and 2 are both broadly expressed in adult tissues, while nectin 3 is expressed mainly in the testes and placenta (63, 69,

71, 111). Expression of nectin 4 is normally restricted to the placenta, but has been reported in ductal breast carcinoma and lung adenocarcinomas (71, 79, 81). Fabre-Lafay et al. demonstrated that the ectodomain of nectin 4 can be cleaved from the cell surface by the metalloproteinase ADAM17 (**A D**isintegrin **A**nd **M**etalloproteinase **17**), and detected in sera by ELISA in both breast and lung cancer patients (79-81).

In this comprehensive study, we sought to validate the overexpression of nectin 4 in ovarian cancer tissues and cell lines compared to their normal ovarian counterparts using a variety of techniques including RT-PCR, qRT-PCR, flow cytometry, Western Immunoblotting, immunohistochemistry, and ELISA. We also sought to determine whether overexpression, either at the tissue or serum level, correlated with relevant clinical outcomes. Tissue microarrays comprised of 500 cases of clinically annotated ovarian cancer allowed us to determine the expression of nectin 4 in various subtypes, stages, and grades of ovarian cancer as well as to evaluate correlations with recurrence and survival. Finally, we used an ELISA to quantify nectin 4 levels in the sera of ovarian cancer patients and normal/benign gynecological cases.

Materials & Methods

Reagents

Cell culture media and supplements were purchased from Invitrogen Corporation (Carlsbad, CA) unless otherwise stated. Chemicals were purchased from Sigma Chemical (St. Louis, MO) unless otherwise stated.

Monoclonal antibodies used were: mouse anti-human nectin 4 (clone 337516, R&D Systems, Minneapolis, MN), mouse anti-human nectin 4 (clone N4.61), mouse anti-human nectin 1 (clone CK8; Invitrogen), mouse anti-human ADAM17 (Clone 111623; R&D Systems), and normal mouse IgG (clone 3-5D1-C9, AbCam, Inc., Cambridge, MA).

Polyclonal antibodies used include: biotin-conjugated goat anti-human nectin 4 (BAF2659, R&D Systems), horseradish peroxidase-conjugated rabbit anti-mouse IgG (ab5762, AbCam, Cambridge, MA), and biotin-conjugated goat anti-mouse IgG F(ab')2 fragment (Jackson ImmunoResearch, West Grove, PA).

Cell Lines

Ovarian cancer cell lines SKOV3, ES2, OVCAR3, HEY, C13, OV2008, OVCA429, OVCA433, A2780s, and A2780cp (provided by Dr. Barbara Vanderhyden, University of Ottawa, Canada), NIH:OVCAR5 (provided by Dr. Judah Folkman, Harvard Medical School, Boston, MA), CAOV3 (provided by Dr. Robert Bast Jr., University of Texas, Houston, TX), and MA148dsRed2 (provided by Dr. Sundaram Ramakrishnan, University of Minnesota, Minneapolis, MN) were maintained as previously described (86-89). SKOV3, ES2, and OVCA429 cell lines were derived from clear cell carcinomas; OV2008 and C13 cells were derived from endometrioid tumors; OVCAR3, OVCAR5, OVCA433, CAOV3, HEY, MA148, and A2780s/cp cell lines were derived from serous adenocarcinomas.

Immortalized normal ovarian surface epithelial (NOSE) cell lines 1816-575, 1816-686, HIO117, HIO135, IMCC3, IMCC5, and 3173-11 (provided by Dr. Patricia Kruk, University of South Florida, Tampa, Florida), IOSE-80 (provided by Dr. Nelly Auersperg, University of British Columbia, Vancouver, BC, Canada) were also maintained as described (90, 91). Cells were maintained in a humidified chamber at 37°C with 5% CO_2 and were routinely subcultured with trypsin/EDTA.

Tissue Samples

Snap-frozen and formalin-fixed, paraffin-embedded tissue blocks were obtained from the University of Minnesota Tissue Procurement Facility after IRB approval. RNA was isolated from snap-frozen tissues while formalin-fixed, paraffin-embedded tissues were used to optimize immunohistochemical staining. Diagnoses for the samples were: cancer, serous papillary (n=5); normal, leiomyomata (n=3), normal ovary (n=2), endometriosis (n=1), and benign peritubal cyst (n=1).

Blood and Ascites Samples

Staff at the University of Minnesota Tissue Procurement Facility ensured that all patients signed an IRB-approved consent form prior to surgery. Blood was collected immediately prior to surgery from women with abdominal masses suspected to be ovarian cancer. Blood was collected from 51 women with serous ovarian cancer (five stage 1, seven stage 2, twenty-eight stage 3, ten stage 4, one unstaged; four Silverberg grade 1, nine Silverberg grade 2, thirty-seven Silverberg grade 3, one ungraded), 14 women with clear cell ovarian cancer (eight stage 1, one stage 2, four stage 3, one not staged; fourteen Silverberg grade 3), 18 women with low malignant potential (LMP) ovarian tumors (10 LMP serous, 3 LMP mucinous, and 5 LMP with no subtype noted), and 51 women with benign gynecological disease (12 benign endometriosis, 10 benign

mucinous cystadenoma, 6 fibroma, 6 benign serous cystadenoma, 17 benign disease not specified). Ascites was collected from 10 women with serous ovarian cancer. Blood and ascites were processed by standard protocols, aliquoted, and stored at -80°C.

Reverse Transcriptase Polymerase Chain Reaction

Total RNA was extracted from cell lines and ovarian tissue samples using the RNeasy Mini kit (Qiagen, Valencia, CA) according to the manufacturer's instructions. A 189 bp sequence corresponding to nectin 4 was amplified with the following primers: Forward, 5'CAAAATCTGTGGCACATTGG3'; Reverse, 5'GCTGACATGGCAGACGTAGA3'. One-step RT-PCR was performed with the RT-PCR Access kit (Promega, Madison, WI), with conditions as follows: 45 min at 45°C; 1 cycle of 94°C, 2 min; 55°C, 1 min; 68°C, 1 min; 25 cycles of: 94°C, 30 sec; 55°C, 1 min; 68°C, 1 min; and a final extension at 68°C for 7 min. Expression of nectin 4 in MCF7 breast cancer cell lines has been reported and was used as a positive control (80). Expression of β-actin in the samples confirmed mRNA was not degraded and that similar amounts of mRNA were loaded.

qRT-PCR

Real time quantification of nectin 4 was performed using the SYBR-green assay (Bio-Rad Laboratories, Hercules, CA) and the iQ5 Real-Time PCR thermocycler (Bio-Rad). Two microliters of cDNA was amplified in a 25 µL reaction containing 13 µL iQ SYBR green supermix (Bio-Rad), 1 µL each of nectin 4 forward and reverse primers (Forward, TGCTCAAGTGCCTGAGTGAA; Reverse, AGACGTAGATGCCGCTGTG), and 8 µL nuclease-free water. Following an initial denaturation step of 95°C for 3 min, 40 cycles of PCR were performed under the following conditions: 95°C, 10 sec (denaturation) and 57°C, 30 sec (annealing/extension). Product size was verified by

agarose gel electrophoresis. Threshold cycle (Ct) values were calculated according to the iQ5 Real-time detection software. Standard curves for nectin 4 and β-actin were generated by plotting Ct versus the log of the initial starting amount of RNA in nanograms (93). Each sample was normalized to the amount of β-actin mRNA present in the sample and the relative amount of each sample was determined as a fold-change increase over the lowest expressing cell line (1816-575).

Flow Cytometry

Cells (1×10^6) were incubated with 1-2.5 µg mouse-anti-nectin 4 (clone 337516), mouse anti-nectin 1, mouse anti-human ADAM17, or a control mouse IgG for 30 min at 4°C. Cells were washed, and then incubated with biotin-conjugated goat anti-mouse IgG F(ab')2 fragment for 30 min at 4°C. After washing, cells were incubated with allophycocyanin-conjugated streptavidin for 20 min at 4°C. After washing, cells were resuspended and run on a FACSCalibur (Becton Dickenson, Franklin Lakes, NJ) and analyzed using Cell Quest Pro software (Becton Dickenson), gating on live cells by forward and side scatter.

Western Immunoblotting

Total protein extracts were derived from confluent monolayers of cells in 50 mM Tris, 150 mM sodium chloride, 1 mM EDTA, 1% Triton X-100, 1% sodium deoxycholate, 0.1% SDS, protease inhibitor cocktail (Roche Applied Science; Basel, Switzerland), and 1 mM PMSF then stored at –80°C. Fifty micrograms of total cell lysate were separated on a 10% SDS Tris-HCl polyacrylamide gel then blotted onto a polyvinylidene difluoride membrane (GE Healthcare Limited; Piscataway, NJ). Membranes were blocked with 5% powdered milk (Roundy's Inc.; Milwaukee, WI) in PBS as previously described (32, 112), and then incubated in 1 µg/mL mouse anti-human nectin 4 (clone N4.61) overnight,

followed by a 2 hr incubation in horseradish peroxidase conjugated rabbit anti-mouse antibody diluted 1/5000. Protein was visualized using the Super Signal West Femto kit (Thermo-Fisher Scientific, Rockford, IL) according to manufacturer's instructions. Membranes were exposed to autoradiography film (Midwest Scientific; Valley Park, MO) and developed.

Tissue Microarrays

TMA slides containing 0.6 mm duplicate core samples for 500 ovarian cancer patients were provided by the Cheryl Brown Ovarian Cancer Outcomes Unit (University of British Columbia; Vancouver, BC, Canada). Patients included in the TMA were chosen based on having been optimally cytoreduced at initial surgery with no macroscopic residual disease remaining. Due to these criteria, a significant proportion of early stage cases were present on the TMA relative to the general population. None of the patients received neoadjuvant therapy and all received platinum-based chemotherapy following surgery. The 500 cases included on the TMA were collected up to 18 years prior to this analysis. Hematoxylin and eosin stained slides for all cases were reviewed by a gynecologic pathologist (C.B.G.) to confirm diagnosis, stage, tumor cell type, and grade prior to TMA inclusion to ensure that the current diagnostic criteria for subclassification of ovarian cancer based on cell type were uniformly applied (9, 94). Samples displaying multiple cell types (mixed tumors) were excluded from the study. Details regarding the cohort used for these TMAs are provided in Table 1 and in Gilks et al (95). Patients were followed for a median of 4.6 (0.1-18) years after the initial surgery.

Immunohistochemical Staining of Tissues

Slides were dried and tissue sections were deparaffinized and rehydrated as previously described (112). Staining was performed manually and antigen retrieval was not performed. Endogenous peroxidase activity was blocked by incubation in 0.3%

hydrogen peroxide, then slides were incubated with 10 µg/mL mouse anti-human nectin 4 (clone 337516) or normal mouse IgG diluted in 1:5 Sniper:PBS (Biocare, Concord, CA) overnight at 4°C. Slides were incubated with horseradish peroxidase conjugated rabbit anti-mouse polyclonal secondary antibody for 20 min. Staining was visualized with Vulcan Fast Red (Biocare) and hematoxylin was used as a counterstain. Slides were dehydrated through a series of ethanol and xylene washes, then coverslipped with VectaMount (Vector Laboratories, Burlingame, CA).

Tissues were graded on a 4 point scale by a pathologist (S.E.P.) in a blinded manner. Sections with no staining were scored as 0, those with less than 10% of cancer cells staining were scored as +1, tissues with 10-50% of the cancer cells staining were scored as +2, and tissues with over 50% of the cancer cells staining were scored as +3. For most of the analysis, the data was binarized to create two groups, where all positive scores (+1, +2, and +3) were grouped together and compared to the negatively scored tissues.

TMA Statistical Analysis

Differential expression for nectin 4 across the histopathological subtypes was assessed with the Pearson Chi-Square statistic. Univariable relapse-free survival for the entire cohort and each histopathologic subtype was examined with Kaplan-Meier survival curves. Results significant in univariable analysis were subjected to multivariable relapse-free survival using the Cox Proportional Hazards test. The level of significance for all comparisons was $p<0.05$. All statistical calculations were computed with JMP v. 6.0.3 (SAS Institute Inc., Carey, NC).

ELISA

A sandwich enzyme-linked immunosorbent assay (ELISA) was used to detect soluble nectin 4 in patients' sera and ascites. Ninety-six well tissue culture plates were coated with 10 µg/mL of mouse anti-human nectin 4 mAb (clone N4.61). After blocking the wells with PBS containing 1% bovine serum albumin (BSA) (R&D Systems), 100 µL of serum or ascites was incubated for 12 hr at 4°C, washed and then 0.5 µg/mL biotinylated goat anti-human nectin 4 antibody was added. Streptavidin-peroxidase in PBS-BSA was incubated for 1 hr at 37°C. One hundred µL of peroxidase substrate was added (One Step ABTS, Pierce) and optical density was read at 405 nm. Three to five wash steps were performed between incubations with PBS containing 0.5% Tween 20. Analyses were done in duplicates. Nectin 4 concentration was calculated using serial dilution of recombinant human nectin 4-Fc protein as previously described (14).

ELISA Statistical Analysis

Serum nectin 4 levels were compared among serous, clear cell, LMP, and benign gynecological disease using the Kruskal Wallis test. Subsequent pairwise comparisons were conducted using the Wilcoxon Rank sum test.

Receiver-operating characteristic (ROC) curves were constructed for nectin 4 alone, CA125 alone, and the combination of CA125 and nectin 4. Youden's index was used to place the optimal threshold point for nectin 4 to distinguish between a serous ovarian cancer mass and benign gynecological disease on the curve; the corresponding sensitivity and specificity of the test was then determined. Exact p-values for the classification table of the test results by the known status were then calculated.

Results

Nectin 4 mRNA is Overexpressed in Ovarian Cancer

When analyzed by RT-PCR, nectin 4 mRNA was present in all five of the serous ovarian cancer tissue samples and absent from all seven normal ovarian tissues (Fig. 1A), confirming our previous microarray data (85). Nectin 4 mRNA was detected in 5 of 13 ovarian cancer cell lines, while none of the eight immortalized NOSE cell lines expressed substantial levels of nectin 4 (data not shown). Expression of nectin 4 in the MCF7 breast cancer cell line was used as a positive control (Fig. 1A). Expression of β-actin in the samples confirmed that mRNA was not degraded and that equal amounts of mRNA were loaded (Fig. 1A).

Quantitative RT-PCR was performed on multiple ovarian cancer and immortalized NOSE cell lines (Fig. 1B). mRNA levels were expressed as a fold-increase over the lowest expressing cell line (1816-575). Levels of nectin 4 mRNA averaged 60-fold higher (range 2.3 – 453.6) in the ovarian cancer cell lines compared to the 1816-575 cell line. In immortalized NOSE cells, nectin 4 mRNA expression averaged only 1.8-fold higher (range 1.5 – 2.8) than the lowest expressing cell line.

Nectin 4 Protein is Overexpressed in Ovarian Cancer

Nectin 4 protein levels in ovarian cancer cell lines were compared to immortalized NOSE cell lines by both Western immunoblotting and flow cytometry analysis. A band of ~66 kDa corresponding to nectin 4 was present in the positive control MCF7 cell extracts (Fig. 2A). Nectin 4 protein was visibly expressed by all thirteen of the ovarian cancer cell lines tested while absent or expressed at very low levels in the five NOSE cell lines tested (Fig. 2A). By FACS analysis, nectin 4 protein was detected on the surface of OVCAR5, C13, and OV2008 ovarian cancer cells, but

not on the immortalized NOSE cell lines HIO117 or 1816-575 (Fig. 2B), confirming our RT-PCR and Western immunoblotting results.

We also investigated the expression of nectin 1 and ADAM17 on these cell lines by flow cytometry. Nectin 1, which can trans-dimerize with nectin 4 on adjacent cells, was present on two of the three ovarian cancer cell lines tested, but not on either of the immortalized NOSE cell lines (Fig. 2B). ADAM17, a metalloproteinase that can cleave the ectodomain of nectin 4 from the surface of the cell, releasing a soluble fragment, was detected on all of the cell lines tested. These results suggest that nectin 4 may be released into the blood of ovarian cancer patients and thus may serve as an accessible biomarker for the disease.

Nectin 4 is Expressed in Ovarian Cancer Patients' Tissues

Immunohistochemical staining of TMAs allowed for simultaneous analysis of 500 patient specimens. Overall, 48.6% of the tissues in the TMA stained positively for nectin 4. Staining was uniformly cytoplasmic with no nuclear staining observed. Nectin 4 protein expression was differentially expressed ($p = 0.008$) across the histological subgroups of ovarian cancer, with the highest expression in endometrioid carcinomas (57.6% of tumors positive), followed by serous (50.5%), clear cell (41.7%), and mucinous (29.0%) (Fig. 3B, Table 1).

Silverberg grade 1 tumors showed a significantly higher percentage of intense nectin 4 staining (i.e. 16% of the grade 1 tumors received scores of +3, compared to only 5% of the grade 2 or grade 3 tumors; $p=.0026$) when positive scores were not binarized (Fig. 3C). However, when binarized as "any staining" vs. "no staining", Silverberg grade 1, 2, and 3 tumors each were approximately 50% positive for nectin 4. Nectin 4 expression was not statistically different for disease stage for any histological subgroups of ovarian cancer when positive scores were binarized (Table 1). Overall, expression of

nectin 4 did not alter relapse-free survival (not shown) or overall survival (Fig. 3D), regardless of subtype, stage, or grade.

Nectin 4 is Elevated in Ovarian Cancer Patients' Serum

Sera from 134 women were analyzed by ELISA to quantify cleaved nectin 4. ROC curves were constructed and Youden's index was used to place the optimal threshold value to distinguish between serous ovarian cancer and benign samples. The threshold value for serum nectin 4 levels was 0 ng/mL; any samples above 0 ng/mL were considered positive and indicative of serous ovarian cancer. Nectin 4 was detected in serum from 53% of patients with serous ovarian cancer, 29% with clear cell, and 16% with benign gynecological diseases. Interestingly, none of the sera samples from patients with LMP tumors demonstrated elevated protein levels. The mean concentration of serum nectin 4 was significantly higher in patients with serous ovarian cancer (3.7 ng/mL) compared to patients with benign disease (0.6 ng/mL) and LMP tumors (0 ng/mL) (Fig. 4A; Table 2, $p=0.001$), but not those with clear cell cancer (0.9 ng/mL). Nectin 4 levels were significantly different among the groups ($p<0.001$) using the Kruskal Wallis test. Subsequent comparisons using the Wilcoxon Rank sum test determined the difference detected was between the serous and both the benign groups and LMP groups.

When 0 ng/mL was used as a threshold value, the area under the curve (AUC) in ROC analysis for serous samples was 68.6% (Fig. 4B; $p= 0.0001$). Nectin 4 was 53% sensitive and had a positive predictive value (PPV) of 77% for serous ovarian cancer, and was 84% specific and had a negative predictive value (NPV) of 64% for benign gynecological disease (Table 2). No associations between stage ($p=0.44$) or grade ($p=0.38$) and nectin 4 concentration were detected.

In the same serous samples, the threshold value for CA125 was 30 U/mL per standard protocol, and the AUC of ROC analysis for CA125 was 66% (Fig. 4B; p=0.0003). While CA125 was more sensitive (92%) in detecting serous ovarian cancer, specificity was reduced greatly at 39% (Table 2). PPV and NPV for CA125 were 60% and 83%, respectively (Table 2). When nectin 4 and CA125 were combined, the AUC for ROC analysis increased to 76% (Fig. 4B; p=0.0013), with a 53% sensitivity and 88% specificity (Table 2). The PPV of the combined markers was 82% and the NPV was 65% (Table 2).

Nectin 4 was detected in all of the serous ovarian cancer ascites fluid samples tested (mean 158 ng/mL; range 13.7 − 270.2 ng/mL). Each of the ten ascites fluid samples had been procured from patients whose corresponding serum samples were also tested by ELISA. Interestingly, only six of the ten sera samples had detectable levels of nectin 4 (range 0 – 31.0 ng/mL). The concentration of nectin 4 was significantly higher in each patient's ascites fluid compared to their sera sample, suggesting that the soluble form of nectin 4 that is being detected by this ELISA may be degraded or cleared from the blood more readily than the ascites fluid.

Discussion

In this study, we have demonstrated increased mRNA and protein expression of nectin 4 in ovarian cancer tissues and cell lines compared to their normal ovarian counterparts using several techniques. These results provide the first validation of our previously published gene microarray data (85). Immunohistochemical staining of TMAs allowed for the study of 500 patients' tissues at one time; overall, 48.6% of the tissues on the TMA stained positively for nectin 4. Early grade tumors had a greater percentage of intensely positive samples (Fig. 3C). This trend toward more intense staining and increased expression in early grade cancers may indicate the feasibility of using nectin 4 to help predict the aggressiveness of ovarian cancer at early time points.

We have also demonstrated that the cleaved ectodomain of nectin 4 can be detected in the sera of ovarian cancer patients. By ELISA, nectin 4 was detected in the serum of 53% of the serous ovarian cancer cases tested. Interestingly, this correlates closely with the TMA results of 50% of serous samples staining positively for nectin 4, indicating that the ELISA may be able to detect all or nearly all positive samples. Using nectin 4 in conjunction with CA125 for the diagnosis of ovarian cancer increases the PPV and specificity compared to CA125 alone, which may help in the triage of patients with a suspicious pelvic mass. One caveat, however, is that ELISA detection of nectin 4 would not distinguish between primary ovarian cancers and primary breast cancers that have metastasized to the pelvic region. However, as breast cancer can be detected by mammogram screening, it should be possible to determine whether a positive ELISA test for nectin 4 is a result of breast or ovarian cancer.

The role of nectin 4 in the development and propagation of ovarian cancer is unknown. The recent discovery of nectin 4 in subsets of breast and lung cancer, along with demonstration that serum levels of nectin 4 correlated with both the number of

metastases and therapeutic efficacy in breast cancer, suggests it may have a conserved role in cancer biology (80, 81).

We identified significantly more patients with elevated serum levels of nectin 4 than had previously been reported (53% vs. 4% by Fabre-Lafay et. al). The reason(s) for the difference in detection rates is unclear, but both case selection and detection bias based on ELISA technique are likely impacting factors. Among the sera samples tested by Fabre-Lafay et. al, only nine were of serous subtype, and these included three low grade tumors. Additionally, we used a different detection antibody for our ELISA, which was more sensitive compared to the previously published ELISA method (data not shown).

Nectin 4 has also been detected in the serum of patients with non small cell lung cancer (NSCLC) (81). Takano et. al developed an ELISA using different monoclonal antibodies against nectin 4 and established a threshold value of 1.0 ng/mL for serum nectin 4 in a panel of normal, chronic obstructive pulmonary disease, and NSCLC patients. They found that high serum nectin 4 levels correlated with poor survival in the NSCLC patients. Additionally, expression of nectin 4 increased lamelliopodia formation, resulting in an increase in invasive potential in lung cancer cell lines, while siRNAs directed against nectin 4 suppressed cell growth.

Besides modulating growth and invasive potential, expression of nectin 4 may increase the survival of ovarian cancer cells when treated with chemotherapeutic agents. Ovarian cancer cells often form spheroids that appear more resistant to chemotherapy; nectin 4 is important in cell-cell adhesion, and spheroids formed from nectin 4 expressing cells may be better able to exclude chemotherapy agents from the cells in the center of the spheroid, promoting resistance. Thus, in addition to determining expression of nectin 4, we also investigated expression of nectin 1 on ovarian cancer cells and immortalized NOSE cells. Nectin 1 was present on two of the three ovarian

cancer cell lines tested. Nectin 4 interacts in trans with either nectin 1 or nectin 4 on adjacent cells. Trans-heterophilic interactions between nectin 1 and nectin 4 are stronger than trans-homophilic interaction; ovarian cancer cells expressing both nectin 1 and nectin 4 may be able to form compact, tight spheroids that aid in survival due to decreased chemosensitivity (113, 114).

Why nectin 4 is shed from the surface of cells remains unknown, and functionality studies were beyond the scope of this study. However, given the apparent relationship between nectin 4 expression and metastases in breast and lung cancers, multiple hypotheses can be considered. It is possible that increased expression of nectin 4 contributes to the formation of ovarian cancer spheroids, which in turn have been demonstrated to be relatively chemotherapy resistant. Reversal of this phenotype may occur once the cells come in contact with an appropriate metastatic site, whereby nectin 4 may be cleaved from the surface, allowing for the cells to better attach to and invade the site. In this study, ADAM17, a metalloproteinase that cleaves the ectodomain of nectin 4 from the cell surface, was detected on ovarian cancer cell lines. The presence of ADAM17 on the ovarian cancer cell surface increases the possibility that nectin 4 may be shed from the cell surface and then be detectable in the ascites fluid or blood of ovarian cancer patients.

We have described the first comprehensive study of the expression of nectin 4 in ovarian cancer. Nectin 4 is overexpressed at both the mRNA and protein level in ovarian cancers and rarely overexpressed in healthy non-pregnant patients, suggesting potential use as a serum biomarker (71). As with most biomarkers, nectin 4 was not able to detect all ovarian cancers. However, several patients with benign gynecological disease and high CA125 levels had no detectable levels of serum nectin 4, leading to an increase in specificity over CA125 alone. This indicates that nectin 4 may help discriminate ovarian

cancer from benign disease when used in conjunction with CA125 in a panel for diagnosis. Identification of a complementary biomarker detecting nectin 4 negative tumors could greatly increase the sensitivity, resulting in improved diagnosis. Functional studies are needed to fully determine the impact of nectin 4 expression on ovarian cancer progression.

Figure 3-1. Nectin 4 gene overexpression in ovarian cancer. A) RT-PCR of nectin 4 in ovarian cancer (C1-C5) and normal ovarian tissue (N1-N7). MCF7 cell line, positive control. – RT, no reverse transcriptase; - RNA, no RNA. B) qRT-PCR analysis of nectin 4 expression in immortalized NOSE and ovarian cancer cell lines. Results expressed as fold-change compared to the lowest expressing cell line (1816-575). *, OVCAR3 mRNA was 454-fold increased over the lowest expressing cell line.

Figure 3-1

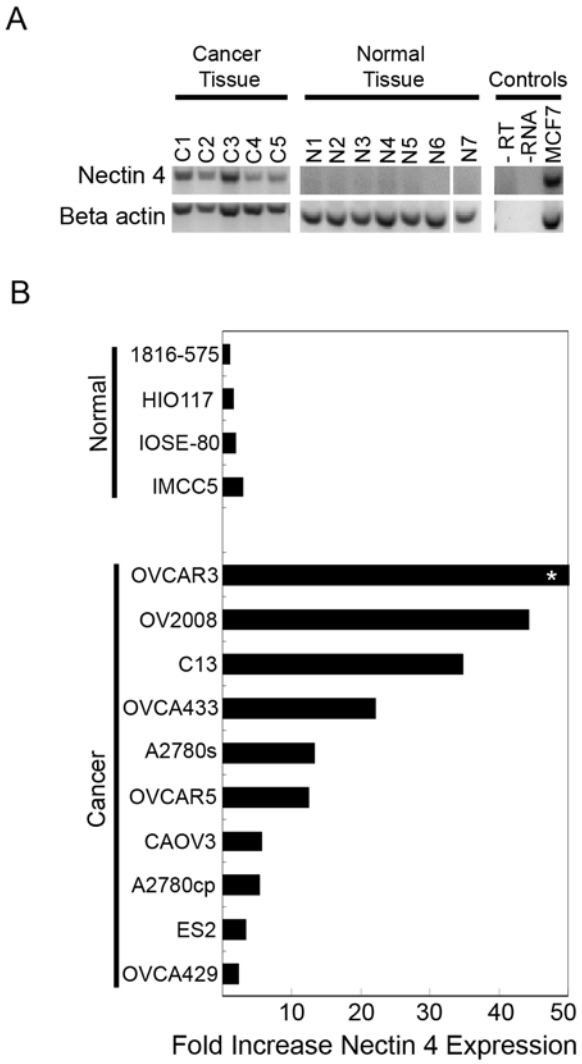
A
Cancer Tissue
Normal Tissue
Controls
C1
C2
C3
C4
C5
N1
N2
N3
N4
N5
N6
N7
- RT
-RNA
MCF7
Nectin 4
Beta actin
B
Normal
1816-575
HIO117
IOSE-80
IMCC5
Cancer
OVCAR3
*
OV2008
C13
OVCA433
A2780s
OVCAR5
CAOV3
A2780cp
ES2
OVCA429
10
20
30
40
50
Fold Increase Nectin 4 Expression

Figure 3-2. Nectin 4 protein expression in ovarian cancer. A) Western immunoblotting of ovarian cancer cell lines and immortalized NOSE cell lines. Nectin 4 appears as a ~66 kDa band. B-actin was used as a loading control. B) FACS analysis of ovarian cancer and immortalized NOSE cell lines for nectin 4 (top row), nectin 1 (middle row), and ADAM17 (bottom row). Dashed line, IgG control stain; solid line, nectin 4, nectin 1, or ADAM17.

Figure 3-2

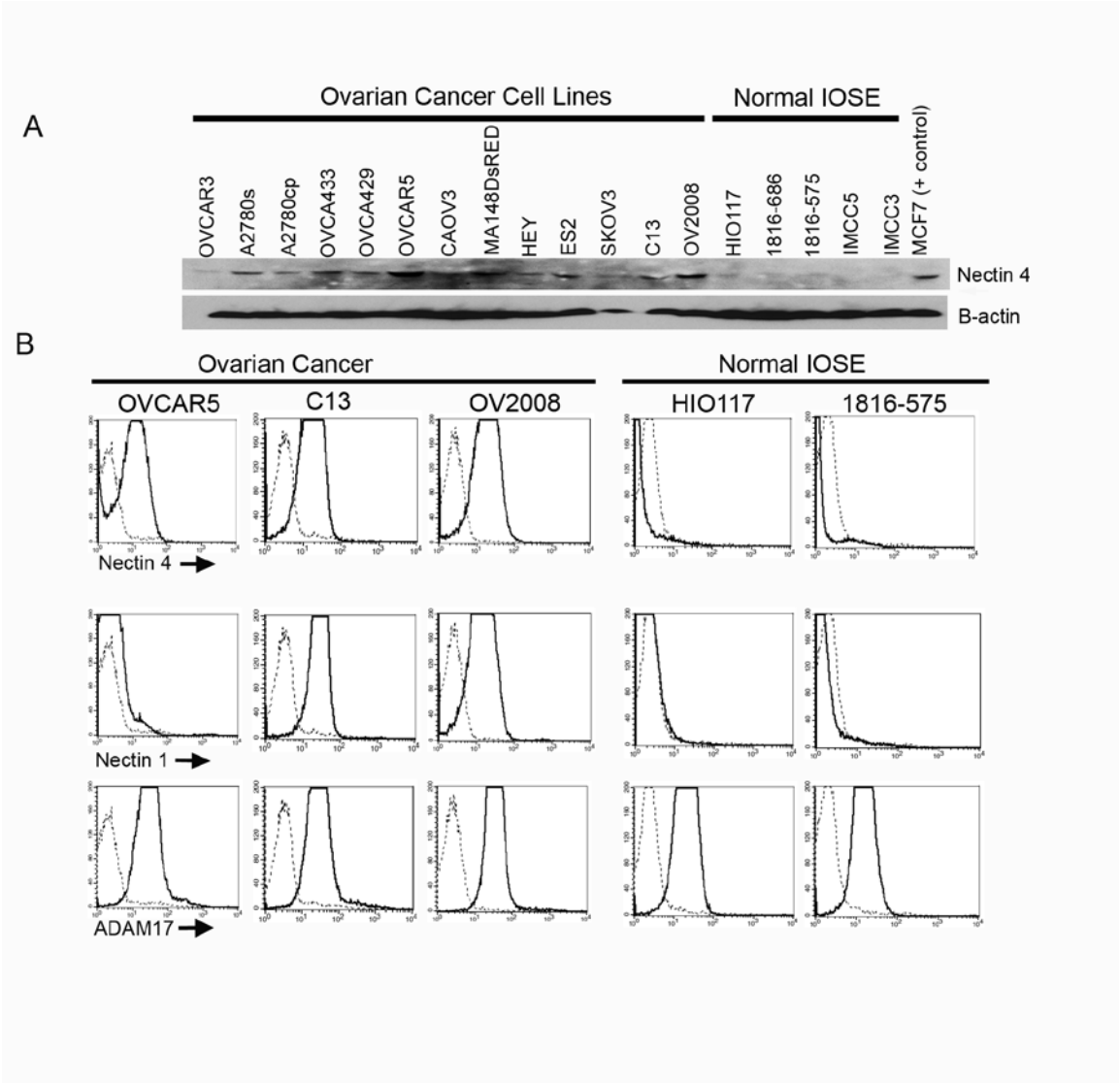
A
Ovarian Cancer Cell Lines
Normal IOSE
OVCAR3
A2780s
A2780cp
OVCA433
OVCA429
OVCAR5
CAOV3
MA148DsRED
HEY
ES2
SKOV3
C13
OV2008
HIO117
1816-686
1816-575
IMCC5
IMCC3
MCF7 (+ control)
Nectin 4
B-actin
B
Ovarian Cancer
Normal IOSE
OVCAR5
C13
OV2008
HIO117
1816-575
Nectin 4
Nectin 1
ADAM17

Table 3-1. Subtype, stage, Silverberg grade, and Nectin 4 score of tissue microarrays.

Subtype	Median Age (range)	Median PreOP* CA125 (range)	Stage	N	Nectin 4 Positive	Silverberg grade	N	Nectin 4 Positive	Nectin 4 Positive Overall
Serous (n=212)	59.6 (33.5 – 86.0)	108 (0 – 23,000)	I	50	29 (58.0%)	1	12	4 (33.3 %)	107 (50.5 %)
			II	93	47 (50.5%)	2	56	30 (53.6%)	
			III	69	31 (44.9%)	3	144	73 (50.7%)	
Endometrioid (n=125)	54.1 (29.4 – 88.1)	130 (8 – 13,000)	I	69	40 (58.0 %)	1	82	49 (59.8 %)	72 (57.6 %)
			II	50	29 (58.0%)	2	35	19 (54.3%)	
			III	6	3 (50.0%)	3	8	4 (50.0%)	
Clear Cell (n=132)	55.0 (28.1 – 89.0)	64 (4 – 7,750)	I	68	34 (50.0%)	1	0†	N/A	55 (41.7 %)
			II	56	17 (30.4%)	2	0†	N/A	
			III	8	4 (50.0%)	3	132	55 (41.7 %)	
Mucinous (n=31)	56.4 (25.4 – 76.7)	45 (7 – 650)	I	18	6 (33.3%)	1	11	2 (18.2%)	9 (29.0%)
			II	12	2 (16.7%)	2	18	6 (33.3%)	
			III	1	1 (100%)	3	2	1 (50.0%)	
Total (n=500)	56.6 (25.4 – 89.0)	98 (0-23,000)	I	205	109 (53.2 %)	1	105	55 (52.4%)	243 (48.6%)
			II	211	95 (45.0 %)	2	109	55 (50.4%)	
			III	84	39 (46.4%)	3	286	133 (46.5%)	

*PreOp, preoperative

†All clear cell carcinomas are considered grade 3 (high grade)

Figure 3-3. Immunohistochemical staining for nectin 4 of ovarian cancer tissue microarrays. A) Staining and grading examples of TMA samples. IgG, control primary stain. +1, <10% of cancer cells staining; +2, 10-50% of cancer cells staining; +3, >50% of cancer cells staining. B) Percent of TMA cases positive for nectin 4 by ovarian cancer subtype. C) Percent of TMA cases positive for nectin 4 by Silverberg grade. D) Kaplan-Meyer survival curve of TMA patients measured in days. Red, staining score 0. Green, staining score +1. Blue, staining score +2. Orange, staining score +3.

Figure 3-3

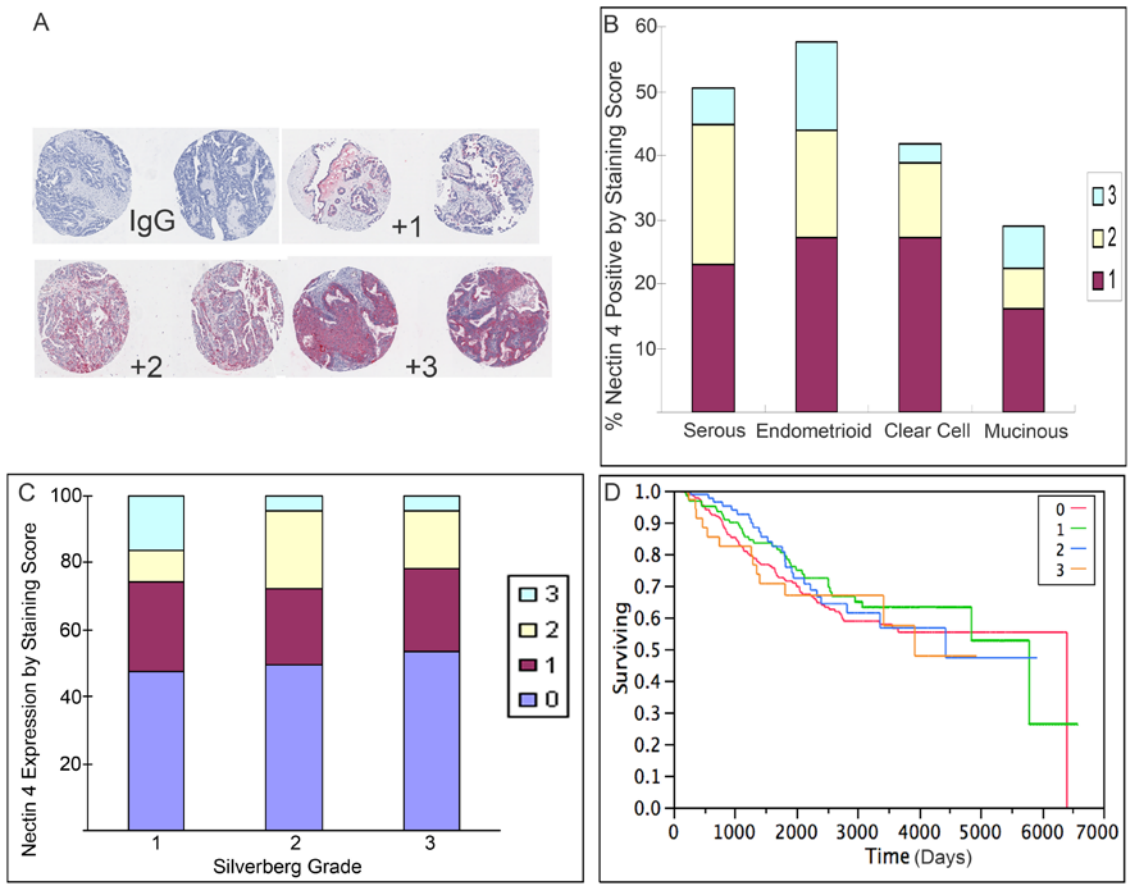
A
IgG
+1
+2
+3
B
% Nectin 4 Positive by Staining Score
Serous
Endometrioid
Clear Cell
Mucinous
C
Nectin 4 Expression by Staining Score
Silverberg Grade
D
Surviving
Time (Days)

Figure 3-4. Nectin 4 ELISA analysis. A) Serum nectin 4 levels (ng/ml) separated by diagnosis. B) ROC curves for nectin 4 alone (dash-dot line), CA125 alone (dashed line), or nectin 4 and CA125 combined (solid line).

Figure 3-4

A

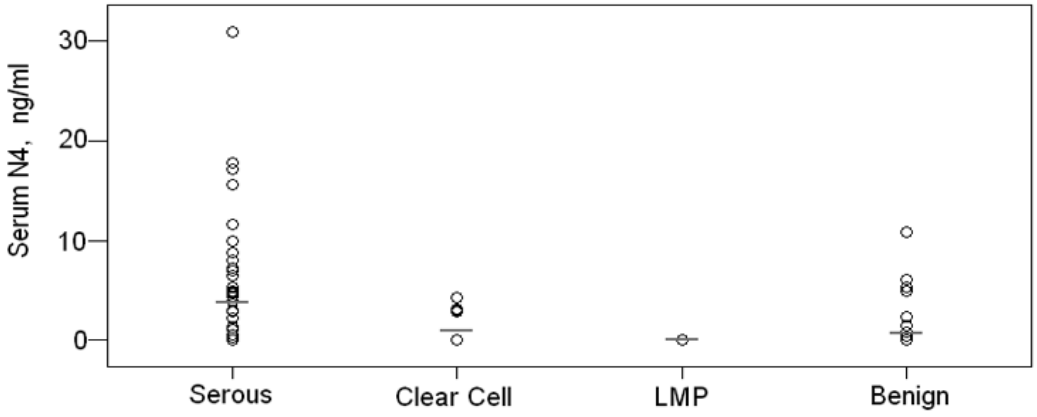
Serum N4, ng/ml
30
20
10
0
Serous
Clear Cell
LMP
Benign

B

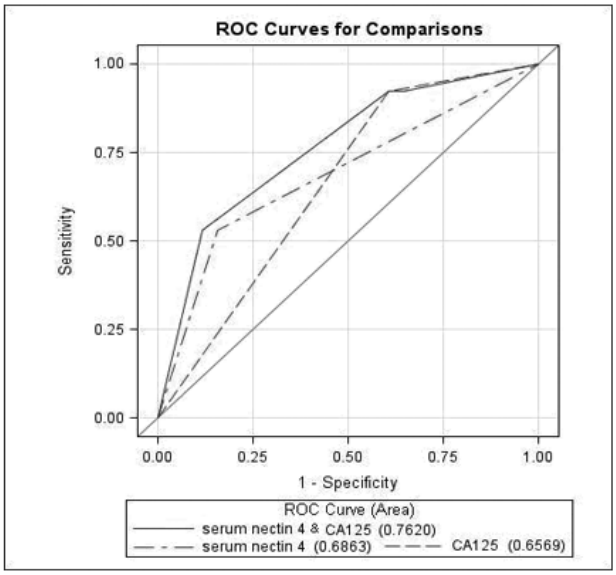
ROC Curves for Comparisons
Sensitivity
1.00
0.75
0.50
0.25
0.00
0.00
0.25
0.50
0.75
1.00
1 - Specificity
ROC Curve (Area)
serum nectin 4 & CA125 (0.7620)
serum nectin 4 (0.6863)
CA125 (0.6569)

Table 3-2. Nectin 4 ELISA analysis of patient serum samples.

Diagnosis	N	# Positive*	Mean N4, ng/ml	Mean CA125, U/ml	Sensitivity	Specificity	PPV†	NPV‡
Serous			3.7	2,246.2				
N4	51	27	(0 – 31.0)	(6 – 22,780)	53		77	
CA125	51	47			92		60	
N4/CA125	51	27			53		82	
Clear Cell			0.9	222.6				
N4	14	4	(0 – 4.2)	(13 – 1,504)	29		33	
CA125	14	11			79		26	
N4/CA125	14	3			21		33	
LMP§			0	264.6				
N4	18	0	(0 – 0)	(6.6 – 1,539)		100		43
CA125	18	14				22		50
N4/CA125	18	0				100		43
Benign			0.7	151.4				
N4	51	8	(0 – 10.9)	(4 – 1,984)		84		64
CA125	51	31				39		83
N4/CA125	51	6				88		65

*****Number positive, nectin 4 (N4) positive, CA125 positive, or both nectin 4 and CA125 positive
†PPV, positive predictive value
‡NPV, negative predictive value
§LMP, low malignant potential

Chapter 4

Functional impact of nectin 4 expression

Abstract

Increased expression of proteins in cancer typically imparts an advantage for the growing tumor. Increased proliferation, freedom from normally required growth factors, and resistance to apoptosis, senescence, and chemotherapy are examples of processes that may occur due to disregulation of gene expression. Determining how disregulated proteins affect tumor progression can help define targets for therapy.

Nectin 4 is a protein recently shown to be highly expressed in breast and lung cancer subsets (80, 81). Takano et. al determined that expression of nectin 4 in lung cancer cell lines increased proliferation both *in vitro* and *in vivo* (81). We recently described that nectin 4 is overexpressed in ovarian cancer. To further our understanding, we performed several experiments to determine how expression of nectin 4 in ovarian cancer cell lines affects proliferation, sensitivity to chemotherapy, spheroid formation, and invasion of mesothelial cell monolayers.

Introduction

Overexpression of proteins in cancer usually results in a functional advantage for the growing tumor. Defining what advantage the proteins impart can help elucidate pathways and targets that may be potential targets for therapy. Nectins play key roles in the formation of AJs and the integrity of epithelial cell layer polarity (61, 63, 65, 108, 109, 111). Nectin 3 has also been shown to be important in cell migration (111, 115).

Because the only expression of nectin 4 in normal tissue is in the placenta, a limited understanding of its function is known (71, 79). Recently, however, two separate studies describing expression of nectin 4 in breast cancer and lung cancer have been published; both detail how expression of nectin 4 resulted in decreased survival (80, 81). However, only one reported on the possible advantages that expression of nectin 4 may impart to growing tumors. Takano et. al determined that expression of nectin 4 in lung cancer cells increased proliferation and invasion in *in vitro* cell cultures. Additionally, when injected into mice, tumors formed by nectin 4 expressing cells grew more rapidly than control cells (81).

We previously described overexpression of nectin 4 in ovarian cancer and determined that it was possible to detect shed nectin 4 in the sera of ovarian cancer patients. We wanted to expand our studies to understand what functions nectin 4 has in the progression of ovarian cancer.

Materials and Methods

Chemicals and Reagents

Cell culture reagents were purchased from Invitrogen (Carlsbad, CA). All chemicals were purchased from Sigma Chemical (St. Louis, MO) unless otherwise stated.

Cell Culture

MA148DSRed2 cells (provided by Dr. Sundaram Ramakrishnan, University of Minnesota) and Met5a mesothelial cells (provided by Dr. Faris Farassati, University of Minnesota) were grown in RPMI 1640 supplemented with 10% FBS and penicillin/streptomycin. Cells were routinely subcultured using trypsin and incubated in a humidified chamber at 37°C.

Cloning and transfection of full length nectin 4

Full length nectin-4 was amplified by Touchdown RT-PCR from SKOV3 mRNA using the following primers: Forward 3' GCGA ATTC ATGC CCCT GTCC CTGG GAGC CGAG ATG 5', and Reverse 3'CGTC TAGA TCAG ACCA GGTG TCCC CGCC CATT GATG 5'. Full-length nectin-4 was cloned into the pCR2.1-TOPO vector and transformed DH5α *E. coli*. Sequencing confirmed the full length sequence was present, but in reverse orientation.

For subcloning into the expression plasmid pcDNA3.1(+), the sequence was reversed by cutting pCR2.1 TOPO:Nectin 4 with HindIII (New England Biolabs, Ipswich, MA) according to the manufacturer's instructions. The sticky ends were then blunted by extension with DNA polymerase I, Large (Klenow) Fragment (New England Biolabs). The target vector pcDNA3.1(+) was digested with XbaI (New England Biolabs) and the sticky ends were blunted as above. Cut plasmid DNA was purified by phenol/chloroform

extraction and dissolved into Tris-EDTA buffer. Both pCR2.1 TOPO:Nectin 4 and pcDNA3.1(+) were then digested in separate reactions with NotI (New England Biolabs) according to the manufacturer's instructions. Reactions were run on an agarose gel and the nectin 4 insert and linearized pcDNA3.1(+) plasmid bands were extracted from the gel using the QIAquick Gel Extraction kit (Qiagen, Valencia, CA) according to the manufacturer's instructions. Ligation of the nectin 4 fragment with the linearized pcDNA3.1(+) plasmid was performed by incubation with T4 DNA ligase (New England Biolabs) according to the manufacturer's instructions. Ligated samples were transformed into DH5α E. coli (Invitrogen) per the manufacturer's instructions. Colonies were selected and grown in luria broth overnight, and then plasmid DNA was isolated using the QIAgen Plasmid Purification kit (Qiagen) according to the manufacturer's instructions.

Correct, full-length sequence was verified both by restriction digest and by sequencing through the BioMedical Genomics Center using the T7 forward and BGH reverse primers. Sequence was compared to the NCBI reference sequence NM_030916.2.

MA148DSRed2 cells were transformed with nectin 4 containing or empty vector pcDNA3.1 (+) using Lipofectamine 2000 (Invitrogen) per the manufacturer's instructions. Stable transfectants were selected in media supplemented with 800 ug/ml G418 according to manufacturer's instructions. Cells were analyzed by flow cytometry to determine expression of nectin-4 after transformation.

Proliferation

Cells were seeded into 96-well tissue culture treated plates (Corning Inc. Life Sciences, Lowell, MA) at 2.5 x 10^5 cells/ml in 200 ul media containing low serum (2% FCS). Cells were grown for 24 or 48 hours, then 3-(4,5-dimethylthiazol-2-yl)-2,5-

diphenyltetrazodiom bromide (MTT) assays were performed to determine proliferation. Twenty-five ul per well of 5 mg/ml MTT in PBS was filtered and added to each well being tested. Plates were incubated for 3 hours at 37°C, and then the media/MTT was removed and replaced by 60 ul/well of a 1:1 mixture of dimethyl sulfoxide and isopropanol. Plates were incubated for 30 minutes at 37°C, and then absorbance was read at 570 nm and 660 nm. Absorbance at 660 nm was subtracted from the absorbance at 570 nm. Each cell type was plated a minimum of 20 times per plate, and the average of the wells was used to compare values between nectin 4 negative and expressing cells. Experiments were performed in triplicate. Statistically significant differences were determined by two-tailed t-tests with a p value of ≤ 0.05 considered significant.

Cytotoxicity Test

Cells were seeded into 96-well tissue culture treated plates (Corning Inc. Life Sciences) at 3.75 x 10^5 cells/ml in 200 ul media with 10% FCS. Cell were allowed to adhere for 2 hours, then the media was removed and replaced with fresh low serum (2% FCS) media containing increasing amounts of cisplatin or taxol. Cells were incubated at 37°C for 24 or 48 hours, and then an MTT assay was performed as described above.

Spheroid Formation

Spheroids were formed in either 6-or 96-well tissue culture treated plates (Corning Inc. Life Sciences) with a 1:1 mixture of 1% SeaKem agarose (Lonza, Rockland, ME) and RPMI. Cells were trypsinized, spun down, and resuspended in full media, then strained through a 70 um cell strainer (Falcon) to ensure single cell suspensions. Cells were counted and then added to the wells (30,000 cells/well in 2 ml media for a 6-well plate; 5,000 – 10,000 cells per well in 200 ul media for a 96-well plate) and allowed to

incubate at 37°C overnight. Spheroids were used the following day for assays.

Single Cell Attachment to Mesothelial Cells

Met5a mesothelial cells were grow to confluency in 96 well tissue culture plates. MA148DSRed2 cells expressing empty vector or nectin 4 were stained red using CellTracker Red according to the manufacturer's instructions (Invitrogen). Single cell suspensions of cells (500 cells/0.1 ml/well) were added to the confluent mesothelial cell monolayers and allowed to attach for 2.5 hours. Unattached cells were gently washed away 3 times then media was replaced. Pictures were taken of 5 random areas per well and the number of attached cells was counted manually. Two-tailed t-tests were performed to determine significance with a $p=0.05$ value considered significant.

Spheroid Adhesion and Invasion Assay

Met5a mesothelial cells were plated in 48-well tissue culture plates, allowed to grow to confluency for 48 hours, and then stained with CellTracker Green (Invitrogen) per the manufacturer's instructions. Spheroids were made as described above except that immediately prior to adding cells to the agar coated wells, the cells were stained with CellTracker Red per manufacturer's instructions (Invitrogen). One spheroid was added per well and allowed to attach and invade the mesothelial cell layer. Pictures were taken at 4, 24, 48, and 96 hours after addition of the spheroids.

The areas of both the spheroid and the cleared area of mesothelial cells were assessed in Adobe Photoshop. The area was determined by outlining either the spheroid or the cleared area and determining the number of pixels.

Spheroid Cytotoxicity Assay

Spheroids were formed as described above for 24 hours. Cisplatin (3-20 uM) or a vehicle control (saline) was added to the media in the wells and the spheroids were allowed to incubate for an additional 48 hours. 2-(4-Iodophenyl)-3-(4-nitrophenyl)-5-(2,4-

disulfophenyl)-2H-tetrazolium, monosodium salt (WST-1) (Boehringer-Mannheim Corporation, Indianapolis, IN) was added to each well and incubated for 2 hours at 37C. The formazan dye product produced by live cells metabolizing WST-1 was quantified by spectrophotometer absorbance readings at 450 nm. Experiments were performed in duplicate.

In Vivo Assay of Tumorogenesis

Eight week old female Harlan-Sprague Dawly athymic nude mice ($Foxn1^{nu}$; Harlan Laboratories; Indianapolis, Indiana) were injected intraperitoneally with 2.0×10^6 cells in 0.5 ml in serum-free RPMI. Fifteen mice were injected with MA148DSRed2:Empty vector (EV) cells; 16 mice were injected with MA148DSRed2:Nectin 4 (N4) cells. Mice were inspected daily for signs of distress and/or apparent tumor growth. Mice were imaged weekly for the presence of tumor, identified by expression of DSRed2 protein. Imaging was performed using the CRi Maestro *in vivo* imaging system. Mice were anesthetized using isoflurane and imaged in groups of two or three. Both white light and fluorescent images were acquired. Mice were placed under a warming lamp and monitored for recovery from anesthesia then returned to their cages.

Three mice per group (3 N4, 3 EV) were euthanized by CO_2 asphyxiation at certain time points (2, 3, 4, 6, 8, and 9 weeks post injection). One mouse was euthanized at week 7 due to distress due to tumor burden (the abdomen was greatly enlarged due to tumor burden and thus the mouse had poor mobility).

Necropsies were performed on all mice. Blood was collected by cardiac puncture, and then spun in a microfuge to separate sera from the cells. Sera were stored at -85°C. If present, ascites was collected and the supernatants stored at -85°C. Tissues were harvested (lungs, liver, spleen, kidneys, bowel, ovaries, and uterus) and fixed in 10% neutral buffered formalin, then stored at 4°C. Ovaries and spleens were measured in

three dimensions using calipers to determine volume. Weight of the organs was also recorded.

Some tissues were processed into FFPE blocks for analysis of micrometastases by hematoxylin and eosin staining.

Results and Discussion

Describing how overexpressed proteins in cancer facilitate tumor progression can help determine potential targets for therapy. Previously, nectin 4 has been shown to increase proliferation and invasion in lung cancer (81). In these studies, we sought to determine if nectin 4 functioned in a similar manner in ovarian cancer, as well as if nectin 4 could influence spheroid formation, invasion, and survival after treatment with chemotherapeutic drugs.

To answer these questions, I first cloned full-length nectin 4 into the pcDNA3.1(+) expression vector (Fig. 4-1A). After confirmation of full-length correct sequence through restriction digest and DNA sequencing, I transfected both the nectin 4 expressing (MA148DSRed2:N4) and the empty pcDNA3.1(+) (MA148DSRed2:EV) into MA148DSRed2 cells using Lipofectamine. Cells were selected in regular media with the addition of G418 to kill non-transfected clones. A population of cells after transfection was positive for nectin 4 expression by flow cytometric analysis (Fig. 4-1B) and the correct molecular weight was demonstrated by Western immunoblotting (not shown). For further studies, these cells were sorted for expression of DSRed 2 and nectin 4 on a FACS Aria cytometer by the Flow Cytometry Core Facility and the Masonic Cancer Center (data not shown).

I next sought to determine whether expression of nectin 4 would affect proliferation; to that end, I performed MTT assays. Initially I tried the assay using the standard media containing 10% FCS and various concentrations of cells (500-2.5x10^5 cells/well) and saw no difference in proliferation at either 24 or 48 hours. Lower concentrations of cells (below 2x10^5 cells/well) did not proliferate as well, thus for all future experiments I used 2.5x10^5 cells/well. I next investigated whether performing the assay in low serum, which can mimic the stress of low nutrient availability in cancer,

would result in different proliferation rates. In the first series of experiments, I plated cells in decreasing amounts of serum (5%, 2%, 1%, 0.5%, and 0.1% FCS) for an MTT assay. Cells were incubated for 24 or 48 hours, and then an MTT test was performed. The greatest difference in proliferation between nectin 4 positive and empty vector control cells occurred when cells were plated at 2% serum for 48 hours (Fig. 4-2). In the second series of experiments, I tested the cells' ability to attach to tissue culture plates when incubated in various concentrations of serum. Equal numbers of cells ($2.5x10^5$ cells/well, MA148DSRed2:N4 and MA148DSRed2:EV) were plated in 12-well tissue culture plates in increasing amounts of serum (0.1%, 0.5%, 1%, or 10%) and incubated overnight or for 48 hours (Fig. 4-3). Both empty vector and nectin 4 cells were able to attach to the plates at all concentrations tested, however, there was a noticeable decrease in the number of cells adhering after incubation in all concentrations that were ≤ 1% FCS. The experiment was repeated using higher concentrations (2%, 4%, and 5% FCS); serum concentrations of 2% allowed for proliferation of cells at a similar level as 10% serum. Based on these two series of experiments, I chose to use 2% FCS and 48 hours time point for future proliferation and cytotoxicity assays.

Expression of nectin 4 significantly increased proliferation over 48 hours (Fig. 4-4, $p>0.001$), which may promote tumor progression *in vivo*. Proliferation was increased in nectin 4 expressing cell lines at 24 hours in preliminary experiments as well. However, the difference was more dramatic at 48 hours, and thus after the preliminary experiments, I chose to use 48 hours as the sole time point.

Expression of adhesion molecules such as nectin 4 could help maintain epithelial cell layer integrity and prevent or minimize the uptake of chemotherapeutic agents. Thus, I next investigated whether expression of nectin 4 influenced the sensitivity of cells following treatment with cisplatin and taxol. No difference in survival in nectin 4 or empty

vector control cells grown in monolayers and treated with cisplatin was evident after 24 or 48 hours (Fig. 4-5). At low concentrations of taxol (2 – 3 nM taxol), no difference in survival was observed between the nectin 4 and empty vector control cells (Fig. 4-6). However, at higher concentrations (4 – 15 nM taxol), cells expressing nectin 4 were significantly more sensitive. This was unexpected, as nectins are important components in AJ and thus help organize and maintain the integrity of epithelial cell layers. Taxol functions by causing the polymerization of microtubules during M phase in the cell cycle. As nectin 4 expression is associated with increased proliferation rate, it is possible that nectin 4 expressing cells are more sensitive because more of the cells are in M phase at any given time.

Nectins form trans-dimers between cells and this may aid in the first steps of metastasis by adhering to mesothelial cells lining the peritoneal cavity. To determine if expression of nectin 4 increased attachment to mesothelial cells, I added single cell suspensions of empty vector or nectin 4 expressing cells to confluent layers of Met5a mesothelial cells. After incubation for 2.5 hours, non-attaching cells were washed away, pictures of 5 random areas per well were taken and attached cells were counted manually. No difference was seen in attachment to mesothelial cells when cells expressed nectin 4 (not shown, $p=0.168$).

To determine if nectin 4 expression aids the formation of spheroids, I plated nectin 4 expressing and empty vector control cells in tissue culture plates with an agar and media mixture coating the bottom of the wells to prevent attachment and monolayer growth. Originally I tried various concentrations of cells (500-50,000 cells/well) in 6-, 24-. or 96-well tissue culture plates. Multiple small spheroids per well were formed in 6-well plates, while a single, large spheroid was formed in both 24- and 96-well plates. Because I wanted to add just one spheroid per well and I wanted the spheroids to be as

uniform of size as possible, I chose to use spheroids formed in 96-well plates for adhesion studies. At three and five hours, the nectin 4 expressing cells attached to each other more so than the empty vector control cells (Fig. 4-7). However, by 24 hours both control and nectin 4 cells formed spheroids similarly well (Fig. 4-7). Whether this would have any influence in disease progression is unclear. Ovarian cancer spheroids have been postulated to increase chemoresistance to standard chemotherapy agents. It is possible that slower formation of spheroids could result in more sensitivity to chemotherapy; however, as most ovarian cancers are diagnosed at late stages when spheroids have already formed, the contribution to chemoresistance may be minimal.

Trans-dimerization of nectins with mesothelial cells may aid in attachment and invasion. To study this interaction, I plated Met5a mesothelial cells; once confluent, I stained them with CellTracker Green. Ovarian cancer spheroids were formed as described above with the exception that cells were stained with CellTracker Red. One spheroid was added per well to the mesothelial cells and allowed to attach. Pictures were taken at various time points; the differential staining allowed for discrimination of both cell types (mesothelial and ovarian cancer) in a single field of view. The area of the spheroid and the area of invasion into the mesothelial cells could then be measured in Adobe Photoshop. When determining invasion into mesothelial cell monolayers, it subjectively appeared that the spheroids composed of nectin 4 cells stayed more compact and did not spread out as much as empty vector control cells (Fig. 4-8). However, due to large variances in the sizes of the spheroids, there was no statistically significant difference. We also investigated whether mesothelial cell lines (LP9 and Met5a) express either nectin 1 or nectin 4 to aid trans-dimerization. By FACS analysis, neither of the mesothelial cell lines expressed nectin 1 or nectin 4, supporting our earlier results that nectin 4 expression on cancer cells does not enhance attachment to

mesothelial cells.

Formation of spheroids in ovarian cancer may decrease the sensitivity of cells to chemotherapy by preventing chemotherapeutic agents from accessing the cells in the center of the spheroid. Nectin 4 spheroids qualitatively appeared to stay more compact; thus, we hypothesized that nectin 4 may influence the sensitivity of the cells to chemotherapeutic agents. We found that expression of nectin 4 did not alter the sensitivity of spheroids to cisplatin (Fig. 4-9. However, both nectin 4 and empty vector control spheroid cultures were less sensitive to cisplatin compared to their corresponding monolayer cultures (Fig. 4-3 vs. Fig. 4-9).

While tissue culture is a useful tool for determining the effects of protein expression, it does not always recapitulate disease in an animal. Differences in tissue culture may not occur in *in vivo* models and vice versa. Thus, the use of animal models is important to understand disease progression. To this end, we used a previously described model of ovarian cancer in athymic, nude mice (88). Two groups of mice were formed, those injected intraperitoneally with MA148DSRed2 cells expressing nectin 4 or empty vector control plasmid. Every week for nine weeks, the mice were imaged for tumor development. At various time points, three mice from each group were euthanized and blood, ascites fluid, and tissues were collected. Mice from both groups had micrometastases of tumor growth by two weeks (1 nectin 4 mouse, 2 EV mice) as determined by hematoxylin and eosin staining of FFPE tissue samples. By three weeks after injection, the 3 EV mice sacrificed and 2 of 3 nectin 4 mice sacrificed had micrometastases on the ovarian surface. Three nectin 4 mice and two EV mice sacrificed 4 weeks after injection had detectable tumors by hematoxylin and eosin staining. Tumors were not visible by imaging until week 3 (Fig. 4-10). At week 4, some tumors were visible at the time of necropsy in some mice. Metastases were found in the

liver, kidneys, intestine, omentum, as well as implants of tumor at the injection site (Table 4-1). No clear difference between mice receiving N4 or EV cells was evident in regards to the number of mice forming tumors, tumor formation time, size of tumors, or site of tumor implantation. It remains to be seen whether this will be a useful model in the future. Analysis of serum levels of nectin 4 in the future may help determine what size of tumor is needed to detect serum nectin 4; this may help determine whether nectin 4 could be useful at detecting small, early stage tumors.

I tried several other techniques to discern the impact of nectin 4 expression in ovarian cancer cells. However, due to technical difficulties, the results were not suitable for analysis and interpretation. Three techniques in particular I will describe further here.

In an attempt to see if expression of nectin 4 altered migration of cells, I tried three different experiments: scratch assays, Boyden chamber assays and single cell tracking. Scratch assays were performed by using a p10 pipet tip to scratch a line through a confluent monolayer of either empty vector or nectin 4 expressing cells. While simple in procedure, the MA148DSRed2 cells are tightly associated once confluent. This resulted in the scratched edges becoming unattached and eventually the remaining cells would detach from the surface, making analysis impossible. Several modifications were tried (coating the tissue culture vessel with fibronectin, nectin 1, or nectin 4, and scratching cells that are ~80% confluent), however none of these were able to keep the cells attached. Another trouble with analysis of scratch assays is that proliferation could be mistaken for migration. As the nectin 4 expressing cells proliferate more, it would be difficult to discern if a narrowing of the scratched area is a result of migration or proliferation.

For the above reasons, I next tried Boyden chamber assays. I had difficulties in loading the top layer of media with cells without air bubbles in the wells. I tried various

different methods, including different pipet tips, angling the pipet tips, and adding the media either slowly or quickly, but no method consistently produced wells without air bubbles. Air bubbles between the porous membrane and the media containing the cells prevented cells from migrating in control wells (10% FCS in the bottom wells, 2% FCS in the top wells). Thus, the results from these experiments could not be analyzed.

I also had several problems with single cell tracking of cells. In general, single cell suspensions were added to 8-well chamber slides and allowed to attach overnight. The following day, the chamber slides were incubated on a heated stage of the Yee lab microscope. Three to five areas of interest (areas with several single cells visible) were found and pictures of each area were taken every 10 minutes for 24 hours. I tried various experimental setups, including coating the chamber slides with nectin 1, nectin 4, fibronectin, or leaving them uncoated. Several occurrences made the data unusable, however. During one run, the computer rebooted after automatically installing safety updates during the middle of the incubation. Another time the table on which the microscope was set was bumped, and the pictures acquired were all off center after that time point, making it impossible to accurately determine the distance the cells moved. When I tried coating the wells with nectin 1 or nectin 4, I used commercially purchased protein (AbNova, Taiwan). However, they were only partial recombinant proteins and did not include the entire X domain required for transdimerization. Collectively, the results were not able to be used or interpreted with any confidence.

I also used shRNA clones (Open BioSystems, Huntsville, AL) directed at nectin 4 to knock down expression of nectin 4 in ovarian cancer cell lines naturally expressing it (C13, OV2008). Five clones (#23-27) were purchased, but only two (#23, #26) knocked down expression by RT-PCR analysis (42% and 30% of original expression, respectively). I transfected both of these shRNA clones into C13 and OV2008 cell lines

and selected for expression by antibiotic resistance (puromycin). Using both shRNA clones did not alter the expression of nectin 4 RNA more than the single clones alone. I did not have time to verify decreased expression by Western immunoblotting or FACS analysis. However, I was able to try colony formation assays. Six well plates were coated with 0.8% agarose in media. Single cell suspensions ($3x10^5$ cells/ml) were mixed with warmed agarose to a final concentration of 0.45% agarose and then layered on top of the bottom agar. Cultures were incubated as per normal protocol and monitored for two weeks to determine if colonies could form. Compared to untransfected cells, there was no difference in cells transfected with nectin 4 shRNA clones. OV2008 cells were able to form small colonies by the end of two weeks, but C13 cells could not. This was true of both control and shRNA transfected cell lines. Decreased protein expression had not been verified, however. Although these results indicate that nectin 4 expression does not influence the ability of cells to form colonies in agar, it is possible that there was no change in protein expression.

In conclusion, nectin 4 expression was associated with proliferation and an increase in sensitivity to taxol at high concentrations. While it is possible that nectin 4 only impacts these two attributes of ovarian cancer progression, it is unlikely. Although we saw no difference in invasion of mesothelial cells by spheroids, it is possible that single cells would be more adept at this function. Many ovarian cancer patients have a mix of single cells and spheroids present in the ascites, and both of these can form new tumor nodules throughout the peritoneal cavity. Further studies of the functional impact of nectin 4 expression in ovarian cancer need to be completed to better understand how it promotes tumor progression, as well as how it may be useful as a therapeutic target for treatment of late stage ovarian cancer.

Figure 4-1. Cloning of full length nectin 4. A) Nectin 4 was cloned into the pcDNA3.1(+) vector using the NotI and XbaI sites. B, C) Flow cytometric analysis for nectin 4 expression of B) MCF7 (positive control) and C) Nectin 4 transfected MA148DSRed2 cells. Shaded peak, mIgG control; line, nectin 4.

Figure 4-1

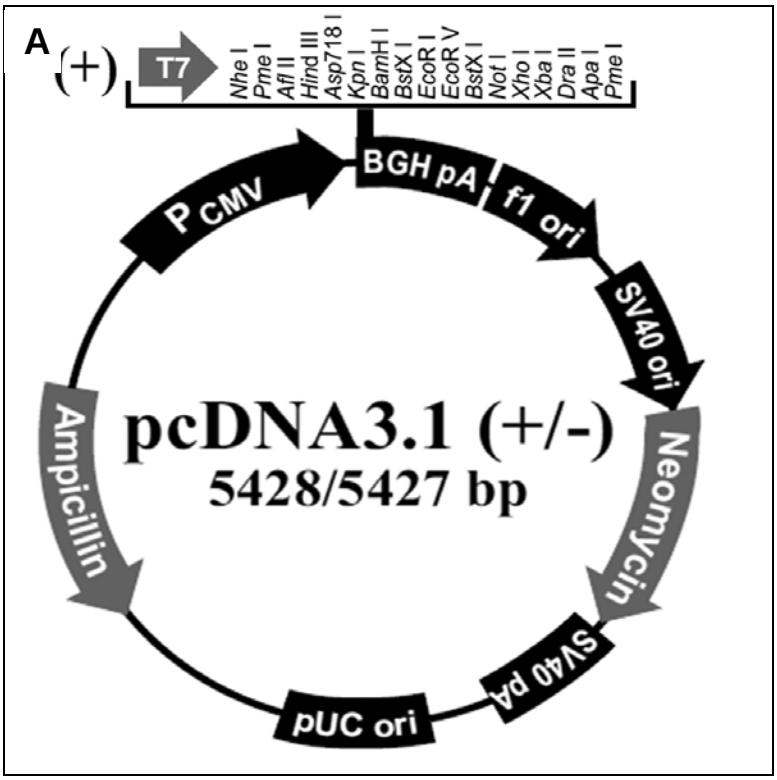
A
(+)
T7
Nhe I
Pme I
Afl II
Hind III
Asp718 I
Kpn I
BamH I
BstX I
EcoR I
EcoR V
BstX I
Not I
Xho I
Xba I
Dra II
Apa I
Pme I
P CMV
BGH pA
f1 ori
SV40 ori
Neomycin
SV40 pA
pUC ori
Ampicillin
pcDNA3.1 (+/-)
5428/5427 bp

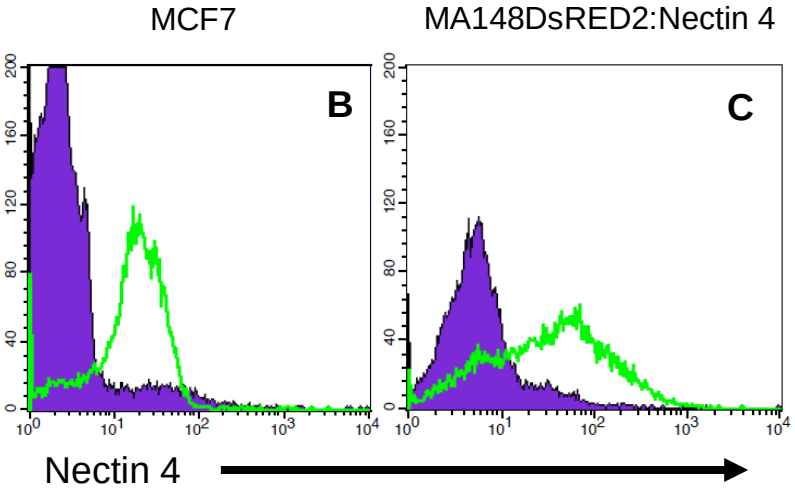
MCF7
MA148DsRED2:Nectin 4
B
C
Nectin 4

Figure 4-2. Proliferation of MA148DSRed2:N4 or :EV cells under low serum conditions. Cells were plated in media with various concentrations of FCS, and then incubated for A) 24 or B) 48 hours. MTT assays were then performed to determine proliferation. Each concentration of FCS and cell type was performed two times in triplicate. Significance was determined by a two-way repeated measures ANOVA followed by the Student-Newman-Keuls t-test. Error bars are standard deviation of the mean; only significantly different comparisons are labeled.

Figure 4-2

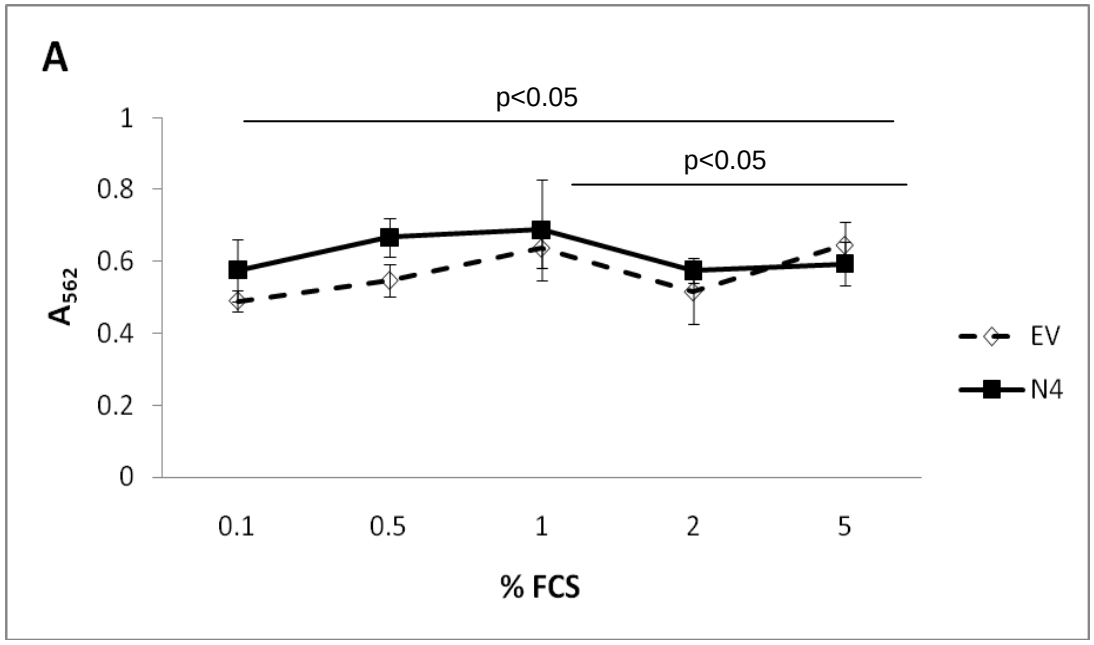
A
p<0.05
p<0.05
1
0.8
0.6
0.4
0.2
0
A562
0.1
0.5
1
2
5
% FCS
EV
N4

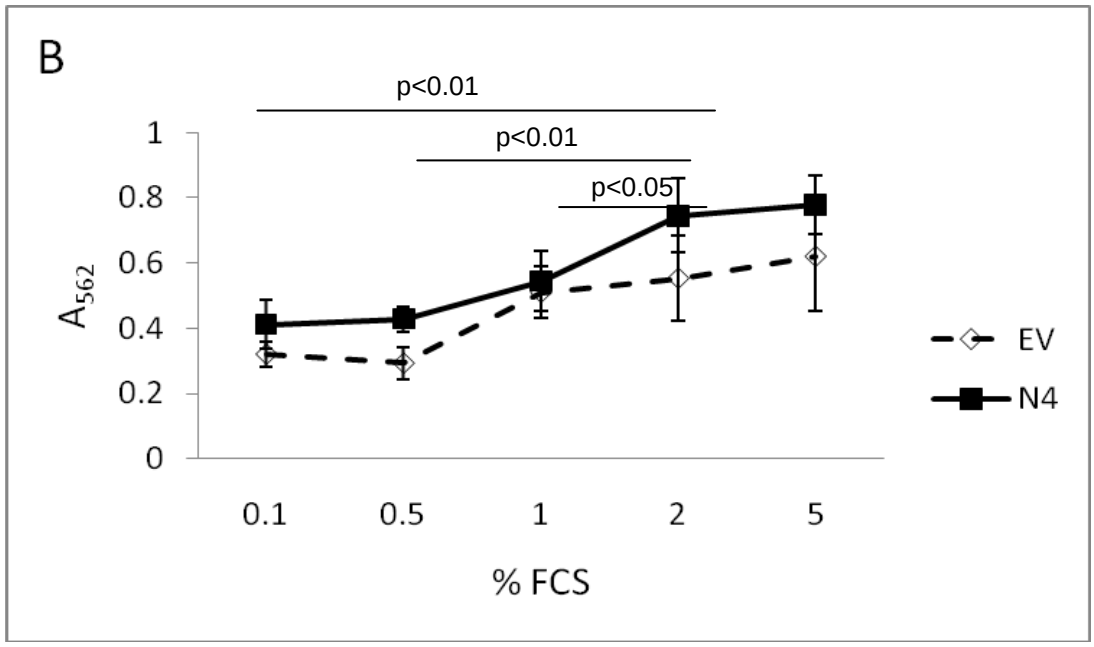
B
p<0.01
p<0.01
p<0.05
1
0.8
0.6
0.4
0.2
0
A562
0.1
0.5
1
2
5
% FCS
EV
N4

Figure 4-3. Growth of MA148DSRed2:N4 or :EV cells under low serum conditions. Equal numbers of cells were plated and incubated overnight. Pictures were taken after 24 hours. All pictures taken at 10x magnification.

Figure 4-3

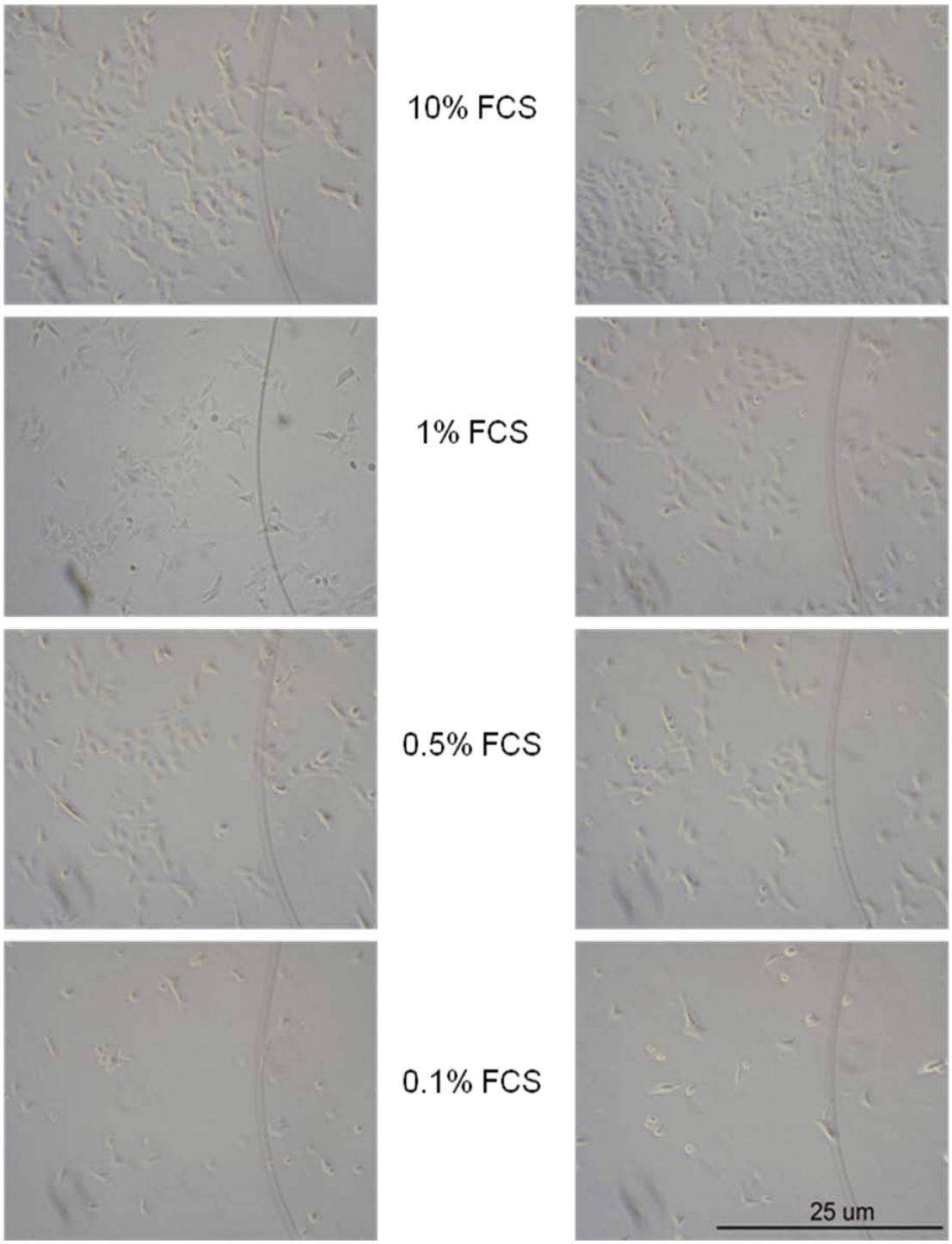

Figure 4-4. Nectin 4 expression in MA148 cells increases proliferation. MA148DSRed2 cells were transfected with empty or nectin 4 expressing pcDNA3.1 (+) vector plasmid and grown in 2% serum. Cells expressing nectin 4 proliferated significantly more than those transfected with the empty vector at 48 hr ($p<0.001$).

Figure 4-4

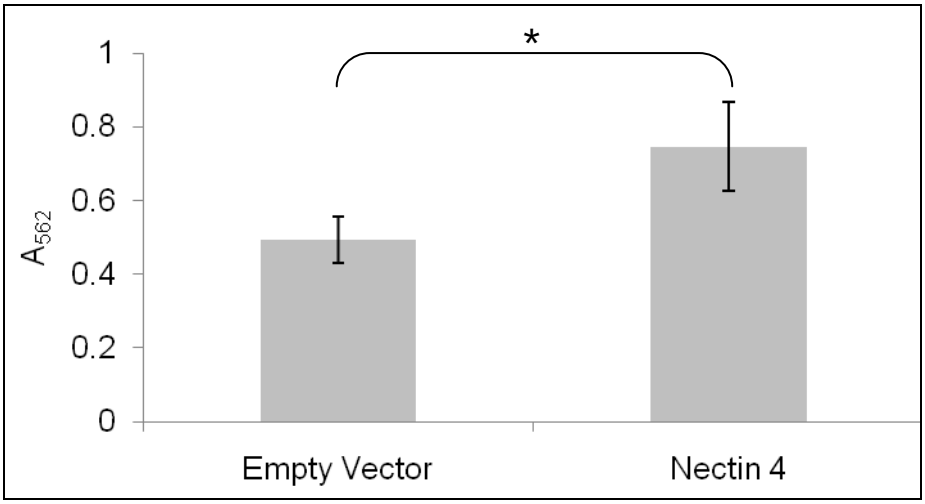

*p<0.001

Figure 4-5. Sensitivity of monolayer cells to cisplatin treatment for 24 or 48 hours. MA148DsRED2 cells transfected with empty vector or nectin 4 containing vector were treated with increasing concentrations of cisplatin for A) 24 hours, or B) 48 hours. MTT assays were performed to determine the percent survival after treatment compared to control treated samples. Each treatment concentration was plated in triplicate and repeated three times. Standard error of the mean was calculated and error bars are present on the graph. Graphs are of a representative experiment.

Figure 4-5

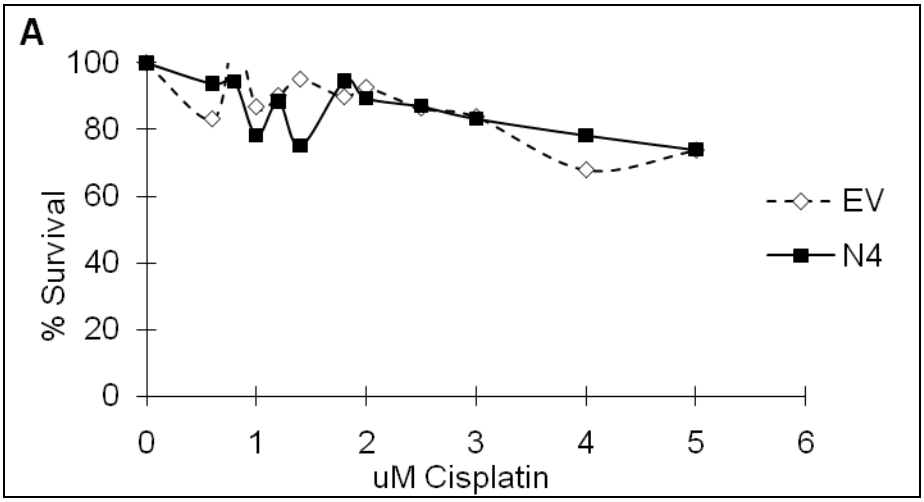
A
100
80
60
40
20
0
% Survival
0
1
2
3
4
5
6
uM Cisplatin
EV
N4

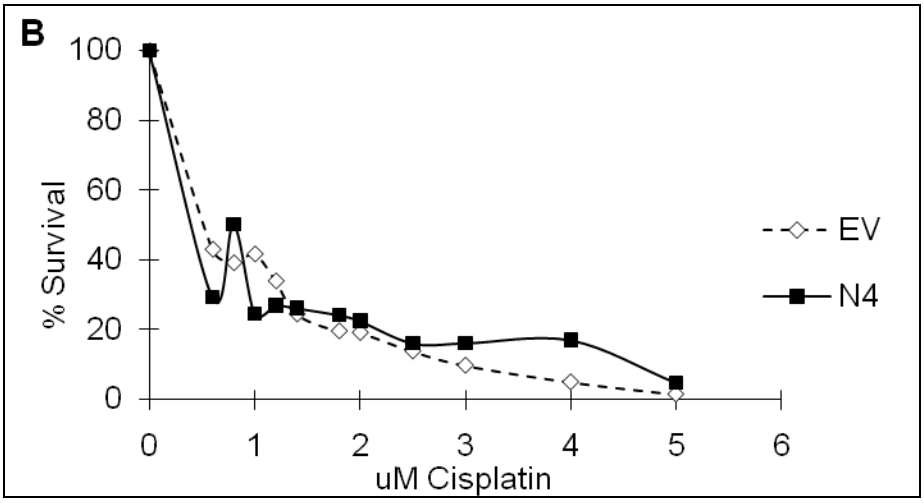
B
100
80
60
40
20
0
% Survival
0
1
2
3
4
5
6
uM Cisplatin
EV
N4

Figure 4-6. Sensitivity of monolayer cells to taxol treatment for 24 or 48 hours. MA148DsRED2 cells transfected with empty vector or nectin 4 containing vector were treated with increasing concentrations of taxol for A) 24 hours, or B) 48 hours. MTT assays were performed to determine the percent survival after treatment compared to control treated samples. Each treatment concentration was plated in triplicate and repeated three times. Standard deviation was calculated and error bars are present on the graph. Student t-tests were used to determine significance. *, $p<0.05$; **, $p<0.01$. Graphs are of representative experiments.

Figure 4-6

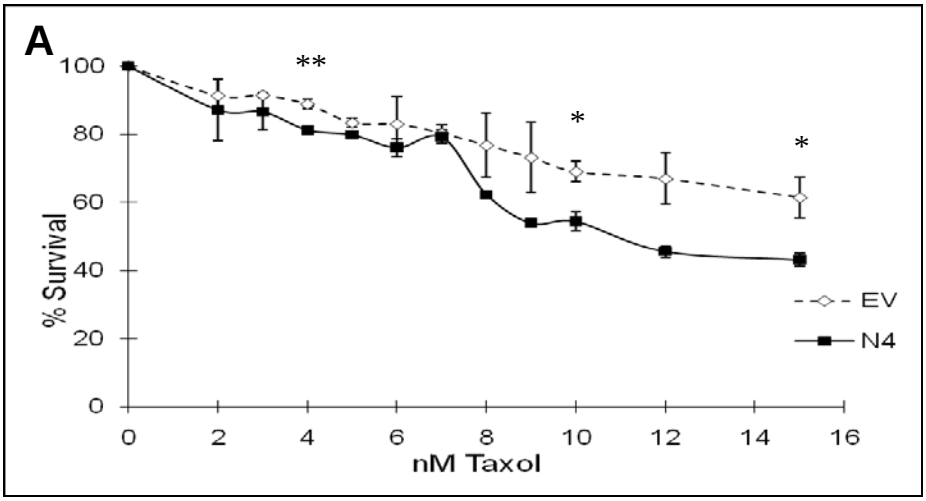
A
100
80
60
40
20
0
% Survival
0
2
4
6
8
10
12
14
16
nM Taxol
**
*
*
EV
N4

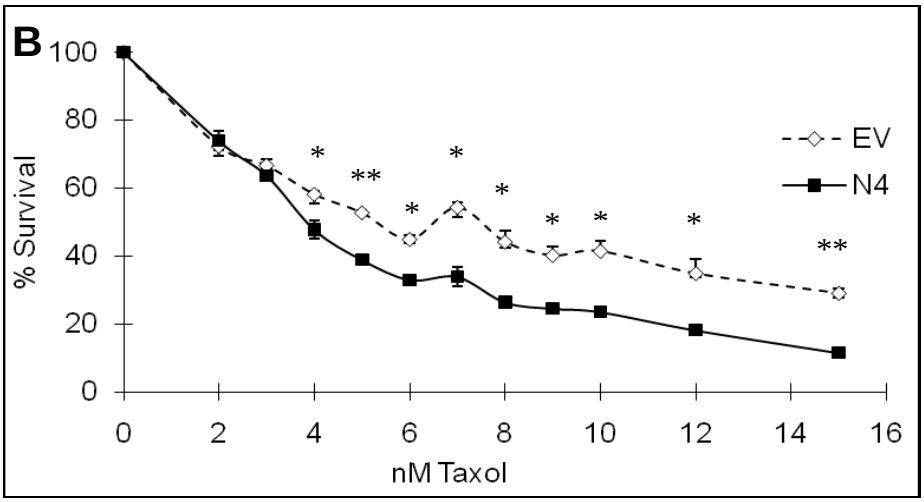
B
100
80
60
40
20
0
% Survival
0
2
4
6
8
10
12
14
16
nM Taxol
*
**
*
*
*
*
*
*
**
EV
N4

Figure 4-7. Spheroid formation of nectin 4 and empty vector control cells. Single cell suspensions of cells were plated in agarose coated tissue culture plates and spheroids were allowed to form over 24 hours. Pictures were taken at 3, 5, and 24 hours. All pictures taken at 4x magnification.

.

Figure 4-7

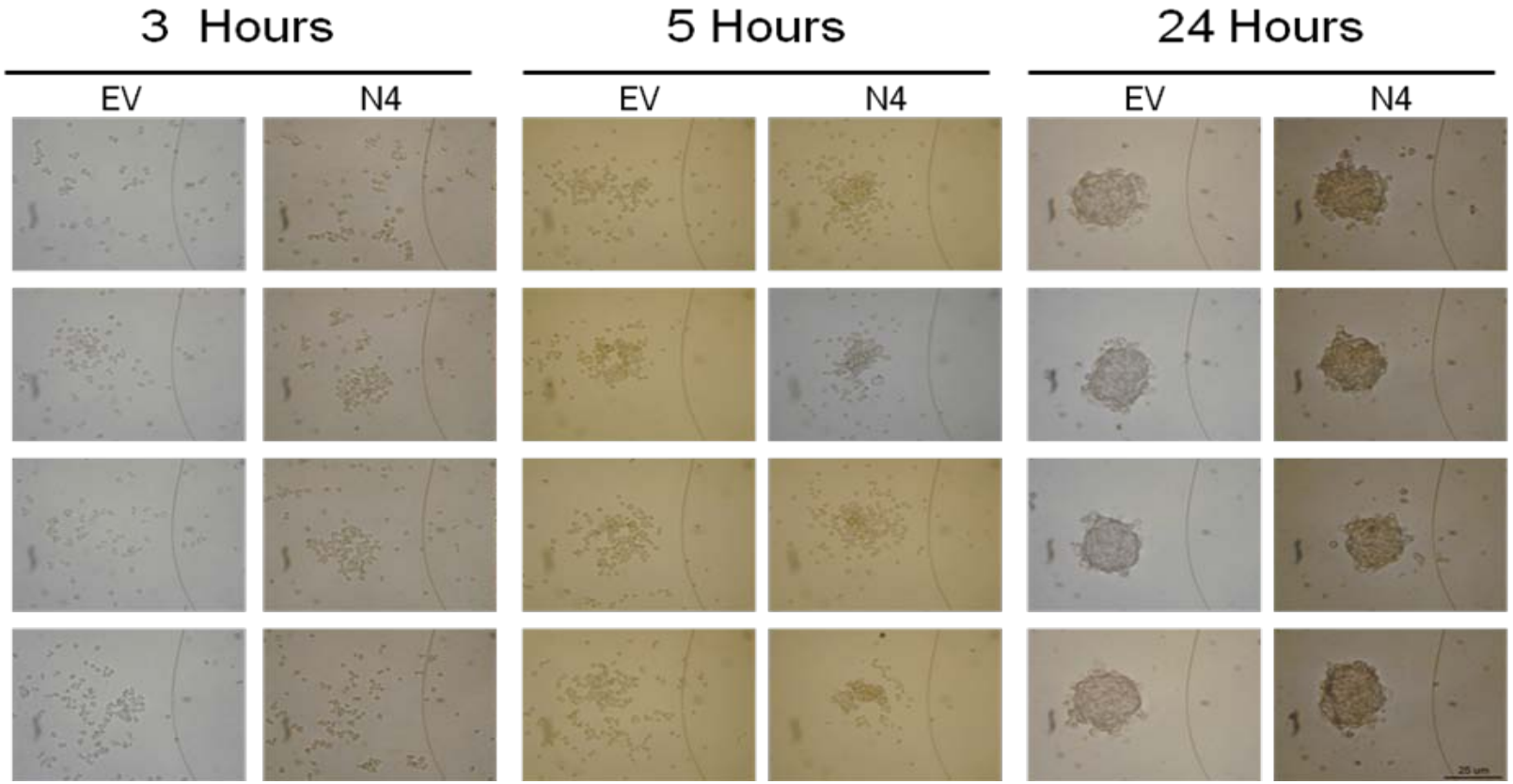

Figure 4-8. Spheroid adhesion to mesothelial cells. MA148DSRed2 empty vector or nectin 4 spheroids (stained with CellTracker Red) were added to confluent monolayers of Met5a mesothelial cells (stained with CellTracker Green) and allowed to attach. Pictures were taken at 4, 24, 48, and 96 hours after spheroids were added. Three representative spheroids are shown for both empty vector control and nectin 4 expressing spheroids.

Figure 4-8

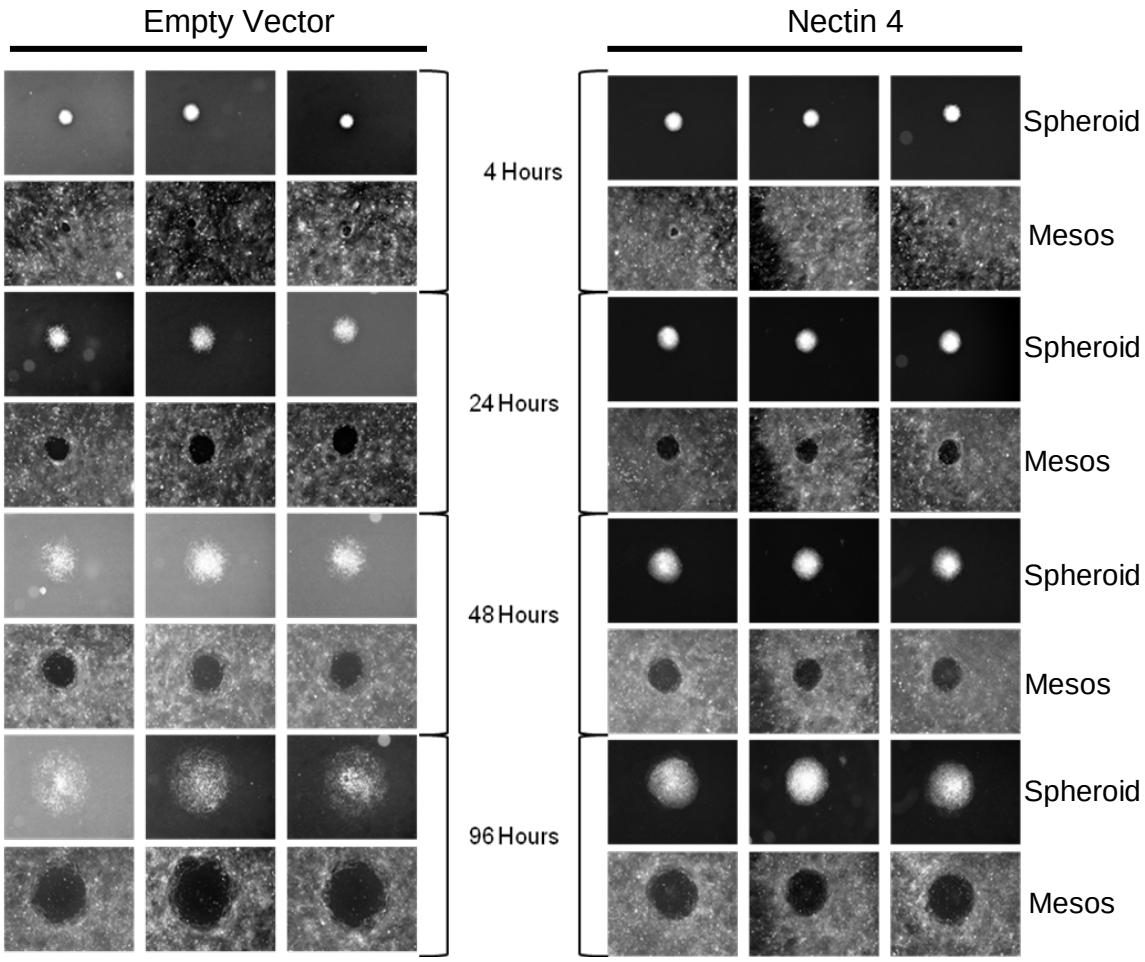
Empty Vector
Nectin 4
4 Hours
24 Hours
48 Hours
96 Hours
Spheroid
Mesos
Spheroid
Mesos
Spheroid
Mesos
Spheroid
Mesos

Figure 4-9. Tumor and mesothelial cell area during spheroid adhesion to mesothelial cells. MA148DSRed2 empty vector or nectin 4 spheroids were added to confluent monolayers of Met5a mesothelial cells and allowed to attach. Pictures were taken at 4, 24, 48, and 96 hours after spheroids were added. Two dimensional area of the A) tumor and B) area cleared of mesothelial cells was measured in Adobe Photoshop by pixel count. Error bars are standard deviation of n=17 for empty vector cell spheroids and n=19 for nectin 4 cell spheroids.

Figure 4-9

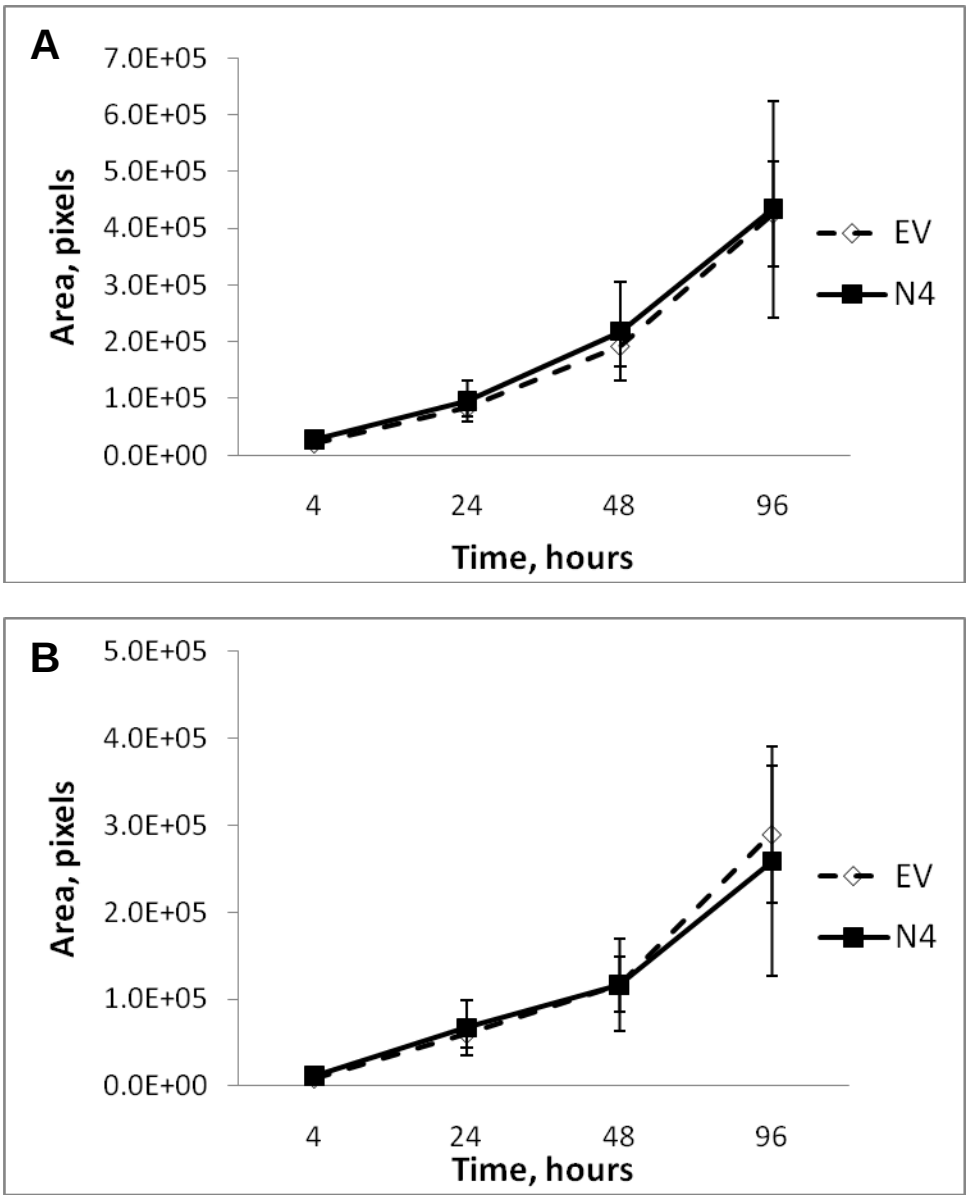
A
7.0E+05
6.0E+05
5.0E+05
4.0E+05
3.0E+05
2.0E+05
1.0E+05
0.0E+00
Area, pixels
4
24
48
96
Time, hours
EV
N4
B
5.0E+05
4.0E+05
3.0E+05
2.0E+05
1.0E+05
0.0E+00
Area, pixels
4
24
48
96
Time, hours
EV
N4

Figure 4-10. Sensitivity of spheroid cells to cisplatin treatment after 48 hours with MA148DsRED2 cells transfected with empty vector or nectin 4 containing vector. Cells were cultured as described to form spheroids. The following day, increasing amounts of cisplatin was added to the media and incubated for 48 hours. After 48 hours, WST-1 was added to measure survival. Cisplatin concentrations were tested in duplicate for each cell line and the experiment was performed twice. Standard error of the mean of duplicate readings was calculated and used for error bars.

Figure 4-10

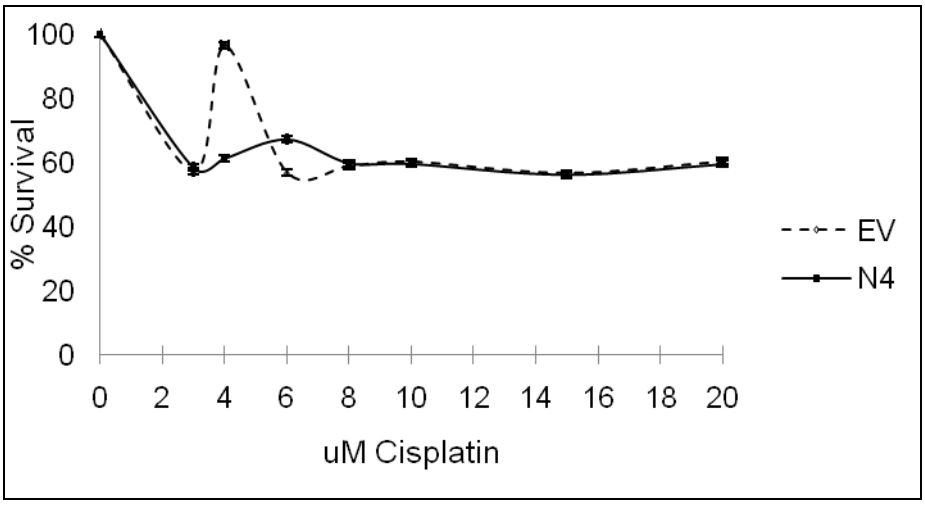
100
80
60
40
20
0
% Survival
0
2
4
6
8
10
12
14
16
18
20
uM Cisplatin
EV
N4

Figure 4-11. In vivo imaging of mice. Mice injected with N4 or EV MA148DSRed2 cells were imaged weekly to detect tumor burden. Images shown are from weeks 3, 6, and 9 post-injection.

Figure 4-11

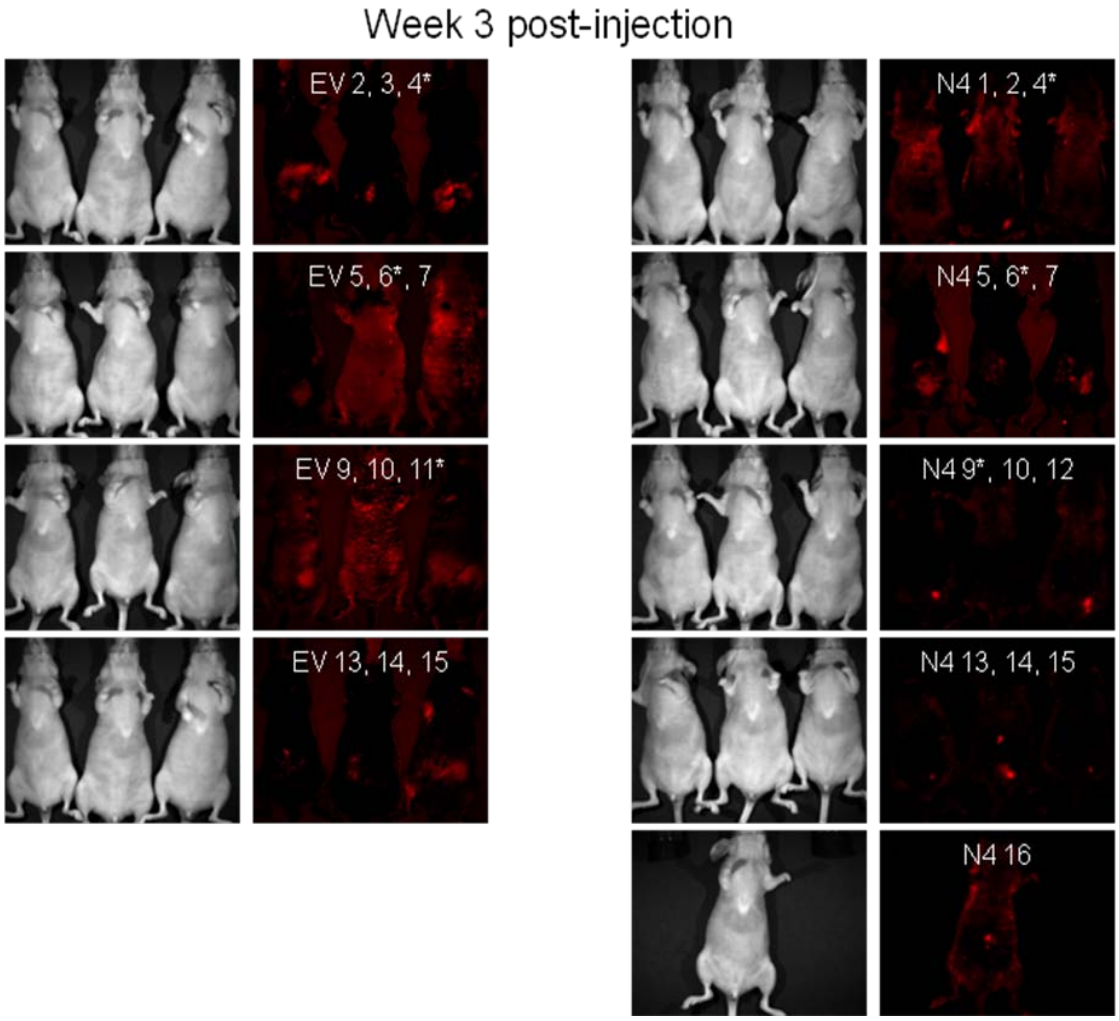
Week 3 post-injection
EV 2, 3, 4*
EV 5, 6*, 7
EV 9, 10, 11*
EV 13, 14, 15
N4 1, 2, 4*
N4 5, 6*, 7
N4 9*, 10, 12
N4 13, 14, 15
N4 16

Figure 4-11

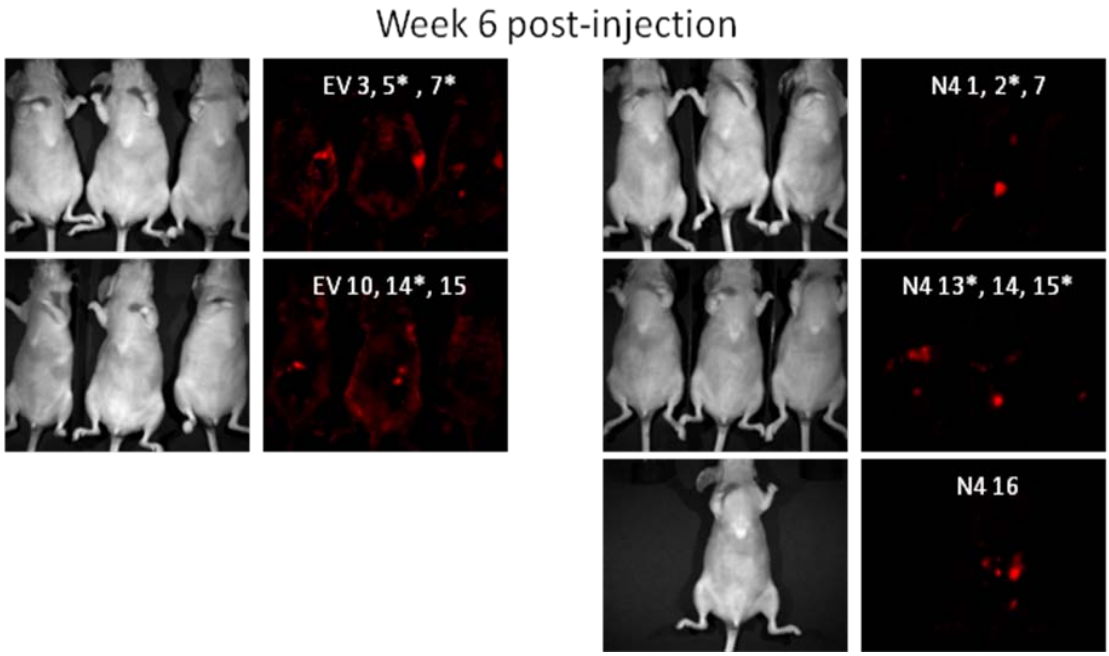

Figure 4-11

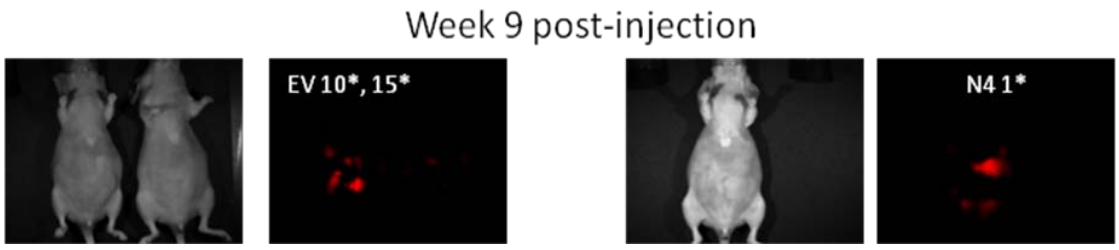

Table 4-1: Summary of data from *in vivo* mouse experiments

Mouse #	Week Sacri-ficed	Ovary, Left (mm^3)	Size	Ovary, Right (mm^3)	Size	Micro-scopic tumor	Spleen (mm^3)	Size	Lung	Liver	Kidneys	Intestine	Omental Mass	Other tumor sites
EV 1	2	6	N*	2.25	N	+‡	980	N	-§	-	-	-	-	N/A
EV 8	2	7.5	N	18	N	+	120	N	-	-	-	-	-	N/A
EV 12	2	24	N	6	N	N	320	N	-	-	-	-	-	N/A
N4 3	2	9	N	7.5	N	+	192	N	-	-	+	-	-	N/A
N4 8	2	11.25	N	18	N	N	165	N	-	-	-	-	-	N/A
N4 11	2	15	N	11.25	N	N	204	N	-	-	-	-	-	N/A
EV 4	3	18	N	5	N	+	315	N	-	-	-	-	-	+/++ (Inj. Site)
EV 6	3	7.5	N	7.5	N	+	238	N	-	-	-	-	-	+ (thoracic mass) ++ (Inj. Site)
EV 11	3	18	N	15	N	+	238	N	-	-	-	-	-	N/A
N4 4	3	9	N	6	N	+	216	N	-	-	-	-	-	N/A
N4 6	3	21.88	N	32	N	+	198	N	-	+	-	-	-	N/A
N4 9	3	18	N	12.5	N	N	234	N	-	+	-	-	-	+ (Inj. Site)
EV 2	4	27	+	30	+	+	196	N	-	-	-	-	-	N/A
EV 9	4	11.25	N	6	N	N	148.5	N	-	-	-	-	-	N/A
EV 13	4	10.5	N	9	N/+	+	165	N	-	+	-	-	-	N/A
N4 5	4	70	N	12	+	+	204	N	-	-	-	-	-	N/A
N4 10	4	36	N	24	+	+	148.5	N	-	-	-	-	-	N/A
N4 12	4	20	N	30	N	+	181.5	N	-	-	-	-	-	+ (Intestinal mass)

Mouse #	Week Sacri-ficed	Ovary, Left (mm^3)	Size	Ovary, Right (mm^3)	Size	Micro-scopic tumor	Spleen (mm^3)	Size	Lung	Liver	Kidneys	Intestine	Omental Mass	Other tumor sites
EV 5	6	12	N	24	N	ND†	351	N	-	-	-	-	-	N/A
EV 7	6	18	N	18	N	ND	511.9	N	-	+	-	-	+	++ (Inj. Site)
EV 14	6	187.5	+	60	+	ND	1120	N	-	+	-	-	-	++ (Inj. Site)
N4 2	6	40.5	N	10.5	N	ND	240	N	-	-	-	-	+	+ (Inj. Site)
N4 13	6	21	N	13.13	N	ND	350	N	-	-	-	-	+	N/A
N4 15	6	47.25	++	819	+	ND	292.5	N	-	-	-	-	-	N/A
N4 7	7	12	N	21	N	ND	285	N	-	+++	-	+	+	+++ (liver mass)
EV 3	8	1347	+++	2088	+++	ND	280	N	-	+	-	-		N/A
N4 14	8	337.5	+	211.8	++	ND	526.5	N	-	+	-	+	++	+ (pelvic mass) + (Inj. Site)
N4 16	8	465.5	+	146.3	++	ND	399	N	-	-	+	+	+++	N/A
EV 10	9	3750	++	198	+++	ND	800	N	-	-	-	+	++	N/A
EV 15	9	495	++	704	++	ND	312	N	-	+	-	+	-	++ (stomach)
N4 1	9	24	++	130	+	ND	612	N	-	-	-	++	+++	N/A

*, N, grossly normal
†, ND, not determined
‡, +, positive
§, -, negative

Chapter 5

Tissue Microarray Analysis of Claudin 4, Cellular Retinoic Acid Binding Protein 1, and Spondin 1

Abstract

Diagnosis of ovarian cancer is often delayed because of subtle symptoms and a lack of a specific, sensitive test useful for the general population. The majority of cases are diagnosed at late stages, after the tumor has metastasized and implanted on many other abdominial organs and cavity surfaces. These secondary tumors are often difficult to completely resect during surgery, thus many women have residual tumor which can cause recurrence. In addition, a paucity of prognostic markers makes it difficult to define which tumors will act aggressively and shorten survival.

New screening tests are needed to diagnose ovarian cancer at earlier stages, prior to spread throughout the abdominal cavity. Tumors at this stage have significantly increased survival times. Diagnosis at these early stages will dramatically increase the overall survival of women with ovarian cancer. New prognostic markers are needed to define which patients would benefit from more aggressive surgery and more frequent monitoring for recurrence. Previously our lab performed gene microarray analysis comparing ovarian cancer tissues to normal ovarian tissues. Sixty-six genes were found to be upregulated in ovarian cancer tissues compared to the normal counterparts. To validate these results, we chose three genes from the 66 and performed IHC analysis to determine their usefulness as biomarkers and prognostic markers for ovarian cancer.

Introduction

Previous work in our lab identified 66 genes overexpressed in ovarian cancer tissues compared to their normal ovarian tissue counterparts (85). A small number of frozen samples were IHC stained with monoclonal antibodies versus seven of these potential biomarkers for validation; however, no comprehensive analysis was performed for these promising biomarkers (85). To address this issue, I optimized the IHC staining technique for three of the proteins in FFPE tissues and then stained TMAs containing 500 cases of ovarian cancer for claudin 4, cellular retinoic acid binding protein 1 (CRABP-1), and spondin 1. These three genes were chosen because monoclonal antibodies were available for them at the time and two of them had previously been reported as being disregulated in ovarian cancer (claudin 4, spondin 1) (116, 117). Since the TMAs were clinically annotated, it was possible to derive clinical correlations from the IHC data.

Claudins are calcium-dependent tight junction molecules. Twenty-four members of the claudin family have been described; members show tissue and developmental specific expression (85, 116, 118, 119). Claudins help organize tight junctions and epithelial cells by maintaining cell polarity and acting as a fence between the apical and basolateral surface of epithelial cells (116). Previous reports have identified overexpression of claudin 4 in ovarian, breast, pancreatic, and prostate cancers (85, 119-121) .

CRABP-1 is a cytoplasmic carrier protein for retinoic acid, regulating its ability to enter the nucleus and bind to nuclear receptors. Previous studies have reported a decrease in expression of CRABP-1 in other cancers, including ovarian, thyroid, and esophogeal cancers, primarily through hypermethylation of the gene (117, 122, 123).

Spondin 1 is a growth factor that stimulates the proliferation of smooth muscle cells

(124) and acts as a guidance molecule for the migration of neurons (125-127). Recently, it has been shown to be increased in ovarian cancer tissues by IHC analysis (128).

Materials and Methods

Tissue Sections

FFPE tissue blocks were obtained from the University of Minnesota Cancer Center's Tissue Procurement Facility after IRB approval and patient consent. Diagnoses were determined by the surgical pathologist and confirmed by two independent pathologists.

Five micron sections of the FFPE tissues were adhered onto slides, then dried at 30°C overnight and for 30 min at 60°C immediately prior to staining to remove any residual water. Sections of normal ovary were only included in analysis if surface epithelium cells were present.

Tissue Microarrays

Tissue microarray slides of 500 cases of ovarian cancer (containing 0.6 mm duplicate core samples for each patient) were provided by the Cheryl Brown Ovarian Cancer Outcomes Unit (Vancouver, Canada). Patients included in the TMA were chosen based on the fact that they were optimally debulked at initial surgery and had no macroscopic residual disease, thereby increasing the proportion of early stage cases on the TMA relative to the general population. None of the patients received neoadjuvant therapy, but all received platinum based chemotherapy following surgery. Because the 500 cases included on the ovarian TMA were originally diagnosed up to 18 years ago and the classification of ovarian cancer histologies has shifted over the years, care was taken to ensure that the current diagnostic criteria for subclassification of ovarian carcinoma based on cell type were uniformly applied (9, 94). Hematoxylin and eosin stained slides for all cases were reviewed by a gynecologic pathologist to confirm diagnosis, stage, tumor cell type, and grade prior to TMA inclusion; samples displaying multiple cell types (mixed tumors) were excluded from the study. Complete details about

the cohort used for these TMAs are provided in Table 5-1 and in Gilks et al (95). Patients were followed for a median of 4.6 (0.1-18) years after the initial surgery. Relapse was defined by visible disease progression by a variety of diagnostic modalities including radiology and physical exam.

Immunohistochemical Staining of Tissues

Tissue sections were deparaffinized and rehydrated through a series of xylene and ethanol washes. Antigen retrieval was performed in a 1x solution of Reveal citrate buffer (Biocare, Concord, CA) for 20 minutes for both claudin 4 and spondin 1, but not for CRABP-1. Endogenous peroxidase activity was blocked with 3% hydrogen peroxide for 10 minutes. Slides were incubated with mouse-anti-human claudin 4 monoclonal antibody (clone 3E2C1 Invitrogen; 0.25 ug/ml), mouse anti-human CRABP-1 monoclonal antibody (clone C-1; AbCam, 1/750), normal mouse IgG1 (clone 3-5D1-C9; AbCam, 1/2000) overnight at 4°C or chicken-anti-human spondin 1 polyclonal antibody (clone ab14271; AbCam, at 5 ug/ml), or normal chicken IgY (ab50579, AbCam) for 1 hour at room temperature. All primary antibodies were diluted in 1:5 Sniper (Biocare):PBS. Slides were washed 2 times with PBS for 5 minutes, then incubated with biotinylated horse-anti-mouse secondary antibody (Vector Laboratories, Burlingame, CA) per the manufacturer's protocol or biotinylated rabbit anti-chicken secondary antibody (1/500, ab6752, AbCam), followed with an avidin:biotin complex (Vector Laboratories) for 30 minutes. Staining was visualized with 3,3'-diaminobenzidine (Biocare) for claudin 4 and with Vulcan Fast Red (Biocare) for CRABP-1 and spondin 1 following the manufacturer's directions. Slides were examined by a pathologist and assigned a score of 0 (no staining); 1 (<10% of neoplastic cells staining); 2 (10-50% of neoplastic cells staining); or 3 (>50% of neoplastic cells staining). For analysis of claudin 4 tissues, scores of 1, 2, and 3 were grouped and considered positive. Positive control tissues and staining

patterns were: intestine (claudin 4, membranous, cytoplasmic); retina (CRABP-1, cytoplasmic), ovary (spondin 1, using two ovarian cancer tissues positive and one tissue negative by Western immunoblotting, not shown, cytoplasmic, extracellular).

Results and Discussion

Claudin 4 expression in the control tissue, intestine, was limited to the epithelial cells lining the intestine (not shown). IHC staining of whole tissue sections revealed claudin 4 was 64% sensitive for serous tumors (21 of 33 tissues positive), 75% sensitive for clear cell tumors (3 of 4 tissues positive), and 81% specific (17 of 21 normal ovarian tissues negative). Ovarian cancer tumor cells, but not stroma, had a high percentage of IHC staining in individual sections, while normal ovarian tissue was either negative or had a slight blush of staining present (Fig. 5-1A, B). Tissue microarray analysis allowed analysis of 500 cases of ovarian cancer simultaneously. Overall, 69.9% of ovarian cancer tissues were positive for claudin 4 (Table 5-1). Endometrioid and mucinous ovarian tumors had the highest expression (77.4% positive for both), followed by serous tumors (72.2%) and clear cell tumors (57.6%).

Expression of claudin 4 was inversely correlated to Silverberg grade in endometrioid ovarian cancers. Low grade tumors had significantly higher expression (81.5%) compared to high grade (37.5%) (Table 5-1, $p=0.04$). No other subtypes had significant differences in claudin 4 expression with regard to grade.

No significant differences were noted in the expression of claudin 4 by stage in any of the subtypes. Additionally, expression of claudin 4 was not associated with a decrease in relapse-free survival or survival times (not shown). The above results confirmed that claudin 4 is overexpressed in ovarian cancer tissues as our previously reported IHC studies had suggested (85).

CRABP-1 expression in the control tissue, eye, was localized to the retina (not shown). In IHC staining of whole sections of tissues, CRABP-1 was 60% sensitive for serous tumors (Figure 5-2, 15 of 25 tissues positive), 25% sensitive for clear cell tumors (1 of 4 tissues positive), and 92% specific (23 of 25 normal tissues negative). However,

only a small number of TMA tissues stained positively for CRABP-1 overall (10.6%). Expression was highest in the serous subtype (15.6%), followed by endometrioid (8.0%), clear cell (6.8%) and mucinous (3.2%) subtypes (Figure 5-2A). Expression was significantly higher in serous tumors compared to the other subtypes (p=0.04). No significant difference in CRABP-1 staining was present by stage (Fig. 5-2B, p=0.23), Silverberg grade (Fig. 5-2C, p=0.14), relapse-free survival (p=0.09), or overall survival (p=0.14).

The majority of TMA samples were positive for spondin 1. Both endometrioid and mucinous tumor stained 100% positive for spondin 1, followed by serous (99.5%) and clear cell (99.2%) tumors. There was no significant difference in staining between subtypes (Fig. 5-3A, p=0.56). There were no significant differences in spondin 1 staining by stage (Fig. 5-3B, p=0.83), Silverberg grade (Fig. 5-3C, p=0.31), or relapse-free survival (not shown, p=0.25). Overall survival was inversely associated with expression of spondin 1 (not shown, p=0.03); however, as only two of the 500 TMA samples were negative for spondin 1, this result should be interpreted with caution.

The results above demonstrate that claudin 4 is a useful marker for ovarian cancer; additionally, the high percentage of tumors that are positive for claudin 4 make it an ideal target for therapy. However, claudin 4 is expressed in several normal tissues, including the intestine epithelial cells, and off-target effects could cause severe reactions.

CRABP-1 was not expressed at high levels in any subtype of ovarian cancer, making it a poor marker. Our original gene microarray analysis determined that mRNA expression of CRABP-1 was increased in ovarian cancer tissues compared to normal ovaries (85), however we were not able to confirm this. It is possible that while the mRNA of CRABP-1 is increased in ovarian cancer tissues, the protein may not be

translated or it may be degraded quickly. When determining the optimal conditions for staining for CRABP-1 using FFPE tissues, we noted that expression of CRABP-1 in tumors was at times heterogeneous; some areas of the tumor stained and others did not. It is possible that the small 0.6 mm punch biopsies of the TMAs do not represent the entire tumor and more tumors may be positive if larger sections of tissue were stained.

Spondin 1 was expressed at high levels in nearly all of the tissues on the TMA. No tissue is listed as positive control on Protein Atlas (accessed on 5/24/10, http://www.proteinatlas.org/gene_info.php?ensembl_gene_id=ENSG00000152268). Thus, we choose to use ovarian cancer tissues we found positive (T050599) and negative (T050586) by Western immunoblotting (not shown). Although optimal conditions for IHC staining were determined using these tissues, it appears that the TMA staining had a high level of background staining present. This could be due to different fixation protocols for the tissues; control tissues were obtained and fixed at the Tissue Procurement Facility at the University of Minnesota, while the TMA tissues were originally fixed at several different hospitals in Canada. Fixation of tissues can alter the antigenic site recognized by antibodies, thus differing methods of fixations could change how well an antibody would be able to detect its target. Therefore, these results should be interpreted with caution.

In summary, we sought to validate the overexpression of three genes in ovarian cancer. We verified the overexpression of claudin 4 and found that expression of claudin 4 was inversely correlated with Silverberg grade in the endometrioid subtype of ovarian cancer. Expression of CRABP-1 in whole ovarian cancer tissue sections was higher than in the TMA tissue cores. There are a few possible explanations for this discrepancy. First, the staining on the whole tissue sections was heterogeneous; some tumor cells stained positively while others did not stain within the same tissue section. Because of

this, it is possible that the tissue cores on the TMA sampled areas that were negative although other areas may have been positive, decreasing the overall sensitivity of the staining. A second possibility is that like CRABP-2, CRABP-1 can readily diffuse out of cells (Dr. Blake Gilks, personal communication), leading to a decrease in staining. Although conditions for spondin 1 staining were worked out, staining in the TMAs was highly non-specific, with only two of the samples on the TMA were negative for spondin 1. It is highly unlikely that only two samples are negative, however, and thus the results should be interpreted with caution.

Figure 5-1. Claudin 4 IHC staining in A) normal ovarian tissue (ovarian surface epithelial cells, arrow), and B) ovarian cancer (tumor, arrow). Staining in ovarian cancer cells was localized to cell membranes. All pictures taken at 20x magnification.

Figure 5-1

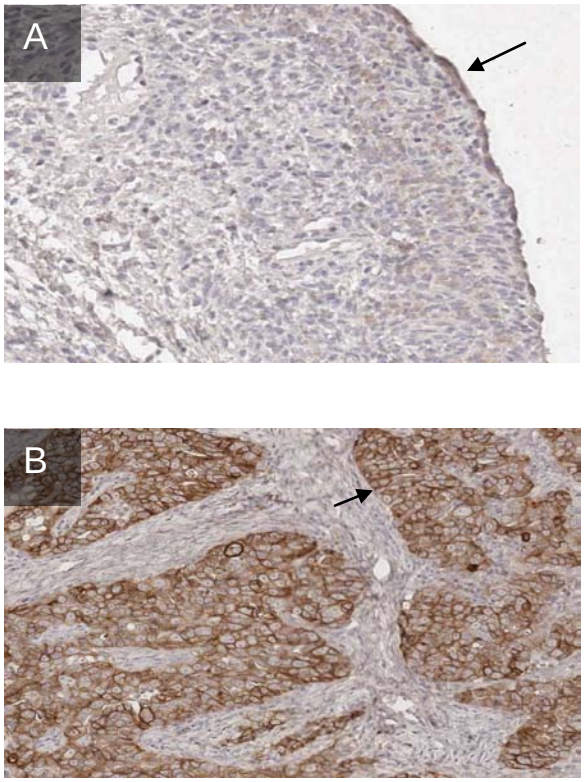

Table 5-1. Subtype, stage, Silverberg grade, and Claudin 4 score of tissue microarrays.

Subtype	Median Age (range)	Median PreOP* CA125 (range)	Stage	N	Claudin 4 Positive	Silverberg grade	N	Claudin 4 Positive	Claudin 4 Positive Overall
Serous (n=212)	59.6 (33.5 – 86.0)	108 (0 – 23,000)	I	50	33 (66.0%)	1	12	7 (58.3%)	153 (72.2%)
			II	93	69 (74.2%)	2	56	37 (66.1%)	
			III	69	51 (73.9%)	3	144	109 (75.7%)	
Endometrioid (n=125)	54.1 (29.4 – 88.1)	130 (8 – 13,000)	I	69	54 (78.3%)	1	82	66 (81.5%)	96 (77.4%)
			II	50	37 (75.5%)	2	35	27 (77.1%)	
			III	6	5 (83.3%)	3	8	3 (37.5%)	
Clear Cell (n=132)	55.0 (28.1 – 89.0)	64 (4 – 7,750)	I	68	45 (66.2%)	1	0†	N/A	76 (57.6%)
			II	56	26 (46.4%)	2	0†	N/A	
			III	8	5 (62.5%)	3	132	76 (57.6%)	
Mucinous (n=31)	56.4 (25.4 – 76.7)	45 (7 – 650)	I	18	15 (83.3%)	1	11	8 (72.7%)	24 (77.4%)
			II	12	8 (66.7%)	2	18	14 (77.8%)	
			III	1	1 (100%)	3	2	2 (100%)	
Total (n=500)	56.6 (25.4 – 89.0)	98 (0-23,000)	I	205	147 (71.7%)	1	105	81 (77.1%)	349 (69.9%)
			II	211	140 (66.4%)	2	109	78 (71.6%)	
			III	84	62 (73.8%)	3	286	190 (66.4%)	

*PreOp, preoperative

†All clear cell carcinomas are considered grade 3 (high grade)

Figure 5-2. CRABP-1 IHC staining in A) normal ovarian tissue (ovarian surface epithelial cells, arrow), and B) ovarian cancer (tumor, arrow). Staining in ovarian cancer cells was localized to the cytoplasm. All pictures taken at 20x magnification.

Figure 5-2

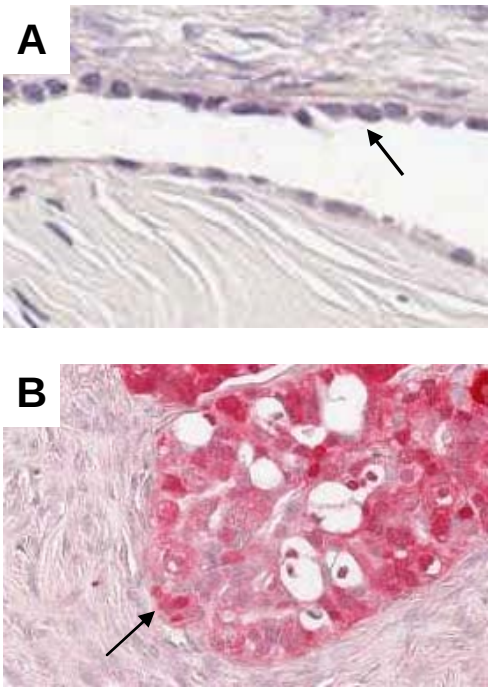

Figure 5-3. CRABP-1 staining of ovarian cancer tissue microarrays. A) Percent of each subtype of ovarian cancer staining positively for CRABP-1. B) Percent positive for CRABP-1 by stage. C) Percent positive for CRABP-1 by Silverberg grade.

Figure 5-3

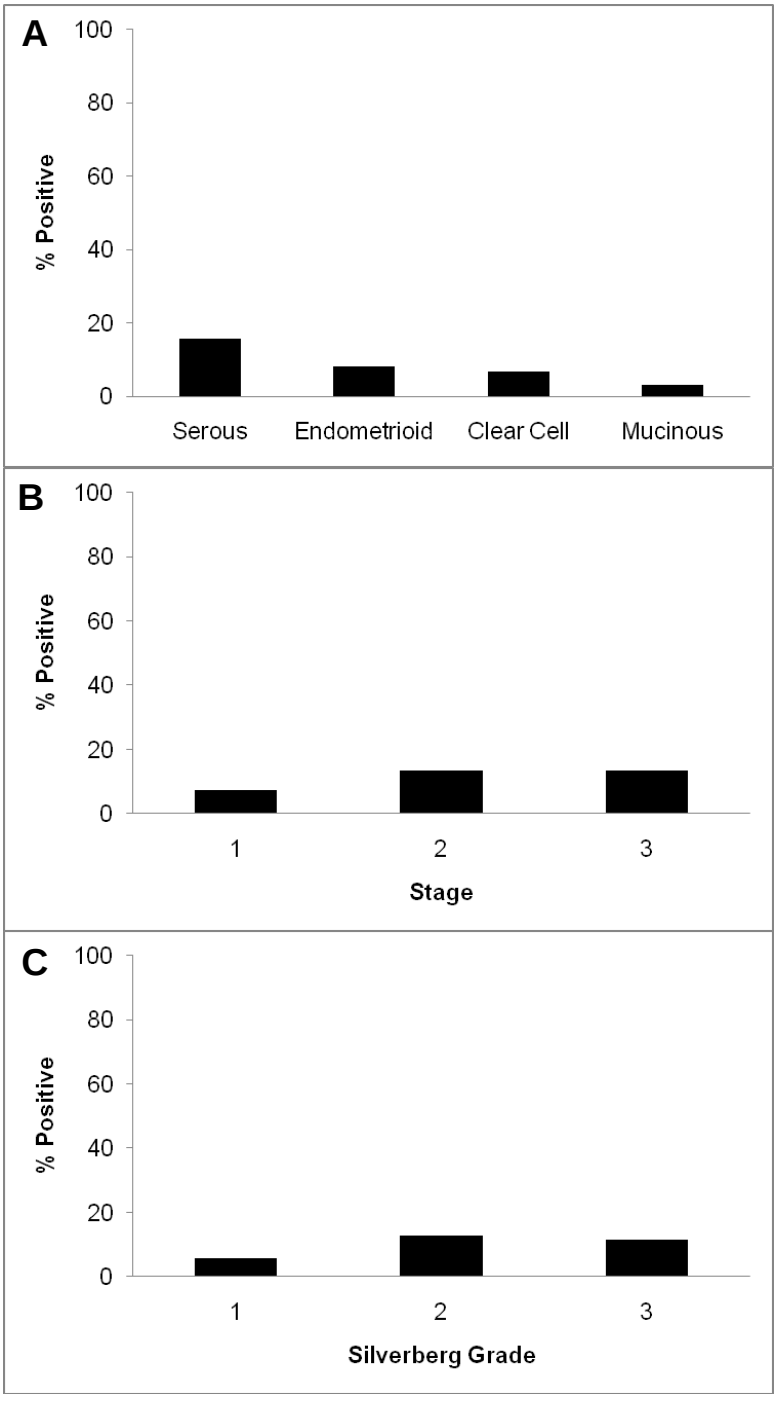
A
100
80
60
40
20
0
% Positive
Serous
Endometrioid
Clear Cell
Mucinous
B
100
80
60
40
20
0
% Positive
1
2
3
Stage
C
100
80
60
40
20
0
% Positive
1
2
3
Silverberg Grade

Table 5-2. Subtype and CRABP-1 scores of tissue microarrays.

Subtype	Median Age (range)	Median PreOP* CA125 (range)	CRABP-1 Positive Overall
Serous (n=212)	59.6 (33.5 – 86.0)	108 (0 – 23,000)	33 (15.6%)
Endometrioid (n=125)	54.1 (29.4 – 88.1)	130 (8 – 13,000)	10 (8.0%)
Clear Cell (n=132)	55.0 (28.1 – 89.0)	64 (4 – 7,750)	9 (6.8%)
Mucinous (n=31)	56.4 (25.4 – 76.7)	45 (7 – 650)	1 (3.2%)
Total (n=500)	56.6 (25.4 – 89.0)	98 (0-23,000)	53 (10.6%)

*PreOp, preoperative

Figure 5-4. Spondin 1 staining of ovarian cancer tissue microarrays. A) Percent of each subtype of ovarian cancer staining positively for spondin 1. B) Percent positive for spondin 1 by stage. C) Percent positive for spondin 1 by Silverberg grade.

Figure 5-4

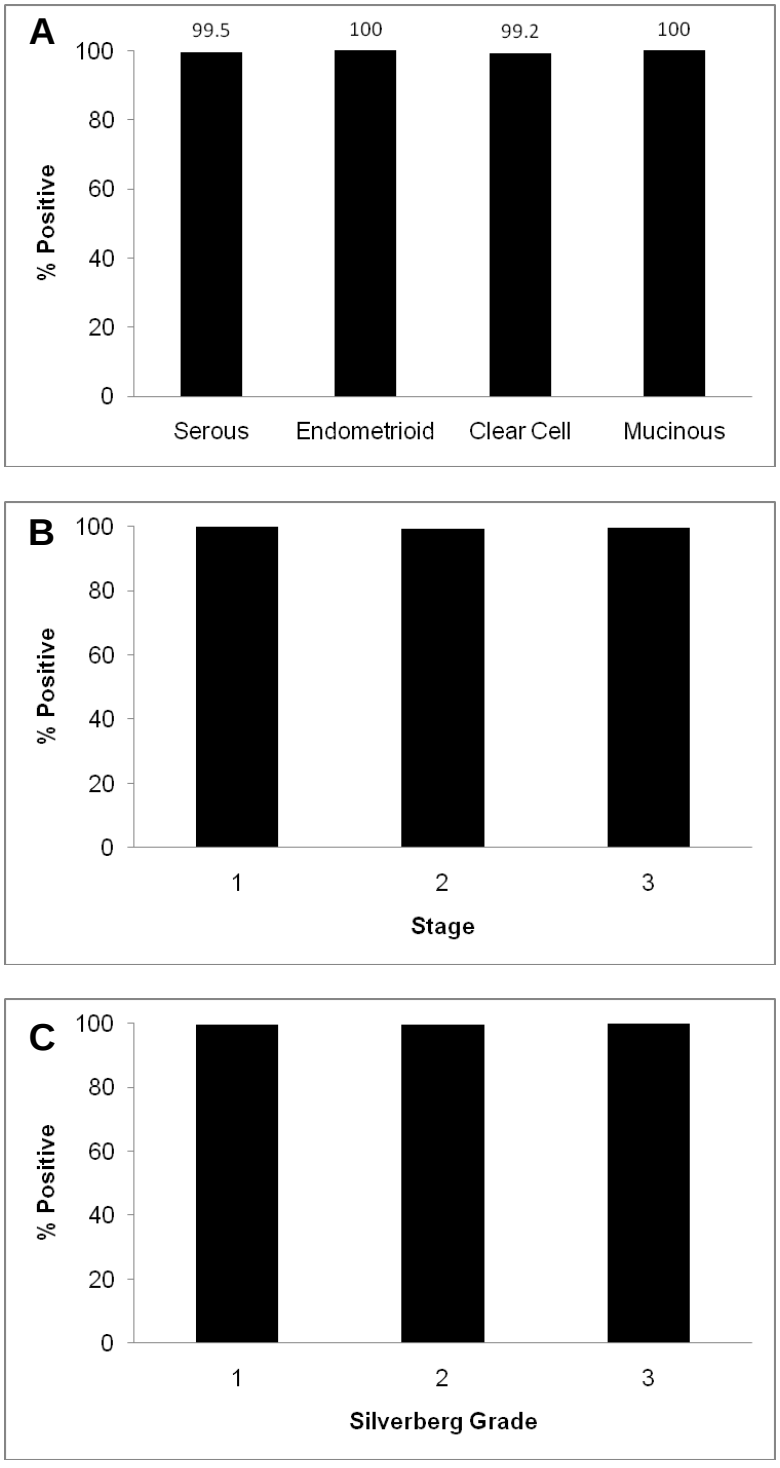
A
99.5
100
99.2
100
100
80
60
40
20
0
% Positive
Serous
Endometrioid
Clear Cell
Mucinous
B
100
80
60
40
20
0
% Positive
1
2
3
Stage
C
100
80
60
40
20
0
% Positive
1
2
3
Silverberg Grade

Table 5-3. Subtype and spondin 1 scores of tissue microarrays.

Subtype	Median Age (range)	Median PreOP* CA125 (range)	Spondin 1 Positive Overall
Serous (n=210)	59.6 (33.5 – 86.0)	108 (0 – 23,000)	209 (99.5%)
Endometrioid (n=123)	54.1 (29.4 – 88.1)	130 (8 – 13,000)	123 (100%)
Clear Cell (n=132)	55.0 (28.1 – 89.0)	64 (4 – 7,750)	131 (99.2%)
Mucinous (n=31)	56.4 (25.4 – 76.7)	45 (7 – 650)	31 (100%)
Total (n=496)	56.6 (25.4 – 89.0)	98 (0-23,000)	494 (99.6%)

*PreOp, preoperative

Chapter 6

Discussion and Future Directions

Discussion

Ovarian cancer diagnosis is difficult; the symptoms that are present are often vague and are commonly mistaken for other problems (27-30). Additionally, there is no specific test for ovarian cancer for the general population. While serum CA125 levels can be screened in patients predisposed to ovarian cancer (BRCA1/2 positive) or used to detect recurrence in women previously diagnosed with ovarian cancer, it is not elevated in all early stage tumors (28, 31). Additionally, many benign conditions have elevated CA125 levels, resulting in a high false positive rate (5, 28). Thus, it is neither specific nor sensitive enough to be useful in screens for the general population.

Detecting ovarian cancer early is critical. Survival greatly decreases after the disease has metastasized in the peritoneal cavity (2). Optimal debulking of tumor masses is crucial, but often it is not possible to detect small implants of ovarian cancer (20, 21). These are missed during surgery and often grow to form secondary tumors. Thus, if surgery can be completed during early stage ovarian cancer, when the cancer cells are still confined to the ovary, surgery is much more effective at eradicating the tumor.

Because most ovarian cancers are diagnosed at late stages, chemotherapeutic agents are given to kill residual cancer cells after surgery (22-24). While effective at first, many ovarian cancers develop resistance and recur, possibly due to the presence of ovarian cancer stem cells with a high capacity for self-renewal (20, 21, 129). Development of new treatment options is necessary to increase survival of late stage, resistant disease. Ideally, the target would be highly expressed in ovarian cancer and have minimal or no expression in other tissues. It is difficult to find such targets, as most often proteins that are overexpressed in cancer have a function in normal tissues, and these tissues would become targets of the therapy. Thus, it is not only imperative to

discover new therapy targets, it is critical to find targets that are specific for ovarian cancer that will not harm nearby, healthy cells and cause further complications.

In this dissertation, I describe studies on two biomarkers of ovarian cancer, S100A1 and nectin 4. Both were previously identified in our lab by gene microarray as being overexpressed in ovarian cancer compared to normal ovarian tissues (85). My thesis work involved validating these results and determining whether they are useful diagnostic or prognostic markers for ovarian cancer.

S100A1 is a calcium binding protein with several cell functions, including regulation of the cell cytoskeleton, muscle contraction, and metabolism (43-51). Studies confirmed that S100A1 expression was increased at both the transcript and protein level in ovarian cancer compared to normal ovary. Differential expression across the four major types of epithelial ovarian cancer was noted, with the highest expression level being in the serous subtype. Overall, expression of S100A1 was associated with a decreased time to relapse. However, when the analysis was broken down by subtype, it was found that the decreased survival only occurred in the endometrioid subtype of ovarian cancer. The percentage of S100A1 positive samples was low (11%), however, and the decrease in survival could have been by chance.

To support our results, we also investigated the expression of S100A1 in endometrioid cancers arising in the endometrium. It has been postulated that these cancers arise in a similar manner and share similar genetic changes. While only 9% of endometrioid endometrial cancers tested were positive for S100A1, a significant decrease in survival was associated with the positive samples, supporting our earlier results.

Prognosis for endometrioid ovarian cancer is often favorable compared to serous ovarian cancer, as it is often diagnosed in early stages before much metastasis occurred

(12, 14). Few prognostic markers for endometrioid ovarian cancer have been described previously. One, type 1 histone deacetylases (HDACs), was studied using the tissue microarrays we used for our analysis (96). Both S100A1 and HDAC expression correlated with poor prognosis, but there was no correlation between S100A1 and HDAC expression found. Thus, these two markers discriminate two distinct populations of endometrioid ovarian cancer with poor prognosis. Combining both of these markers into a clinical test may be useful for determining which patients might benefit from more aggressive therapy and more frequent monitoring for recurrence.

How S100A1 exerts its influence in ovarian cancer is not known. One possible mechanism is through activation of RAGE (41, 58). Other S100 proteins can bind to and activate RAGE, leading to the activation of several downstream signaling cascades, including MAP kinases and NF-κB (40, 41, 58). These may promote cell proliferation and survival. S100A1 added to the media of cells can bind to and activate RAGE, however there is little evidence of S100A1 being secreted like some other S100 proteins (40, 58). Several experiments could be performed to investigate this matter. Determination of RAGE expression on ovarian cancer cells would be a required first step. If expressed, addition of exogenous S100A1 to cell cultures may increase downstream signaling cascades, which signaling cascade is activated by RAGE ligation is both ligand and concentration specific. Adding various amounts of S100A1, in addition to adding either homodimers of S100A1 or heterodimers of S100A1 and S100A4 may result in activation of several different signals, and teasing apart which ones are important may be difficult. Utilization of specific inhibitors may help delineate which signaling cascades are critical in S100A1 tumors.

Nectin proteins are important in the formation of adherens junctions (61-65). Studies of nectin 4 have been limited, but previous reports have found that it is

increased in both breast and lung cancer and associated with decreased survival (80, 81). I first validated overexpression of nectin 4 in ovarian cancer cell lines and tissues. Studies confirmed that nectin 4 was expressed in both ovarian cancer cell lines and tissues but not in normal ovarian tissues or cell lines. Expression was significantly different among the four main subtypes of epithelial ovarian cancer, with the highest expression in endometrioid subtype, followed by serous subtype. More early Silverberg grade tumors were graded +3 (>50% of the tumor cells staining) compared to mid and late grade tumors. No other association was found between nectin 4 expression and stage, grade, or survival.

Nectin 4 can be enzymatically cleaved by the protease ADAM17 (79). To determine if soluble nectin 4 was detectable in the blood of ovarian cancer patients, sera samples from women undergoing surgery for suspected ovarian cancer were subjected to a sandwich ELISA. Nectin 4 was 53% sensitive and had a positive predictive value of 77% in detecting serous ovarian cancer. While the sensitivity was lower than that of CA125 (92%), the positive predictive value was higher than that of CA125 (60%). When nectin 4 and CA125 were combined, the positive predictive value increased to 82%. Of note, one patient with benign gynecological disease was removed from the study after further review of her case file. The patient had very high levels of serum nectin 4, but on further study, it was found that at the time the blood was drawn, the patient was pregnant. Nectin 4 is expressed in the placenta, and it could not be ruled out that the high level of serum nectin 4 was due to pregnancy.

Specificity of nectin 4 was significantly increased over that of CA125 in both low malignant potential tumors and benign samples. Nectin 4 was not detected in any of the 18 low malignant potential tumors and in only eight of the 51 benign serum samples. CA125, in comparison, was increased in 14 of 18 low malignant potential tumors and 31

of the 51 benign samples. Combining nectin 4 and CA125 increased the specificity from 39% to 88% for benign disease. These results indicate that nectin 4 is good candidate serum biomarker that can help discriminate between serous ovarian cancers and benign gynecological disease. Recently, the Food and Drug Administration approved the OVA1 test, which measures the levels of five serum proteins (apolipoprotein A1, beta 2 microglobin, CA125, prealbumin, and transferrin) (130). While the OVA1 test does not detect early stage cancers, it is 92% sensitive in detecting ovarian cancer and may be useful in prompting women with suspicious ovarian masses to go to gynecologic oncologists for primary surgery, where the tumor is likely to be more thoroughly debulked. Unfortunately, the OVA1 test has a high false positive rate of 64%. While OVA1 is more specific than the combination of CA125 and nectin 4, the high rate of false positive results will result in many women undergoing invasive surgery. Adding nectin 4 to the combination of proteins tested may help increase the sensitivity, resulting in a better diagnostic test.

Nectin 4 expression was found to increase proliferation of ovarian cancer cells, similar to what has been previously reported for lung cancer (81). Expression of nectin 4 did not alter resistance to cisplatin but did increase sensitivity to high concentrations of taxol in monolayer culture.

Both control and nectin 4 expressing cells were able to form spheroids equally well. Invasion of mesothelial cells was also unaltered by expression of nectin 4. Nectin 4 positive and control spheroids were similar in their response to cisplatin as well. While both the control and nectin 4 positive spheroids were able to survive at higher concentrations of cisplatin than 2D cultures of the cell were, there was no significant difference between spheroids of the two cell types.

We were not able to discriminate any differences in an *in vivo* model of ovarian

cancer using both nectin 4 expressing and empty vector control cells. Both cell types were able to form tumors at early time points (by two weeks post-injection) and attach to and form tumors on several organs in the peritoneal cavity (ovaries, liver, kidneys, and intestines).

Further studies are needed to better understand the function of nectin 4 in ovarian cancer, since several questions remain. Two isoforms of nectin 4 exist, full length nectin 4 and nectin 4 with a deletion in the cytoplasmic tail (71). mRNA of both isoforms is present in ovarian cancer (unpublished data); however, it is unclear at this time if the shorter isoform is translated into protein and what its function is. Determining the significance of the alternatively spliced isoform could be achieved by several steps. Cloning and expression of the shorter isoform in ovarian cancer cells would be the first project. Once expressed in cells, soluble nectin 4 could be added to mimic trans-dimerization and the signaling cascade could then be examined. It is possible that the short isoform is unable to recruit E-cadherin or initiate the signaling cascade that results in activation of Rac and CDC42.

Nectin 4 may be useful as a therapeutic target; normal expression is limited to the placenta (71). Thus, using nectin 4 as a target should have few side effects of off-target killing of normal cells. Another possibility would be to use nectin 4 peptides to prime the immune system, resulting in generation of cytotoxic CD8+ and antibody producing CD4+ T cells. Dendritic cells could be exposed to nectin 4 peptides resulting in processing and presentation to T cells via the major histocompatiblity complex. Primed cytotoxic T cells could then be added to cultures of nectin 4 positive and negative cells and assayed to determine if specific killing occurs. This type of therapy is dependent on no expression of nectin 4 in normal tissues, however, and more thorough studies to ensure this would be required.

Another question regarding nectin 4 is whether the cleaved ectodomain has functional significance. It may be able to bind to cells expressing nectin 1 or nectin 4 and initiate trans-dimerization signaling. Additionally, this may be an obstacle in using nectin 4 as a therapeutic target. If soluble nectin 4 is present, it may bind to and sequester therapeutic agents targeting nectin 4, limiting the effectiveness of therapy.

Several *in vivo* studies could help elucidate the function of nectin 4 as well. Forcing expression of nectin 4 in the OSE of mice using an ovarian specific promoter (e.g., OSP-1 or Müllerian inhibiting substance receptor type II (131, 132)) could allow for many investigations. First, it could be determined whether expression of nectin 4 is sufficient for tumor formation. This model would also be ideal to different therapy options. Treatment with a taxol and a platinum agent would mimic current treatments for ovarian cancer. This could help determine whether nectin 4 contributes to chemoresistance. Additionally, anti-nectin 4 antibodies could be bound to therapeutic agents such as radioisotopes and toxins (133), however the possibility of immune complexes forming with soluble nectin 4 would have to be investigated.

In addition to the studies on S100A1 and nectin 4, I also did preliminary work on three other potential biomarkers previously identified in our lab, claudin 4, CRABP-1, and spondin 1 (85). Claudins are tight junction proteins and claudin 4 has been previously shown to be increased in several cancers, including ovarian cancer (116, 134). We found that claudin 4 was expressed highly in all subtypes of ovarian cancer tested (69.9% positive overall), and that expression of claudin 4 was inversely associated with Silverberg grade in endometrioid ovarian cancer. These results warrant further study to determine how claudin 4 expression influences ovarian cancer progression.

CRABP-1 is a protein involved in shuttling retinoic acid in the cell. Although IHC analysis in whole tissue sections found 55.2% positive, the TMAs were only 10.6%

positive overall. This could be due to the fact that CRABP-1 can diffuse out of the cell similar to CRABP-2 (Dr. B.C. Gilks, personal communication), or because the cores on the TMAs are not representative of the entire tumor. Because of the low staining results of the TMAs, we chose not to pursue CRABP-1 as a biomarker for ovarian cancer.

Spondin 1 has been identified as a guidance molecule for migrating neurons (125). It has previously been reported as upregulated in ovarian cancer; however, the company responsible for the work was bought out by another company and no further studies were performed (128). Although analysis in whole tissue sections showed appropriate staining patterns, the tissues on the TMAs were almost uniformly positive for spondin 1 (only 2 tissues were scored negative). It is possible that different fixation techniques resulted in this discrepancy. Until further experiments can confirm this high level of expression, the results should be interpreted with caution.

In short, the main studies described in this dissertation have explored the use of two biomarkers that may be useful in the detection, diagnosis, and prognosis of ovarian cancer. Our data supports the use of both S100A1 and nectin 4 in a clinical setting for ovarian cancer. S100A1 expression would be clinically relevant in determining appropriate therapy and monitoring of patients with endometrioid ovarian cancer. Serum nectin 4 levels can help discriminate benign gynecological disease from serous ovarian cancer and could assist physicians in triage of patients with suspicious pelvic masses.

References

1. Boyle P, Levin B. World Cancer Report 2008. Lyon Cedex: International Agency for Research on Cancer; 2008.
2. Jemal A, Siegel R, Ward E, Hao Y, Xu J, Thun MJ. Cancer statistics, 2009. CA Cancer J Clin. 2009; 59: 225-49.
3. Feeley KM, Wells M. Precursor lesions of ovarian epithelial malignancy. Histopathology. 2001; 38: 87-95.
4. Bell DA. Origins and molecular pathology of ovarian cancer. Mod Pathol. 2005; 18: S19-S32.
5. Karst AM, Drapkin R. Ovarian cancer pathogenesis: A model in evolution. Journal of Oncology. 2010: 1-13.
6. Jarboe E, Folkins AK, Drapkin R, Ince TA, Agoston ES, Crum CP. Tubal and ovarian pathways to pelvic epithelial cancer: a pathological perspective. Histopathology. 2008; 53: 127-38.
7. Silverberg SG. Histopathologic grading of ovarian carcinoma: A review and proposal. Int J Gynecol Pathol. 2000; 19: 7-15.
8. Heintz APM, Odicino F, Maisonneuve P, et al. Carcinoma of the ovary. International Journal of Gynecology & Obstetrics. 2003; 83: 135-66.
9. McCluggage WG. My approach to and thoughts on the typing of ovarian carcinomas. J Clin Pathol. 2008; 61: 152-63.
10. Hauptmann S, Dietel M. Serous tumors of low malignant potential of the ovary - molecular pathology: part 2. Virchows Archiv. 2001; 438: 539-51.
11. Kaku T, Ogawa S, Kawano Y, et al. Histological classification of ovarian cancer. Med Electron Microsc. 2003; 36: 9-17.
12. Seidman JD, Kurman RJ. Pathology of ovarian carcinoma. Hematol Oncol Clin North Am. 2003; 17: 909-25.
13. Gilks CB. Subclassification of ovarian surface epithelial tumors based on correlation of histologic and molecular pahtologic data. Int J Gynecol Pathol. 2004; 23: 200-5.
14. Rosen DG, Yang G, Liu G, et al. Ovarian cancer: pathology, biology, and disease models. Front Biosci. 2009; 14: 2089-102.
15. Shih I, Kurman RJ. Ovarian tumorigenesis: a proposed model based on morphological and molecular genetic analysis. Am J Pathol. 2004; 164: 1511-18.
16. Storey DJ, Rush R, Stewart M, et al. Endometrioid epithelial ovarian cancer. Cancer. 2008; 112: 2211-20.
17. Young RC, Decker DG, Wharton JT, et al. Staging laparotomy in early ovarian cancer. JAMA. 1983; 250: 3072-6.
18. Zanetta G, Chiari S, Rota S, et al. Conservative surgery for stage I ovarian carcinoma in women of childbearing age. Br J Obstet Gynaecol. 1997; 104: 1030-5.
19. Hoskins WJ. Surgical staging and cytoreductive surgery of epithelial ovarian cancer. Cancer. 1993; 71: 1534-40.
20. Aletti GD, Dowdy SC, Gostout BS, et al. Aggressive Surgical Effort and Improved Survival in Advanced-Stage Ovarian Cancer. Obstet Gynecol. 2006; 107: 77-85.
21. Berman ML. Future directions in the surgical management of ovarian cancer. Gynecologic Oncology. 2003; 90: S33-S9.

22. DuBois A, Lueck HJ, Meier W, et al. Cisplatin/paclitaxel vs carboplatin/paclitaxel in ovarian cancer: update of an Arbeitsgemeinschaft Gynaekologiesche Onkologie (AGO) study group trial. Proc Am Soc Clin Oncol. 1999; 18: 1374.
23. Johnston SRD. Ovarian cancer: Review of the National Institute for Clinical Excellence (NICE) Guidance Recommendations. Cancer Investigations. 2004; 22: 730-42.
24. Ozols R, Bundy B, Fowler J, et al. Randomized phase III study of cisplatin (CIS)/paclitaxel (PAC) versus carboplatin (CARBO)/PAC in optimal stage III epithelial ovarian cancer (OC): a Gynecologic Oncology Group trial (GOG 158). Proc Am Soc Clin Oncol. 1999; 18: 1373.
25. Meyer T, Rustin GJS. Role of tumour markers in monitoring epithelial ovarian cancer. Br J Cancer. 2000; 82: 1535-8.
26. Canevari S, Gariboldi M, Reid JF, Bongarzone I, Pierotti MA. Molecular predictors of response and outcome in ovarian caner. Critical Reviews in Oncology Hematology. 2006; 60: 19-37.
27. Fields MM, Chevlen E. Ovarian cancer screening: a look at the evidence. Clin J Oncol Nurs. 2006; 10: 77-81.
28. Anderson L. Ovarian cancer: The search for an accurate screening technique. Journal of the American Academy of Physician Assistants. 2009; 22: 22-5.
29. Mani R, Jamil K, Vamsy MC. Specificity of serum tumor markers (CA125, CEA, AFP, Beta HCG) in ovarian malignancies. Trends Med Res. 2007; 2: 128-34.
30. Martin VR. Ovarian cancer: an overview of treatment options. Clin J Oncol Nurs. 2007; 11: 201-7.
31. Yurkovetsky ZR, Linkov FY, Malehorn D, Lokshin AE. Multiple biomarker panels for early detection of ovarian cancer. Future Oncol. 2006; 2: 733-41.
32. Andersen JD, Boylan KLM, Xue FS, et al. Identification of candidate biomarkers in ovarian cancer serum by depletion of highly abundant proteins and differential in-gel electrophoresis. Electrophoresis
2010; 31: 599-610.
33. Zhang H, Kong B, Qu X, Jia L, Deng B, Yang Q. Biomarker discovery for ovarian cancer using SELDI-TOF-MS. Gynecologic Oncology. 2006; 102: 61-6.
34. Yu JS, Ongarello S, Fiedler R, et al. Ovarian cancer identification based on dimesionality reduction for high-throughput mass spectrometry data. Bioinformatics. 2005; 21: 2200-9.
35. Lee CJ, Ariztia EV, Fishman DA. Conventional and proteomic technologies for the detection of early stage malignancies: Markers for Ovarian Cancer. Critical Reviews in Clinical Laboratory Sciences. 2007; 44: 87-114.
36. Michael IP, Sotiropoulou G, Pampalakis G, et al. Biochemical and enzymatic characterization of human kallikrein 5 (hK5), a novel serine protease potentially involved in cancer progression. J Biol Chem. 2005; 280: 14628-35.
37. Moscova M, Marsh DJ, Baxter RC. Protein chip discovery of secreted proteins regulated by the phosphatidylinositol 3-kinase pathway in ovarian cancer cell lines. Cancer Res. 2006; 66: 1376-83.
38. Donato R. Intracellular and extracellular roled of S100 proteins. Microscopy Research and Technique. 2003; 60: 540-51.
39. Emberley ED, Murphy LC, Watson PH. S100 proteins and their influence on pro-survival pathways in cancer. Biochem Cell Biol. 2004; 82: 508-15.
40. Heizmann CW, Ackermann GE, Galichet A. Pathologies involving the S100 proteins and RAGE. Sub-cellular biochemistry. 2007; 45: 93-138.

41. Bierhaus A, Hupert PM, Morcos M, et al. Understanding RAGE, the receptor for advanced glycation end products. J Mol Med. 2005; 83: 876-86.
42. Zimmer DB, Cornwall EH, Landar A, Song W. The S100 protein family: history, function, and expression. Brain Res Bull. 1995; 37: 417-29.
43. Landar A, Caddell G, Chessher J, Zimmer DB. Identification of an S100A1/S100B target protein: phosphoglucomutase. Cell Calcium. 1996; 20: 279-85.
44. Donato R. S100: a multigenic family of calcium-modulated proteins of the EF-hand type with intracellular and extracellular functional roles. Int J Biochem Cell Biol. 2001; 33: 637-68.
45. Baudier J, Bergeret E, Bertacchi N, Weintraub H, Gagnon J, Garin J. Interactions of myogenic bHLH transcription factors with calcium-binding calmodulin and S100a (aa) proteins. Biochemistry. 1995; 34: 7834-46.
46. Zimmer DB, Van Eldik LJ. Identification of a molecular target for the calcium-modulated protein S100. Fructose-1,6-bisphosphate aldolase. J. Biol. Chem. 1986; 261: 11424-8.
47. Zimmer DB, Dubuisson JG. Identification of an S100 target protein: glycogen phosphorylase. Cell Calcium. 1993; 14: 323-32.
48. Duda T, Goraccziak RM, Sharma RK. Molecular characterization of S100A1 - S100B protein in retina and its activation mechanism of bovine photoreceptor guanylate cyclase. Biochemistry. 1996; 35: 6263-66.
49. Ivanenkov VV, Dimlich RVW, Jamieson JGA. Interaction of S100a0 protein with the actin capping protein, CapZ: Characterization of a putative S100a0 binding site in CapZ[alpha]-subunit. Biochemical and Biophysical Research Communications. 1996; 221: 46-50.
50. Sorci G, Agneletti AL, Donato R. Effects of S100A1 and S100B on microtubule stability. An in vitro study using triton-cytoskeletons from astrocyte and myoblast cell lines. Neuroscience. 2000; 99: 773-83.
51. Bianchi R, Giambanco I, Donato R. S100 protein, but not calmodulin, binds to the glial fibrillary acidic protein and inhibits its polymerization in a Ca2+-dependent manner. J Biol Chem. 1993; 268: 12669-74.
52. Wang G, Rudland PS, White MR, Barraclough R. Interaction in vivo and in vitro of the metastasis-inducing S100 protein, S100A4 (p9Ka) with S100A1. J. Biol. Chem. 2000; 275: 11141-6.
53. Li G, Barthelemy A, Feng G, et al. S100A1: a powerful marker to differentiate chromophobe renal cell carcinoma from renal oncocytoma. Histopathology. 2007; 50: 642-7.
54. Teratani T, Watanabe T, Kuwahara F, et al. Induced transcriptional expression of calcium-binding protein S100A1 and S100A10 genes in human renal cell carcinoma. Cancer Lett. 2002; 175: 71-7.
55. Li G, Gentil-Perret A, Lambert C, Genin C, Tostain J. S100A1 and KIT gene expressions in common subtypes of renal tumors. Eur J Surg Oncol. 2005; 31: 299-303.
56. Rocca PC, Brunelli M, Gobbo S, et al. Diagnostic utility of S100A1 expression in renal cell neoplasms: an immunohistochemical and quantitative RT-PCR study. Mod Pathol. 2007; 20: 722-8.
57. Wang G, Zhang S, Fernig DG, Martin-Fernandez M, Rudland PS, Barraclough R. Mutually antagonistic actions of S100A4 and S100A1 on normal and metastatic phenotypes. Oncogene. 2005; 24: 1445-54.

58. Huttunen HJ, Kuja-Panula J, Sorci G, Agneletti AL, Donato R, Rauvala H. Coregulation of neurite outgrowth and cell survival by amphoterin and S100 proteins through receptor for advanced glycation end products (RAGE) activation. J. Biol. Chem. 2000; 275: 40096-105.
59. Harris AL. Hypoxia-a key regulatory factor in tumour growth. Nat Rev Cancer. 2002; 2: 38-47.
60. Helmlinger G, Yuan F, Dellian M, Jain RK. Interstital pH and pO_2 gradients in solid tumors *in vivo*: High-resolution measurements reveal a lack of correlation. Nat Med. 1997; 3: 177-82.
61. Miyoshi J, Takai Y. Nectin and nectin-like molecules: biology and pathology. Am J Nephrol. 2007; 27: 590-604.
62. Takai Y, Shimizu K, Ohtsuka T. The roles of cadherins and nectins in interneuronal synapse formation. Curr Opin Neurobiology. 2003; 13: 520-6.
63. Irie K, Shimizu K, Sakisaka T, Ikeda W, Takai Y. Roles and modes of action of nectins in cell-cell adhesion. Seminars in Cell & Developmental Biology. 2004; 15: 643-56.
64. Rikitake Y, Takai Y. Interactions of the cell adhesion molecule nectin with transmembrane and peripheral membrane proteins for pleiotropic functions. Cell Mol Life Sci. 2007; 65: 253-63.
65. Takahashi K, Nakanishi H, Miyahara M, et al. Nectin/PRR: An immunoglobulin-like cell adhesion molecule recruited to cadherin-based adherens junctions through interaction with afadin, a PDZ domain-containing protein. J. Cell Biol. 1999; 145: 539-49.
66. Lopez M, Eberle F, Mattei M-G, et al. Complementary DNA characterization and chromosomal localization of a human gene related to the poliovirus receptor-encoding gene. Gene. 1995; 155: 261-5.
67. Eberle F, Dubreuil P, Mattei M-G, Devilard E, Lopez M. The human PRR2 gene, related to the human poliovirus receptor gene (PVR), is the true homolog of the murine MPH gene. Gene. 1995; 159: 267-72.
68. Lopez M, Aoubala M, Jordier F, Isnardon D, Gomez S, Dubreuil P. The human poliovirus receptor related 2 protein Is a new hematopoietic/endothelial homophilic adhesion molecule. Blood. 1998; 92: 4602-11.
69. Reymond N, Borg J-P, Lecocq E, et al. Human nectin3/PRR3: a novel member of the PVR/PRR/nectin family that interacts with afadin. Gene. 2000; 255: 347-55.
70. Lopez M, Eberl・ F, Mattei M-G, et al. Complementary DNA characterization and chromosomal localization of a human gene related to the poliovirus receptor-encoding gene. Gene. 1995; 155: 261-5.
71. Reymond N, Fabre S, Lecocq E, Adelaide J, Dubreuil P, Lopez M. Nectin4/PRR4, a new afadin-associated member of the nectin family that trans-interacts with Nectin1/PRR1 through V domain interaction. J. Biol. Chem. 2001; 276: 43205-15.
72. Yasumi M, Shimizu K, Honda T, Takeuchi M, Takai Y. Role of each immunoglobulin-like loop of nectin for its cell-cell adhesion activity. Biochemical and Biophysical Research Communications. 2003; 302: 61-6.
73. Fabre S, Reymond N, Cocchi F, et al. Prominent role of the Ig-like V domain in trans-Interactions of nectins. Nectin 3 and nectin 4 bind to the predicted C-C'-C''-D beta -strands of the the nectin 1 V domain. J. Biol. Chem. 2002; 277: 27006-13.

74. Niessen CM. Tight junctions/adherens junctions: Basic structure and function. J Invest Dermatol. 2007; 127: 2525-32.
75. Takai Y, Miyoshi J, Ikeda W, Ogita H. Nectins and nectin-like molecules: roles in contact inhibition of cell movement and proliferation. Nat Rev Mol Cell Biol. 2008; 9: 603-15.
76. Honda T, Shimizu K, Fukuhara A, Irie K, Takai Y. Regulation by nectin of the velocity of the formation of adherens junctions and tight junctions. Biochemical and Biophysical Research Communications. 2003; 306: 104-9.
77. Ooshio T, Irie K, Morimoto K, Fukuhara A, Imai T, Takai Y. Involvement of LMO7 in the association of two cell-cell adhesion molecules, nectin and E-cadherin, through afadin and a-actinin in epithelial cells. J Biol Chem. 2004; 279: 31365-73.
78. Hoshino T, Shimizu K, Honda T, et al. A novel role of nectins in inhibition of the E-cadherin-induced activation of Rac and formation of cell-cell adherens junctions. Mol. Biol. Cell. 2004; 15: 1077-88.
79. Fabre-Lafay S, Garrido-Urbani S, Reymond N, Goncalves A, Dubreuil P, Lopez M. Nectin-4, a new serological breast cancer marker, is a substrate for Tumor NecrosisFactor-{alpha}-converting Enzyme (TACE)/ADAM-17. J. Biol. Chem. 2005; 280: 19543-50.
80. Fabre-Lafay S, Monville F, Garrido-Urbani S, et al. Nectin-4 is a new histological and serological tumor associated marker for breast cancer. BMC Cancer. 2007; 7: 73-89.
81. Takano A, Ishikawa N, Nishino R, et al. Identification of nectin-4 oncoprotein as a diagnostic and therapeutic target for lung cancer. Cancer Res. 2009; 69: 6694-703.
82. Jemal A, Siegel R, Ward E, et al. Cancer statistics, 2008. CA Cancer J Clin. 2008; 58: 71-96.
83. Verheijen RHM, von Mensdorff-Pouilly S, van Kamp GJ, Kenemans P. CA 125: fundamental and clinical aspects. Semin Cancer Biol. 1999; 9: 117-24.
84. Bast RC, Jr., Urban N, Shridhar V, et al. Early detection of ovarian cancer: promise and reality. Cancer Treat Res. 2002; 107: 61-97.
85. Hibbs K, Skubitz KM, Pambuccian SE, et al. Differential gene expression in ovarian carcinoma: Identification of potential biomarkers. Am J Pathol. 2004; 165: 397-414.
86. Shaw TJ, Senterman MK, Dawson K, Crane CA, Vanderhyden BC. Characterization of intraperitoneal, orthotopic, and metastatic xenograft models of human ovarian cancer. Mol Ther. 2004; 10: 1032-42.
87. Burleson KM, Hansen LK, Skubitz APN. Ovarian carcinoma spheroids disaggregate on type I collagen and invade live human mesothelial cell monolayers. Clin Exp Metastasis. 2004; 21: 685 - 97.
88. Subramanian IV, Bui Nguyen TM, Truskinovsky AM, Tolar J, Blazar BR, Ramakrishnan S. Adeno-associated virus-mediated delivery of a mutant endostatin in combination with carboplatin treatment inhibits orthotopic growth of ovarian cancer and improves long-term survival. Cancer Res. 2006; 66: 4319-28.
89. Skubitz APN, Campbell KD, Goueli S, Skubitz KM. Association of [beta]1 integrin with protein kinase activity in large detergent resistant complexes. FEBS Lett. 1998; 426: 386-91.
90. Nicosia SV, Wilbanks GD, Saunders B, et al. Cytology of human ovarian surface epithelial brushings. Cancer Cytopathology. 2004; 102: 1-10.

91. Kruk PK, Maines-Bandiera S, Auersperg N. A simplified method to culture human ovarian surface epithelium. Lab Invest. 1990; 63: 132-6.
92. Skubitz APN, Pambuccian SE, Argenta PA, Skubitz KM. Differential gene expression identifies subgroups of ovarian carcinoma. Transl Res. 2006; 148: 223-48.
93. Fronhoffs S, Totzke G, Stier S, et al. A method for the rapid construction of cRNA standard curves in quantitative real-time reverse transcription polymerase chain reaction. Mol Cell Probes. 2002; 16: 99-110.
94. Soslow RA. Histologic subtypes of ovarian carcinoma: an overview. Int J Gynecol Pathol. 2008; 27: 161-74.
95. Gilks CB, Ionescu DN, Kalloger SE, et al. Tumor cell type can be reproducibly diagnosed and is of independent prognostic significance in patients with maximally debulked ovarian carcinoma. Hum Pathol. 2008; 39: 1239-51.
96. Weichert W, Denkert C, Noske A, et al. Expression of class I histone deacetylases indicates poor prognosis in endometrioid subtypes of ovarian and endometrial carcinomas. Neoplasia. 2008; 10: 1021-7.
97. Malpica A, Deavers MT, Lu K, et al. Grading ovarian serous carcinoma using a two-tier system. Am J Surg Pathol. 2004; 28: 496-504.
98. Delys L, Detours V, Franc B, et al. Gene expression and the biological phenotype of papillary thyroid carcinomas. Oncogene. 2007; 26: 7894-903.
99. Dubeau L. The cell of origin of ovarian epithelial tumors and the ovarian surface epithelium dogma: Does the emperor have no clothes? Gynecol Oncol. 1999; 72: 437-42.
100. Dubeau L. The cell of origin of ovarian epithelial tumours. Lancet Oncol. 2008; 9: 1191-7.
101. Boni R, Burg G, Doguoglu A, et al. Immunohistochemical localization of the Ca2+ binding S100 proteins in normal human skin and melanocytic lesions. Br J Dermatol. 1997; 137: 39-43.
102. Sato E, Olson SH, Ahn J, et al. Intraepithelial CD8+ tumor-infiltrating lymphocytes and a high CD8+/regulatory T cell ratio are associated with favorable prognosis in ovarian cancer. Proc Natl Acad Sci USA. 2005; 102: 18538-43.
103. Hamanishi J, Mandai M, Iwasaki M, et al. Programmed cell death 1 ligand 1 and tumor-infiltrating CD8+ T lymphocytes are prognostic factors of human ovarian cancer. Proc Natl Acad Sci USA. 2007; 104: 3360-5.
104. Clarke B, Tinker AV, Lee C-H, et al. Intraepithelial T cells and prognosis in ovarian carcinoma: novel associations with stage, tumor type, and BRCA1 loss. Mod Pathol. 2008; 22: 393-402.
105. Heierhorst J, Kobe B, Feil SC, et al. Ca2+ /S100 regulation of giant protein kinases. Nature. 1996; 380: 636-9.
106. Yamasaki R, Berri M, Wu Y, et al. Titin-actin interaction in mouse myocardium: passive tension modulation and its regulation by calcium/S100A1. Biophys. J. 2001; 81: 2297-313.
107. Kim K-S, Sengupta S, Berk M, et al. Hypoxia enhances lysophosphatidic acid responsiveness in ovarian cancer cells and lysophosphatidic acid induces ovarian tumor metastasis in vivo. Cancer Res. 2006; 66: 7983-90.
108. Sakisaka T, Takai Y. Biology and pathology of nectins and nectin-like molecules. Current Opinion in Cell Biology. 2004; 16: 513-21.

109. Sakisaka T, Ikeda W, Ogita H, Fujita N, Takai Y. The roles of nectins in cell adhesions: cooperation with other cell adhesion molecules and growth factor receptors. Current Opinion in Cell Biology. 2007; 19: 593-602.
110. Yamada A, Fujita N, Sato T, et al. Requirement of nectin, but not cadherin, for formation of claudin-based tight junctions in annexin II-knockdown MDCK cells. Oncogene. 2006.
111. Nakanishi H, Takai Y. Roles of nectins in cell adhesion, migration and polarization. Biological Chemistry. 2004; 385: 885-92.
112. DeRycke MS, Andersen JD, Harrington KM, et al. S100A1 expression in ovarian and endometrial endometrioid carcinomas is a prognostic indicator of relapse-free survival. American Journal of Clinical Pathology. 2009; 132: 846-56.
113. Herrmann R, Fayad W, Schwarz S, Berndtsson M, Linder S. Screening for compounds that induce apoptosis of cancer cells grown as multicellular spheroids. J Biomol Screen. 2008; 13: 1-8.
114. Shield K, Ackland ML, Ahmed N, Rice GE. Multicellular spheroids in ovarian cancer metastases: Biology and pathology. Gynecologic Oncology. 2009; 113: 143-8.
115. H. Ogita WIYT. Roles of cell adhesion molecules nectin and nectin-like molecule-5 in the regulation of cell movement and proliferation. Journal of Microscopy. 2008; 231: 455-65.
116. Agarwal R, D'Souza T, Morin PJ. Claudin-3 and claudin-4 expression in ovarian epithelial cells enhances invasion and is associated with increased matrix metalloproteinase-2 activity. Cancer Res. 2005; 65: 7378-85.
117. Wu Q, Lothe R, Ahlquist T, et al. DNA methylation profiling of ovarian carcinomas and their in vitro models identifies HOXA9, HOXB5, SCGB3A1, and CRABP1 as novel targets. Molecular Cancer. 2007; 6: 45.
118. Rangel LBA, Agarwal R, D'Souza T, et al. Tight Junction Proteins Claudin-3 and Claudin-4 Are Frequently Overexpressed in Ovarian Cancer but Not in Ovariana Cystadenomas. Clin Cancer Res. 2003; 9: 2567-75.
119. D'Souza T, Agarwal R, Morin PJ. Phosphorylation of claudin-3 at threonine 192 by cAMP-dependent protein kinase regulates tight junction barrier function in ovarian cancer cells. J. Biol. Chem. 2005; 280: 26233-40.
120. Rangel LBA, Agarwal R, D'Souza T, et al. Tight junction proteins claudin-3 and claudin-4 are frequently overexpressed in ovarian cancer but not in ovarian cystadenomas. Clinical Cancer Research. 2003; 9: 2567-75.
121. Morin PJ. Claudin proteins in human cancer: Promising new targets for diagnosis and therapy. Cancer Res. 2005; 65: 9603-6.
122. Ying H, Albert de la C, Natalia SP. Hypermethylation, but not LOH, is associated with the low expression of MT1G and CRABP1 in papillary thyroid carcinoma. International Journal of Cancer. 2003; 104: 735-44.
123. Lind GE, Kleivi K, Meling GI, et al. ADAMTS1, CRABP1, and NR3C1 identified as epigenetically deregulated genes in colorectal tumorigenesis. Cell Oncol. 2006; 28: 259-72.
124. Miyamoto K, Morishita Y, Yamazaki M, et al. Isolation and characterization of Vascular Smooth Muscle Cell Growth Promoting Factor from bovine ovarian follicular fluid and its cDNA cloning from bovine and human ovary. Archives of Biochemistry and Biophysics. 2001; 390: 93-100.

125. Burstyn-Cohen T, Tzarfaty V, Frumkin A, Feinstein Y, Stoeckli E, Klar A. F-spondin is required for accurate pathfinding of commissural axons at the floor plate. Neuron. 1999; 23: 233-46.
126. Young HM, Anderson RB, Anderson CR. Guidance cues involved in the development of the peripheral autonomic nervous system. Autonomic Neuroscience. 2004; 112: 1-14.
127. Zisman S, Marom K, Avraham O, et al. Proteolysis and membrane capture of F-spondin generates combinatorial guidance cues from a single molecule. J. Cell Biol. 2007; 178: 1237-49.
128. Pyle-Chenault RA, Stolk JA, Molesh DA, et al. VSGP/F-spondin: A new ovarian cancer marker. Tumor Biology. 2005; 26: 245-57.
129. Alvero AB, Chen R, Fu HH, et al. Molecular phenotyping of human ovarian cancer stem cells unravels the mechanisms for repair and chemoresistance. Cell Cycle. 2009; 8: 158-66.
130. Johannes L. Test to help determine if ovarian masses are cancer. The Wall Street Journal. 2010 March 9, 2010.
131. Selvakumaran M, Bao R, Crijns APG, Connolly DC, Weinstein JK, Hamilton TC. Ovarian epithelial cell lineage-specific gene expression using the promoter of a retrovirus-like element. Cancer Res. 2001; 61: 1291-5.
132. Connolly DC, Bao R, Nikitin AY, et al. Female mice chimeric for expression of the simian virus 40 TAg under control of the MISIIR promoter develop epithelial ovarian cancer. Cancer Res. 2003; 63: 1389-97.
133. Sharkey RM, Goldenberg DM. Targeted therapy of cancer: New prospects for antibodies and immunoconjugates. CA Cancer J Clin. 2006; 56: 226-43.
134. Honda H, Pazin MJ, Ji H, Wernyj RP, Morin PJ. Crucial roles of Sp1 and epigenetic modifications in the regulation of the CLDN4 promoter in ovarian cancer cells. J. Biol. Chem. 2006; 281: 21433-44.

Appendix

NATURE PUBLISHING GROUP LICENSE
TERMS AND CONDITIONS

Apr 13, 2010

This is a License Agreement between Melissa S DeRycke ("You") and Nature Publishing Group ("Nature Publishing Group") provided by Copyright Clearance Center ("CCC"). The license consists of your order details, the terms and conditions provided by Nature Publishing Group, and the payment terms and conditions.

All payments must be made in full to CCC. For payment instructions, please see information listed at the bottom of this form.

License Number	2406930281693
License date	Apr 13, 2010
Licensed content publisher	Nature Publishing Group
Licensed content publication	Nature Reviews Molecular Cell Biology
Licensed content title	Nectins and nectin-like molecules: roles in contact inhibition of cell movement and proliferation
Licensed content author	Yoshimi Takai, Jun Miyoshi, Wataru Ikeda, Hisakazu Ogita
Volume number	
Issue number	
Pages	
Year of publication	2008
Portion used	Figures / tables
Number of figures / tables	2
Identify high-res figures	Figure 2, Figure 3
Requestor type	Student
Type of Use	Thesis / Dissertation
High-res requested	Yes
Billing Type	Invoice
Company	Melissa S DeRycke
Billing Address	805 Como Ave #10 Saint Paul, MN 55103 United States

Customer reference info

Total 74.75 USD

Terms and Conditions

Terms and Conditions for Permissions

Nature Publishing Group hereby grants you a non-exclusive license to reproduce this material for this purpose, and for no other use, subject to the conditions below:

1. NPG warrants that it has, to the best of its knowledge, the rights to license reuse of this material. However, you should ensure that the material you are requesting is original to Nature Publishing Group and does not carry the copyright of another entity (as credited in the published version). If the credit line on any part of the material you have requested indicates that it was reprinted or adapted by NPG with permission from another source, then you should also seek permission from that source to reuse the material.

2. Permission granted free of charge for material in print is also usually granted for any electronic version of that work, provided that the material is incidental to the work as a whole and that the electronic version is essentially equivalent to, or substitutes for, the print version. Where print permission has been granted for a fee, separate permission must be obtained for any additional, electronic re-use (unless, as in the case of a full paper, this has already been accounted for during your initial request in the calculation of a print run). NB: In all cases, web-based use of full-text articles must be authorized separately through the 'Use on a Web Site' option when requesting permission.

3. Permission granted for a first edition does not apply to second and subsequent editions and for editions in other languages (except for signatories to the STM Permissions Guidelines, or where the first edition permission was granted for free).

4. Nature Publishing Group's permission must be acknowledged next to the figure, table or abstract in print. In electronic form, this acknowledgement must be visible at the same time as the figure/table/abstract, and must be hyperlinked to the journal's homepage.
5. The credit line should read:

   Reprinted by permission from Macmillan Publishers Ltd: [JOURNAL NAME] (reference citation), copyright (year of publication)

   For AOP papers, the credit line should read:

   Reprinted by permission from Macmillan Publishers Ltd: [JOURNAL NAME], advance online publication, day month year (doi: 10.1038/sj.[JOURNAL ACRONYM].XXXXX)

6. Adaptations of single figures do not require NPG approval. However, the adaptation should be credited as follows:

   Adapted by permission from Macmillan Publishers Ltd: [JOURNAL NAME] (reference citation), copyright (year of publication)

7. Translations of 401 words up to a whole article require NPG approval. Please visit http://www.macmillanmedicalcommunications.com for more information. Translations of up to a 400 words do not require NPG approval. The translation should be credited as follows:

   Translated by permission from Macmillan Publishers Ltd: [JOURNAL NAME] (reference citation), copyright (year of publication).

We are certain that all parties will benefit from this agreement and wish you the best in the use of this material. Thank you.

v1.1

Gratis licenses (referencing $0 in the Total field) are free. Please retain this printable license for your reference. No payment is required.

If you would like to pay for this license now, please remit this license along with your payment made payable to "COPYRIGHT CLEARANCE CENTER" otherwise you will be invoiced within 48 hours of the license date. Payment should be in the form of a check or money order referencing your account number and this invoice number RLNK10766597.
Once you receive your invoice for this order, you may pay your invoice by credit card. Please follow instructions provided at that time.

Make Payment To:
Copyright Clearance Center
Dept 001
P.O. Box 843006
Boston, MA 02284-3006

If you find copyrighted material related to this license will not be used and wish to cancel, please contact us referencing this license number 2406930281693 and noting the reason for cancellation.

Questions? customercare@copyright.com or +1-877-622-5543 (toll free in the US) or +1-978-646-2777.

American Society for Clinical Pathology

33 West Monroe Street, Suite 1600
Chicago, Illinois 60603-5617

T 312.541.4999
F 312.541.4998
www.ascp.org

27 May 2010

Name: Melissa DeRycke
Skubitz Lab
University of Minnesota
Address: Microbiology, Immunology, and Cancer Biology Ph.D. Program
Phone: 612-625-4942
E-mail : deryc004@umn.edu

Dear Melissa DeRycke,

In response to your request, the ASCP grants you permission to use/distribute, the following material(s) for educational use:

1) Manuscript ID # ACJP-2010-04-0183; and,

2) Melissa S. DeRycke, John D. Andersen, Katherine M. Harrington, Stefan E. Pambuccian, Steve E. Kalloger, Kristin L.M. Boylan, Peter A. Argenta, and Amy P.N. Skubitz. "S100A1 Expression in Ovarian and Endometrial Endometrioid Carcinomas is a Prognostic." *AJCP* 2009 132(6):846-856.

Note: Materials will not be provided by ASCP.

This permission is granted on the following four conditions:

- proper credit is given to the ASCP as copyright holder of the material. The following **must** be included in/on the printed and electronic materials:
  - ©2009-2010 American Society for Clinical Pathology and ©2009-2010 *American Journal of Clinical Pathology;*
- the full scientific citation must be included in the list of references (if necessary);
- per the program's requirements, the manuscript (which will be included in its entirety in our dissertation) will be published and submitted online to ProQuest. ProQuest will electronically reproduce the full text of my dissertation abstract, and inquiries using terms in the title or abstract will be searchable.

Further use of the material beyond this will require additional written permission requests.

If you need any further assistance, please feel free to contact me.

Regards,

Brian Oliver

Digitally signed by Brian Oliver
DN: cn=Brian Oliver, o=American Society for Clinical Pathology, ou=Archives, email=brian.oliver@ascp.org, c=US
Date: 2010.05.27 09:28:54 -05'00'

Brian Oliver, MLIS
Archivist and Medical Librarian
American Society for Clinical Pathology
33 West Monroe, Suite 1600
Chicago, Illinois, 60603